Understanding Chronic Lung Infections after Correcting the Basic Cystic Fibrosis Defect

Samantha L. Durfey

A dissertation

submitted in partial fulfillment of the

requirements for the degree of

Doctor of Philosophy

University of Washington

2023

Reading Committee:

Pradeep K. Singh, Chair

Colin Manoil

Lucas Hoffman

Program Authorized to Offer Degree:

Microbiology

University of Washington

Abstract

Understanding Chronic Lung Infections after Correcting the Basic Cystic Fibrosis Defect

Samantha L. Durfey

Chair of the Supervisory Committee:

Pradeep K. Singh

Microbiology

Cystic fibrosis (CF) is a genetic disease caused by mutations in the cystic fibrosis transmembrane conductance regulator (CFTR) gene. In 2012, the first drug that can correct the physiologic defect was approved. These drugs, called “CFTR modulators”, offer great hope to people with CF, as many clinical measures of health improve, including lung function, nutritional status, and frequency of disease flares. Unfortunately, despite marked improvements in overall health, there are hints that modulators cannot restore patients to full health. Early studies indicate chronic bacterial infections persist in many patients, and these patients’ lungs remain inflamed. This is important because before modulators, chronic infection and inflammation were the main drivers of lung disease progression and death. The failure of modulators to resolve these pathologies suggests that lung disease may continue to progress in persistently infected patients taking CFTR modulators.

The goal of my thesis work was to better understand persistent post-modulator lung infections. In chapter 2, I describe a method we developed to enumerate and quantify the bacterial strains present in a pool of thousands of cultured isolates or directly from the sputum of people with CF. This method enables new questions to be addressed regarding the frequency of multi-strain infections and the degree of strain turnover during infections before and after modulator therapy. In chapter 3, we test an eradication protocol that combined intensive antibiotic treatment with modulator therapy. While antibiotics have not previously been able to clear chronic infections, we hypothesized modulator-induced changes in the lung

environment could make antibiotics more effective. Finding that infections generally persisted after combined treatment inspired me to develop a deeper understanding of the causes of persistent infection after modulators. In chapter 4, we used bronchoscopy to sample many lung regions within each subject to identify characteristics of regions which remain persistently infected compared to those that clear infection. Results from this study suggest that structural lung damage may allow bacterial pathogens to persist, and show persistent infection is strongly associated with levels of inflammation after modulators. The work presented in this thesis reveals difficulties in eradicating chronic infection after modulators, and sheds light on the underlying causes of this difficulty.

Table of Contents

Acknowledgements

First, from the bottom of my heart, I'd like to thank every single person who contributed to the work presented in this thesis. Without your dedication and expertise, none of this would have been possible.

Thank you so, so much to my advisor, Pradeep. I really appreciate all the time and effort you've dedicated to my training. In particular, you've coached my writing and presenting skills to heights I did not think I could achieve. I can't say how much I appreciate you always being in my corner, and giving me the opportunity to work on the thesis project of my dreams.

Thank you to everyone in the Singh, Parsek, and Hoffman labs over the years. In particular: Maria, Sumedha, Gilbert, Anna, Anh, Kailee, Wendy and Sara. Your support and friendship have meant the world to me. Y'all made these years so much fun! Thank you also to the postdocs and senior scientists who contributed so much to my training: Sarah Morgan, Richard Siehnel, Courtney Reichhardt, and Chris Pope.

Thank you to my committee members: Luke Hoffman, Colin Manoil, Steve Salipante, and Evgeni Sokurenko. I appreciate all of your advice! Thank you especially to Luke and Colin for serving on my reading committee.

Thank you to my cohort! We really went through the ringer, but we made it through together. In particular, Julia and Lauren – your friendship helped me thrive through all the ups and downs of grad school.

To the whole Seattle CF community: What a vibrant place to study! From legends like Bonnie Ramsey, Margaret Rosenfeld, Moira Aitken, Chris Goss; to the incredible resources provided by the TDN; to the many CF microbiologists; training here gave me access to all your wisdom and energy. It's inspiring to know people like you exist. It makes me think that maybe I can become one of you, too, when I grow up.

To the greater CF community: I deeply appreciate the time and advice you've showered on me over the years. Thank you in particular to Katie Hisert, Boo Tseng, Peter Jorth, Katherine Tuggle, JP Clancy, Ranjani Somayajii, and Meghan Kiedrowski for your support.

Thank you to my parents, Sue and Lance Durfey, for your love and support, and for nurturing my love of STEM from an early age. I appreciate all your encouragement and patience.

Finally, thank you to Luke Wylie. You are the kindest, most loving, and most supportive person I know. I love you very much.

CHAPTER 1: Introduction

A brief history of cystic fibrosis

Cystic fibrosis (CF) is the most common life-limiting genetic disease among Caucasians, affecting at least 100,000 people around the world (1). CF is caused by mutations in a cyclic AMP-regulated membrane anion channel, the cystic fibrosis transmembrane conductance regulator (*CFTR*), which normally transports chloride and bicarbonate across apical cell membranes.

The hallmark clinical manifestation of CF is lung disease, characterized by lifelong bacterial infections, frequent disease flares, continual lung function decline, and eventual death from pulmonary complications. However, this predominance of lung disease is relatively new – for the first decades after the disease was described, it was thought of predominantly as a gastrointestinal disease.

Cystic fibrosis was first described as being a separate disease from celiac disease by Dr. Dorothy Andersen in 1938 (2). Using autopsies, she identified mucus plugging in the glandular ducts of the pancreas, and termed the disease “cystic fibrosis of the pancreas”. She characterized the disease as having malabsorption of fat and protein, excess fat in the stool, growth failure, and lung infection.

In 1946, Andersen and Hodges described CF as a genetic disease (3). Prior to their work, there were multiple hypotheses regarding the cause of CF: genetics; dietary deficiency during pregnancy or early infancy; intrauterine infection; or infection during early infancy. Measuring the frequency of diagnosis among families, they found the 25% inheritance from carrier parents expected of a Mendelian recessive trait and thus concluded it was a highly penetrant genetic disease.

The first clue that CF involved a defect in epithelial ion transport came following a 1948 New York City heatwave, when babies with CF were suffering from heat exhaustion at higher rates than healthy babies (4). This led Paul Di Sant’Agnese in 1953 to hypothesize and demonstrate that babies with CF had abnormal salt levels in their sweat (5). His work offered a convenient diagnostic tool, and rapidly led to the first standardized sweat test in 1959 developed by Gibson and Cooke (6). The sweat test was revolutionary as it was very specific (only a few other clinically distinct conditions resulted in elevated sweat chloride) and allowed mild cases of CF to be identified.

Chloride transport was identified as the primary defect by Paul Quinton in 1983 (7). Contemporaneously, sodium absorption was suggested as a cognate defect by Knowles et al (8) and

Boucher et al (9). However, the sodium absorption hypothesis has been disputed (10) and remains controversial.

CF as a field changed drastically with the discovery of the CFTR gene in 1989 (11–13). Within 2.5 years, over 300 mutations were identified with at least 230 associated with disease, thanks in large part to the efforts of the CF Genetic Analysis Consortium (14). Now, >2000 CFTR variants have been reported to the Cystic Fibrosis Mutation Database (http://www.genet.sickkids.on.ca/cftr/StatisticsPage.html, accessed March 7, 2023), with 400 known to be disease causing (https://cftr2.org/mutations_history, accessed March 10, 2023). About 1/3 of CFTR variants occur in 5 or fewer people and have not been well characterized (15). CFTR variants can be categorized into multiple distinct classes based on their functional abnormalities (15–17). The most recent classification system divides mutations into 7 classes, primarily based on therapeutic strategies/potential (17). I will discuss the classes in a later section about therapies that correct CFTR.

Prior to the discovery of the CFTR gene, treatments focused on managing patients' symptoms. Pancreatic enzyme replacement and nutritional supplementation treated the most severe of gastrointestinal symptoms (18). Hypertonic saline and recombinant DNase were developed to improve airway clearance and respiratory function (19, 20). Airway physiotherapy, characterized by rapid chest percussion, vibration and shaking, additionally improves airway clearance (21). Several antibiotics were adapted for use as chronic therapies to slow life-threatening lung infections (22, 23), and chronic prescription of macrolides like azithromycin reduced airway inflammation and disease flares (24). While these therapies improved patient symptoms and extended their lifespans, patients with CF still had shorter lifespans than people without CF (25). Critically, none of these maintenance therapies have treated the basic defect in CF.

Then, in 2009, the way in which we treat CF fundamentally changed. The era of only managing symptoms ended with the introduction of a new therapeutic strategy to directly correct the underlying CFTR defect. This strategy uses small molecule drugs to interact with the mutant CFTR protein and restore its function. The first of these small molecule drugs, termed "CFTR modulators", was approved for use in the US in 2012, and has revolutionized CF treatment. The newest and most effective was approved in 2019. I will discuss these in much greater detail in a later section on CFTR modulators.

The progress achieved in CF can be seen starkly through improvements in the expected life span of people with CF. When Dorothy Andersen first described CF, it was a fatal diagnosis, with infants typically living to only 6 months of age, and many dying in the first week of life (26). At this time, the primary causes of death were meconium ileus (impaction of the gut), malnutrition, and lung infections. The median predicted lifespan of people with CF rose into their 40's just before the introduction of CFTR modulators (27). With the introduction of the newest, most effective CFTR modulator therapy, the CF Foundation now estimates that babies born in the US from 2017-2021 will likely live into their 50's (28). For many people, CF is no longer a fatal diagnosis or even a crippling disability. In the 2021 report on people in the US with CF, the Foundation found that 55% of adults held full time or part time jobs, and 40% had earned college degrees.

From the first description of CF in 1938, to its discovery as a genetic disease in 1946, to the identification of the CFTR gene in 1989, to the approval of CFTR-targeting therapies in 2012, CF is a disease characterized by rapid progress in diagnosis, treatment, and extending patients' lifespans. However, a median life expectancy of 53 years for people with CF is about 2 decades short of the national median life expectancy (76.1 years) (29), indicating we still have much to discover to help patients lead their fullest lives.

Clinical manifestations of CF

Epithelial cells are the cell types with the highest expression of CFTR and are found in many organs, including the sweat duct, airway, pancreatic duct, intestine, biliary tree, and the vas deferens. CFTR dysfunction in these cell types is responsible for many of the characteristic manifestations of CF – elevated sweat chloride, lung and sinus infection and obstruction, pancreatic insufficiency (severely reduced amounts of the digestive enzyme, pancreatic lipase), intestinal obstruction, biliary cirrhosis, and congenital bilateral absence of the vas deferens. Interestingly, the types of cells that express CFTR is still an area of active investigation. For example, in 2018, Plasschaert and colleagues (30) and Montoro and colleagues (31) simultaneously discovered a new sub-type of epithelial cell called the "ionocyte" for its very high level of CFTR expression. The significance of this discovery for CF disease is not yet known.

The current primary manifestation of CF is progressive lung failure brought on by chronic lung infection (32–34), inflammation, and lung damage in the form of bronchiectasis and small airway obstruction (35–37). CF lung disease changes over the course of a patient's lifetime. Recent studies have demonstrated that by age 3, children with CF have evidence of lung damage on CT, mucus obstruction, neutrophilic inflammation, and infection (38–40). As people age, lung damage accumulates, levels of inflammation increase, and infection evolves. Infection is particularly dependent on age. As newborns/ young infants, CF patients' lungs are likely not colonized by organisms, as bronchoscopy samples are typically indistinguishable from paired reagent controls (41–43). The first pathogens to colonize young CF patients are *Staphylococcus aureus* (*Sa*) and *Haemophilus influenzae* in early childhood. As many as 80% of US children with CF have a *Sa* infection (28). As children with CF reach puberty, gram negative pathogens like *Pseudomonas aeruginosa* (*Pa*), *Stenotrophomonas maltophilia, Achromobacter* spp., and *Burkholderia cepacia* complex begin colonizing the lung, with *Pa* responsible for most of the infections. As adults, ~40-50% of CF patients will be colonized by *Pa*, and ~40-60 % will be colonized by *Sa*, the 2 most common pathogens (28). While it was initially presumed that *Pa* generally displaces *Sa*, recent work shows the two organisms more frequently coexist for long periods of time (44).

Pa infections are responsible for much of the reduction in quality and length of life in people with CF (45–48). When *Pa* infection first begins, there is often a period where the infection is considered "intermittent". This period is characterized by inconsistent culture positivity, and antimicrobial treatments are generally more effective for eradicating the infection (49–51). However, despite the use of antibiotics, *Pa* infections will eventually develop into "chronic" infections, where respiratory samples are consistently culture positive and typically a single strain of *Pa* persists (52). These chronic infections often require frequent use of antibiotics, with some administered as maintenance therapy of monthly on-off cycles of inhaled antibiotics (22) and others are administered as intravenous and oral antibiotics to treat disease flares, termed "exacerbations", that are associated with overall lung function decline (45, 46). Despite this frequent antibiotic exposure, chronic infections are very rarely eradicated, and the same strain of *Pa* generally persists through a patient's life.

What enables *Pa* to successfully infect the lungs of people with CF? The lung in CF is altered in several ways that could contribute to susceptibility to *Pa* infection. Unfortunately, animal models that

recapitulate the characteristics of human lung disease have been difficult to develop. This challenge has recently been mostly overcome (53–55), but the early lack of animal models slowed mechanistic understanding of which abnormalities are directly dependent on loss of CFTR, and which abnormalities are secondary effects of those primary defects (56). However, studies in humans and the newly developed pig model (53), ferret model (54), and rat model (55) reveal differences between the airways of healthy and CF individuals. First, mucus secretion and mucus properties are altered, leading to the accumulation of mucus in the airway (43, 57, 58). Second, altered pH of the airway surface liquid decreases antimicrobial activity (59–64). Finally, immune responses within the lungs of CF patients appear altered. For example, children with CF exhibit excess inflammation for a given bacterial load when compared to non-CF children (65–67). Neutrophils recruited to the CF lung may persist longer than non-CF neutrophils due to slower apoptosis in response to the elevated pro-inflammatory cytokines (68–72). The proteases secreted by excess neutrophils inhibit phagocytosis and bacterial killing (73–76). Finally, monocytes may also exhibit abnormal responses in the lung (77), including LPS tolerance (78) and deficient adhesion (79).

Finally, individuals with CF exhibit marked intra-patient heterogeneity in lung disease. This is very well studied with regards to structural lung damage, catalyzed by the relative ease of acquiring non-invasive measurements via computed tomography (CT) or magnetic resonance imaging (MRI) (80–86). These numerous studies reveal that some areas of a person's lung may appear normal and other areas may be irreversibly damaged. Intra-patient heterogeneity in inflammatory and microbiologic parameters has also been observed, but is much less well understood (42, 85–91), owing to the comparative difficulty in obtaining regional samples within the lung. Regional heterogeneity has been observed in the bacterial species detected (42, 85, 91), bacterial density (42, 87, 90), bacterial phenotypes (89, 92), and concentration of inflammatory markers (42, 86, 90). However, their interrelatedness at the regional level is less certain, as many studies conflict with each other. Davis and colleagues identified and sampled the highest and lowest damage regions in children, and found that highest damage regions had higher inflammation and tended to have higher bacterial density. On the other hand, Hogan and colleagues found that in adults, regions with significantly different degrees of damage did not have different *Pa*

densities. Both studies are small, so the different findings may be due to small numbers of subjects; or it may be that regional heterogeneity changes over the lifetime of a patient.

Development of CFTR modulators

A recent advance in the treatment of CF is the development of a new class of small molecule drugs, called “CFTR modulators”, that restore function to the mutated CFTR protein. They generally function by binding to the mutated CFTR protein and altering function (as opposed to correcting the genetic mutation). CFTR modulators are transformational treatments as they mark the first time the underlying cause of CF can be treated, as opposed to treating symptoms.

Mutations in the CFTR gene can be classified based on their functional abnormalities and the therapeutic strategies necessary to overcome their malfunction (16, 17). There have been mutations found that affect every major step of a protein’s lifecycle, from synthesis of the mRNA to the rate of degradation of the protein after it successfully reaches the membrane. Defects at each step require a unique therapeutic strategy (until genetic therapies are developed). While classification is limited as a single variant can have multiple class defects, the classification system has none-the-less proved incredibly useful for understanding the underlying defect within the cell and for understanding why different CFTR modulators are necessary for different mutations. Using the 7-class system (17), the classes are as follows:

Class	Functional abnormality	Therapeutic strategy (any approved?)
I	No protein (early stop codon)	Read through compounds (no)
II	No trafficking to the membrane	Correctors (yes)
III	Impaired gating	Potentiators (yes)
IV	Reduced conductance/flow of ions	Potentiators (yes)
V	Less protein (usually splicing issues)	Antisense oligonucleotides (no)
VI	Reduced stability/increased degradation	Stabilizers (no)
VII	No mRNA	Stimulate alternative channels (no)

Correctors support the trafficking of mutated CFTR to the cell surface and increase the number of CFTR proteins at the apical plasma membrane. **Potentiators** enhance ion transport through the channel of CFTR proteins that make it to the surface.

The activity of the first CFTR modulator, ivacaftor, was described in 2009 (93). It was identified as part of a high-throughput screen of 228,000 diverse compounds performed in a cell-based fluorescence membrane potential assay. The membrane potential assay measures ion flow across a membrane, and thus identified **potentiators** that enhanced ion transport through a mutant CFTR. **Potentiators** can only treat Class III/IV mutations, which are found in ~6% of the US CF population (94). Ivacaftor (originally called "VX-770" in the literature) was selected because it could potentiate several mutant CFTRs, had in vitro selectivity, and had a favorable preclinical pharmacokinetic profile.

The first proof of concept study using ivacaftor in humans was published shortly after by Frank Accurso, Bonnie Ramsey, and colleagues in 2010 (95). They treated 39 patients with a particular Class III/gating mutation (*G551D*) for 28 days and measured nasal potential difference, sweat chloride, and lung function before and during treatment. Nasal potential difference measures the voltage across the nasal epithelium, which reflects CFTR activity due to CFTR's transepithelial ion transport activity (96). The response was greatest as measured by sweat chloride, the best clinical indicator of CFTR activity (97). Indeed, sweat chloride improved enough to no longer meet the diagnostic threshold for CF. However, both the nasal potential difference and lung function improvements were modest, foreshadowing the modest lung responses to CFTR modulators observed in many subsequent studies.

Ivacaftor was approved by the FDA in January 2012 for adults and children as young as 12 years with the *G551D* mutation. This mutation has a prevalence of ~4% in the US population (28). Ivacaftor was then approved in Europe and Canada in late 2012, followed by Australia and New Zealand in 2013 (98). FDA approvals for younger age groups came steadily: ages 2-5 years in March 2015 (https://www.cff.org/press-releases/2015-03/fda-approves-ivacaftor-children-ages-2-5-certain-rare-cf-mutations), ages 1-2 years in August 2018 (https://www.cff.org/node/1086), ages 6 months to 1 year in 2019, and 4-6 months in 2020 (https://www.cff.org/node/711). Ivacaftor has now been approved for 38

different CFTR variants, in both class III and class IV (99), which has enabled ~10% of the US population to access this drug (28).

Following ivacaftor, the next CFTR modulator developed was lumacaftor, which was used in conjunction with ivacaftor (100). Lumacaftor is significant because it is the first **corrector** developed (helps traffic CFTR to the cell surface and increase the number of CFTR proteins in the cell membrane), which treats people with the most common CFTR mutation, Δ*F508* (found in ~70% of US patients (28)). Lumacaftor was soon replaced by tezacaftor (101), and then this dual combination was quickly rendered obsolete by the introduction of elexacaftor (28).

The next (and most recent) highly effective CFTR modulator developed was elexacaftor, which is a next generation **corrector** and treats people with the Δ*F508* mutation. Following a head to head comparison of 2 different candidates in early 2019 (102, 103), elexacaftor was selected and the triple combination of elexacaftor/ tezacaftor/ ivacaftor (ETI) was approved by the FDA in November 2019. The initial clinical trial demonstrated increased efficacy; in patients already taking tezacaftor/ivacaftor, adding elexacaftor produced an additional 11% increase in lung function. In treatment naïve individuals, the benefit was +14%. For comparison, ivacaftor produced a +10% improvement in people with gating mutations (97) and tezacaftor/ivacaftor produced a +3.8% improvement in people with Δ*F508* (101). These marked improvements in lung function were recapitulated in a large, real world observational study (104).

However, worldwide access to these expensive drugs remains a challenge – a recent report estimated that only ~20,000 people worldwide are currently prescribed ETI, about 20% of the global diagnosed population (1). Many factors contribute to low uptake. First, the estimated cost per year of ETI is USD $311,741 (1). The lowest European market rate the authors found was $254,000, and by the end of 2020 only the USA, UK, Ireland, Denmark, Germany, and Slovenia had reimbursement agreements with Vertex (the sole producer of ETI) (1). In developing countries, access is delayed because Vertex is not selling ETI in these countries, while also seeking to block local companies from producing it (https://www.nytimes.com/2023/02/07/health/cystic-fibrosis-drug-trikafta.html). Finally, access to CFTR modulators will be generally harder for people of African and Asian descent, as the treatable CFTR

mutations are less common in these populations. For example, the Δ*F508* mutation is estimated to be present in only 12-31% of Asian patients with CF (105) as compared to 70% of Caucasian patients. So, while CFTR modulators are transforming care for many patients of Caucasian descent in high-income nations, achieving worldwide coverage remains a key challenge.

A host of additional CFTR-targeting therapies are in the clinical development pipeline (https://apps.cff.org/trials/pipeline/; accessed March 12, 2023). They range from improving dosing of current modulators, to delivering mRNA or gene therapy to correct CFTR no matter the underlying mutation. As such, CFTR-targeting therapies and their impacts on disease will remain an active area of research for years to come.

Ivacaftor and lung infections

Ivacaftor has been repeatedly demonstrated to improve patient outcomes such as sweat chloride, lung function, exacerbations, and nutritional status (97, 106, 107). Ivacaftor also modifies the lungs in ways that could affect the infecting bacterial populations. For example, ivacaftor improves mucociliary clearance in people (108) and mucus hydration in cell cultures (109). It also improves airway surface liquid pH in a CFTR activity-dependent manner (60), which could increase the activity of antimicrobial peptides. There are also early indications that ivacaftor can correct some immune response pathologies. For example, neutrophil (76, 110, 111) and monocyte (112–114) functions appear to improve with ivacaftor.

A surprising finding from studies of ivacaftor is that treatment has only modest effects on a cardinal manifestation of CF, chronic lung infections caused by *Pa*, *Sa*, and other pathogens. For example, Hisert and colleagues used culture-based methods to show that ivacaftor produced rapid reductions in sputum *Pa* density in chronically infected subjects and reduced lung inflammation (115). However, *Pa* density rebounded after ~1 year, and *Pa* strains present pretreatment were found to persist for at least 6 years of follow-up (116). Epidemiological studies analyzing patient registry data (108, 117–120) and studies using DNA-based methods (108, 121, 122) also indicate that chronic infections usually persist in modulator-treated patients. In one study with a decrease in *Pa* culture positivity (108),

subsequent analysis demonstrated that this decrease was driven by patients who were intermittently infected with *Pa* and those with chronic *Pa* rarely became culture negative (117). These studies suggest that ivacaftor does not generally eradicate chronic CF infections.

Elexacaftor / tezacaftor / ivacaftor (ETI) and lung infections

The effects of ivacaftor may be predictive of the response to ETI, as sweat chloride and lung function improvements appear similar (103). As discussed above, studies of ivacaftor-treated subjects show that chronic CF lung infections generally persist after treatment (108, 115, 117, 118, 120–122) and this trend appears to be holding true for ETI, although very little is known yet about infections after ETI. In two papers from Ben Kopp's group, possibly examining the same patient cohort, they found that registry-reported culture positivity decreased from about 50% before ETI to about 25% after 1 year of ETI (123, 124). The PROMISE microbiology study (125) was the first to quantify bacterial abundance in prospectively collected sputum before and after ETI treatment, and examined ~200 patients during the first 6 months of ETI treatment. They found that within 30 days of treatment, the concentration of *Pa* and *Sa* decreased 100-fold. However, they also found low rates of infection clearance. Only 5/50 *Pa*-positive patients became repeatedly negative for *Pa* culture and *Pa* DNA in the 6 months after initiating ETI, and only 2/83 *Sa*-positive patients became repeatedly negative for *Sa* culture and *Sa* DNA (125). Taken together, these studies suggest that many patients will continue to harbor infections, even after initiating the most effective CFTR modulator to date.

Summary and Objective:

Despite the promise of CFTR modulators, persistent infection will remain a pressing problem for people with cystic fibrosis. The goal of my doctoral thesis work in the Singh lab has been to better understand persistent post-modulator lung infections. In chapter 2, we develop a method to characterize the number and relative abundance of bacterial strains present in a mixed population. This method enables new questions to be addressed regarding the frequency of multi-strain infections and the degree of strain turnover in chronic infections before and after modulator treatment. In chapter 3, we test an

eradication protocol that combines intensive antibiotics and initiation of a CFTR modulator to try to increase eradication of chronic infections. After finding that most infections persisted, despite this combined treatment, I was inspired to develop a deeper understanding of the causes of persistent infection after modulators. In chapter 4, I present the results from a clinical study in which we used bronchoscopy to sample many lung regions within each subject to identify characteristics of regions which remain persistently infected compared to those that clear infection. My thesis work provides insights into the challenges of treating chronic infections and sheds light on the causes of this difficulty.

CHAPTER 2: A Population-level Strain Genotyping Method to Study Pathogen Strain Dynamics in Human Infections

Published as: Sarah J Morgan*, Samantha L Durfey*, Sumedha Ravishankar, Peter Jorth, Wendy Ni, Duncan Skerrett, Moira L Aitken, Edward F Mckone, Stephen J Salipante, Matthew C Radey & Pradeep K Singh. JCI Insight. 2021;6(24):e152472.

Author contributions: SJM and SLD contributed equally. SJM, SLD, and PKS conceived the study; SJM, SLD, and MCR designed the methodology; MCR developed the software; SJM, SLD, and WN validated data; PKS, SJM, SLD, SR, and DTS investigated; PKS, MLA, SJS, PJ, and EFM provided resources; SJM, SLD, and PKS wrote the manuscript; PKS supervised; and PKS acquired funding. All authors have read and agreed to the published version of the manuscript.

Abstract

A hallmark of chronic bacterial infections is the long-term persistence of one or more pathogen species at the compromised site. Repeated detection of the same bacterial species can suggest that a single strain or lineage is continually present. However, infection with multiple strains of a given species, strain acquisition and loss, and changes in strain relative abundance can occur. Detecting strain-level changes and their effects on disease is challenging as most methods require labor intensive isolate-by-isolate analyses, thus, only a few cells from large infecting populations can be examined. Here we present a population-level method for enumerating and measuring the relative abundance of strains called "PopMLST". The method exploits PCR amplification of strain-identifying polymorphic loci, next-generation sequencing to measure allelic variants, and informatic methods to determine whether variants arise from sequencing errors or low abundance strains. These features enable PopMLST to simultaneously interrogate hundreds of bacterial cells that are either cultured *en masse* from patient samples, or are present in DNA directly extracted from clinical specimens without *ex vivo* culture. This method could be used to detect epidemic or super-infecting strains, facilitate understanding of strain dynamics during chronic infections, and enable studies that link strain changes to clinical outcomes.

Introduction

Serial culturing of chronic infection sites often repeatedly yields the same pathogen species. For instance, chronic wounds can consistently grow *Staphylococcus* and *Pseudomonas* species (126), subjects with urinary tract anomalies can be persistently infected by *Escherichia coli* (127), and chronically-infected sinuses can recurrently yield the same anaerobes (126–128). The chronic infections that afflict people with cystic fibrosis (CF) are a prime example, as the same pathogen species are frequently cultured from patients' lung secretions for long periods. Some species, like *Pseudomonas aeruginosa* (*Pa*) and *Staphylococcus aureus* (*Sa*), can be highly abundant in the lungs of individual patients for decades or even life-long (52, 129–133).

Repeated detection of the same bacterial species over time can imply that a single strain or lineage is continually present. However, even though most strain-level genotyping studies examine very few isolates from each infection, studies on chronic wound, urinary tract, ear, gastrointestinal, and lung infections suggest more complexity. For example, strain-level genotyping methods have shown that close to a third of people with CF and *Sa* lung infections simultaneously harbor more than one *Sa* strain (129, 130, 134, 135). Likewise, some studies have shown that up to 40% of people with CF are simultaneously infected by more two or more *Pa* strains (136–138), although other work has suggested a lower frequency of multi-strain infections (52, 92, 139–143). In addition, strain relative abundance can change over time, and strains can be gained or lost in individual patients (137, 141, 142). Notorious examples are *Pa* epidemic strains that can infect and eventually become dominant in already-colonized patients, and markedly worsen disease (144–146).

Identifying infecting strains is important for several reasons. First, strains of the same species can differ markedly in traits like the capacity for injury, transmissibility, and resistance to antibiotics (92, 145–150). Thus, the presence of multiple strains or changes in strain relative abundance could have clinical consequences. Second, strain abundance changes could provide information about the status of host defenses, treatment efficacy, or pathogen functioning. For example, strains may recede when host defenses or treatments to which they are susceptible intensify, or when deleterious mutations arise.

Likewise, new strain acquisition could indicate that host conditions have become more permissive, and analysis of succeeding strains could increase understanding of bacterial functions important *in vivo*. Third, sensitive methods for strain detection could reveal outbreaks and lapses in infection control procedures. Finally, early detection of new strains could spur eradication attempts, which may be more successful soon after strains are acquired (151–155).

Established methods for strain-level identification such as pulse-field gel electrophoresis (PFGE), multi-locus sequence typing (MLST), whole genome sequencing (WGS), and others must generally be performed on one cultured isolate at a time (140, 156–159). Because pathogen populations can be extremely large and colonies from different strains may look identical (160–164), analyzing a few colonies per sample could miss multi-strain infections and strain acquisition and loss events. Newer methods using amplification of species-specific variable regions (165, 166) are not easily adaptable to multiple pathogens, and shotgun sequencing of clinical samples (164, 167) can be limited if non-target DNA (e.g. host or other bacterial DNA) is abundant. To address these limitations, we developed PopMLST ("population MLST"), a method to enumerate and measure the relative abundance of strains present in pools of hundreds of cultured isolates, or in DNA directly extracted from clinical samples.

Results

Overview. In conventional MLST, bacterial colonies are isolated in pure culture, Sanger sequencing is used to identify allelic variation in MLST loci within conserved housekeeping genes (7 loci in the case of *Sa* and *Pa*), and loci allele types are determined by comparison to a database (168–170). Because a single clone is analyzed, the loci are known to be linked, in that they originate from the same bacterial isolate. Thus, loci allele identities can be combined to define the MLST type of a pure culture isolate.

In contrast, the goal of PopMLST is to enumerate the pathogen strains and measure strain relative abundance in samples that could contain multiple strains, even when the infection site contains a vast excess of non-target (e.g. human) DNA. To achieve this, PopMLST uses PCR to amplify MLST loci from complex samples, and next-generation sequencing to measure allele relative abundance. The PCR primers act as probes to find conserved sequences flanking MLST loci (even when the targeted species is rare), and as vectors to amplify the strain-discriminating MLST loci. Amplicons are Illumina sequenced, and bioinformatic tools are used to distinguish rare variants from errors, bin “like” sequences, and measure their relative abundance (Figure 1). A drawback to this approach is that PCR amplification and Illumina sequencing from complex mixtures is more error-prone than Sanger sequencing of individual clones. Errors could be confused for low-abundance variant strains, particularly since different MLST loci can differ only at a few positions (168–170).

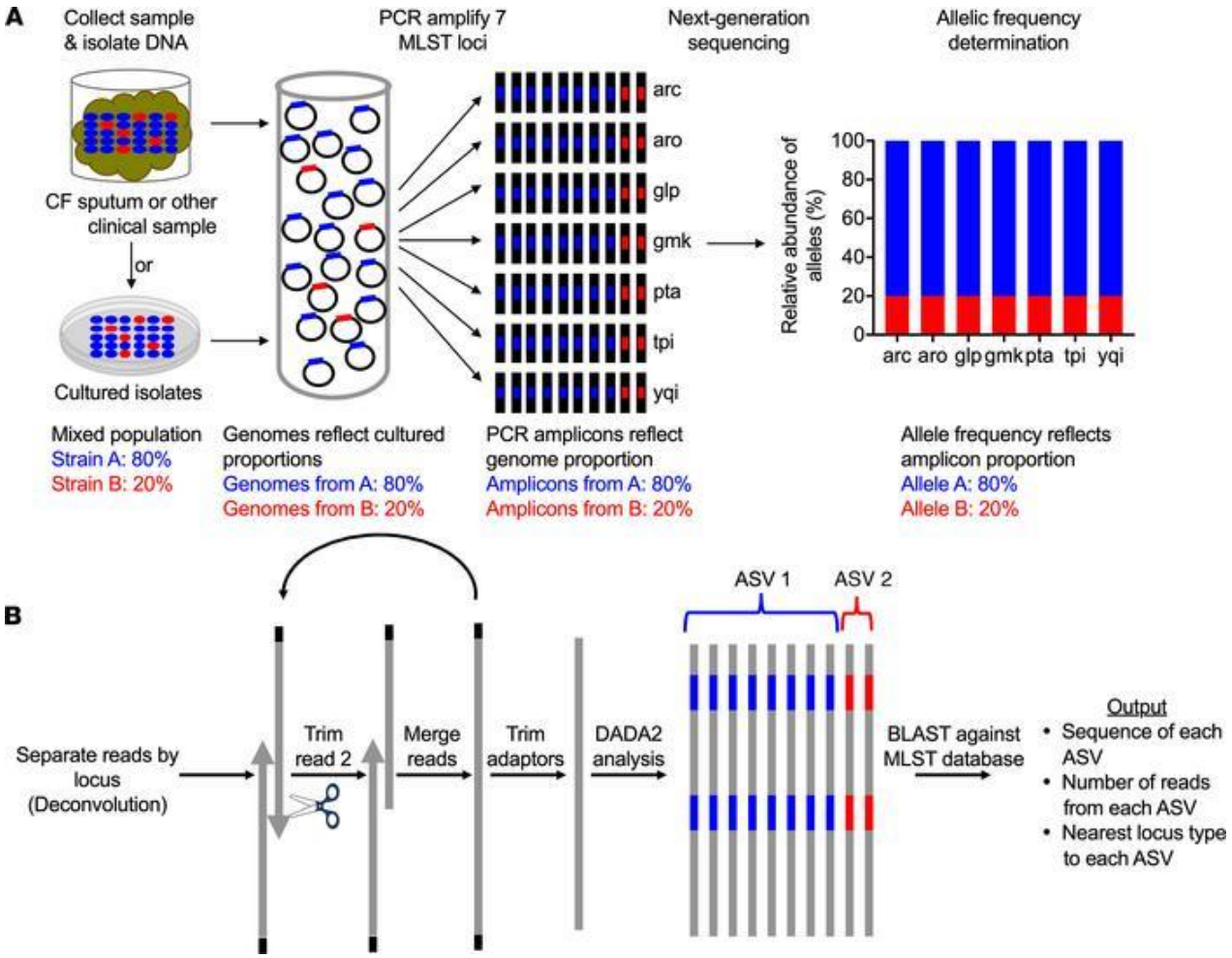

Figure 1. PopMLST methods. **(A)** PopMLST can be performed on clinical specimens (without culturing) or cultured isolates. MLST loci are PCR amplified in separate reactions, amplicons Illumina-sequenced, and the relative abundance of reads representing MLST loci are measured. **(B)** Bioinformatic analysis deconvolves reads using permissive alignment to assign them to MLST loci, iteratively tests reverse read trimming lengths to optimize merging of paired-end reads, removes adaptors, identifies amplicon sequence variants (ASVs) using DADA2, and uses BLAST to identify closest MLST locus type.

We addressed this problem in several ways. (1) We used high fidelity polymerases and as few PCR cycles as possible to reduce error and PCR chimeras. (2) We adapted the DADA2 analysis pipeline for uses on MLST loci amplicons. *DADA2* (171) is designed for 16S rRNA amplicon sequencing and uses statistical methods to distinguish sequencing errors from low abundance variants (Figure 1B)) (166, 171). (3) We developed bioinformatic methods to adaptively trim the lower-quality ends of the reverse read generated by Illumina sequencing to facilitate accurate read merging (see methods and Figure 1B). (4) We amplified each MLST locus in triplicate and pooled the data to reduce random, preferential amplification of templates (i.e. "jackpot" amplifications) (172). (5) We omitted a GC-repeat rich *Pa* MLST locus (*aro*) that was challenging to sequence with Illumina chemistries (Figure S1 A-C) (173, 174). Control analyses (Figure S1D and E) showed that omission of *aro* had only a minor effect on strain discrimination. Together these approaches mitigate, but do not fully eliminate the effects PCR and sequencing errors.

Data interpretation. While the PCR and Illumina sequencing used in PopMLST enable analysis of complex mixtures containing multiple strains and excess non-target DNA, information from MLST loci are unlinked. Many (up to hundreds of) of isolates are analyzed *en masse* and sequence reads reporting alleles from each locus are derived from separate PCR reactions. This issue does not generally limit PopMLST's ability to enumerate and measure strain relative abundance, which can be determined by examining the loci with the highest number of alleles represented.

This approach is effective because even though strains sometimes share MLST alleles (and PopMLST will report the sum of the shared loci's relative abundances in these cases), the large number of alleles for each locus (e.g. *Sa* MLST loci have 484-892 distinct alleles*,* and *Pa* MLST loci have 137-278 distinct alleles) make it unlikely that strains would have identical alleles at enough MLST loci to prevent strain enumeration. However, in mixed populations containing many strains, the likelihood that multiple strains share alleles increases, which would cause PopMLST to underestimate the number of strains present in the population.

The MLST types of strains within mixtures can also often be determined from PopMLST data. When a limited number of strains co-exist, inference can determine which MLST alleles originate from the same strain, as linked alleles will be detected at a similar relative abundance. For example, if PopMLST finds that each locus contains 3 alleles at a relative abundances of ~70% : ~25%: ~5%, it is likely that the alleles identified at 70% relative abundance belong to one strain, alleles at 25% come from a second strain, and alleles at 5% come from a third strain. When many strains are present, if strains co-exist at similar relative abundances, or if strains happen to share several alleles, inference can fail. If knowledge of the specific MLST types is important, conventional MLST can be performed on a few cultured colonies to determine which alleles are linked to one another to guide analysis of population-level data generated by PopMLST.

Once it is determined which MLST locus types likely belong to the same isolates (by inference, or by conventional MLST on single isolates) the relative abundance of each MLST type in the sample is calculated by averaging the relative abundance of all loci that differentiate the two strains. Averaging MSLT loci abundances dampens the effect of error that could occur in individual loci measurements.

PopMLST identifies single strains after *in vivo* diversification. As an initial test of the method, we performed PopMLST on pure cultures containing single strains of Sa and Pa and found that >99% of reads correctly reported a single MLST type in each of 21 independent experiments (Table 1).

Table 1. PopMLST correctly identifies single *Sa* and *Pa* isolates as a single MLST type.

Sample	Percent of reads mapping to single loci type (SEM)
S. aureus	
NCTC8325	100% (0)
NCTC8325 (repeat)	100% (0)
MN8	100% (0)
MN8 (Repeat)	100% (0)
Newman	100% (0)
CF isolate	100% (0)
CF isolate	100% (0)
CF isolate	100% (0)
CF isolate	100% (0)
CF isolate	100% (0)
P. aeruginosa	
PA14	100% (0)
PA14 (repeat)	99.96% (0.0272)*
LES	100% (0)
LES (repeat)	100% (0)
PAO1	100% (0)
PAO1 (repeat)	100% (0)
CF isolate	100% (0)
CF isolate	100% (0)
CF isolate	100% (0)
CF isolate	100% (0)
CF isolate	99.6% (0.006)**
CF isolate	100% (0)
Wound isolate	100% (0)
Wound isolate	100% (0)

* Three of the six loci indicated the presence of a second locus type at less than 1% likely due to sequencing error.

* Four of the six loci indicated the presence of a second locus type at less than 1% likely due to sequencing error.

In CF and other chronic infections, strains genetically diversify during infection (92, 134, 148–150, 175, 176), and within-strain genetic diversity could be mistaken for strain differences. Thus, we tested PopMLST on pools of 90-96 clonally related *Pa* isolates collected from different lung regions, from three different CF patients undergoing lung transplantation. Whole genome sequencing showed that isolates from each subject were clonally related to each other, but had genetically diversified via *in vivo* evolution (19). Importantly, two of the three collections exhibited hypermutator phenotypes due to mutations in either *mutL* or *mutS* mismatch repair genes and whole genome sequencing showed that the mutator populations contained far higher levels of genetic variation that the non-mutator population (92). Core genomes of 96 isolates from the subject that was not infected with a hypermutator contained a total 328 SNP differences, and the 96 isolates from subjects with hypermutator lineages contained 3169 and 1653 SNP differences (92).

Despite this extensive evolved diversity, PopMLST correctly identified each of the populations as containing a single MLST type (< 0.01% of reads erroneously reported a second MLST allele) (Figure 2, Table S1). These data suggest that the measures we used to mitigate PCR amplification and sequencing errors are effective for pure-culture isolates and diversified clonally related populations.

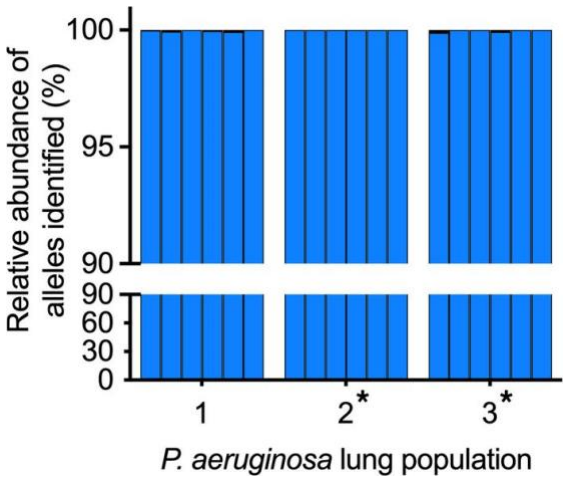

Figure 2. PopMLST correctly identifies genetically diversified, clonally related *Pa* as a single MLST type. PopMLST was performed on pools of 90-96 clonally related *Pa* isolates collected from different lung regions, from three CF patients undergoing lung transplantation. Plot shows the relative abundance of each MLST allele (from pool) that matches the known MLST sequence (determined by whole genome sequencing, see table S1). The six bars for each sample show the relative abundance of *acs, gua, mut, nuo, pps,* and *trp* loci (in order). Black bars indicate any additional MLST loci types detected and in all cases were less than 0.2%. *indicates hypermutable populations due to *mutS* (population 2) or *mutL* (population 3) mutations.

PopMLST accurately measures pathogen strains in experimental mixtures. A key assumption of the PopMLST approach is that the relative abundance of MLST loci present in samples is maintained through DNA extraction, amplification, sequencing, and enumeration steps (Figure 1). We therefore began testing PopMLST's ability to detect multiple strains using defined mixtures of purified DNA from different strains. PopMLST identified the expected ratios (within 2-fold) of mixtures containing two *Sa* or *Pa* strains over a wide relative abundance range (Figure 3). Replicate experiments using different sequencing runs and different MLST types produced similar results (Figure 3 and S2-S3). Linear regression of data from the experimental mixtures indicated close agreement between expected the results and average MLST allele loci measurements ($R^2 = 0.9916$ for *Sa* and $R^2 = 0.9901$ for *Pa*) with slopes approximating 1 (*Sa*: 1.017 [95% CI: 0.9872-1.047]; *Pa*: 0.9806 [95% CI: 0.9454-1.016]).

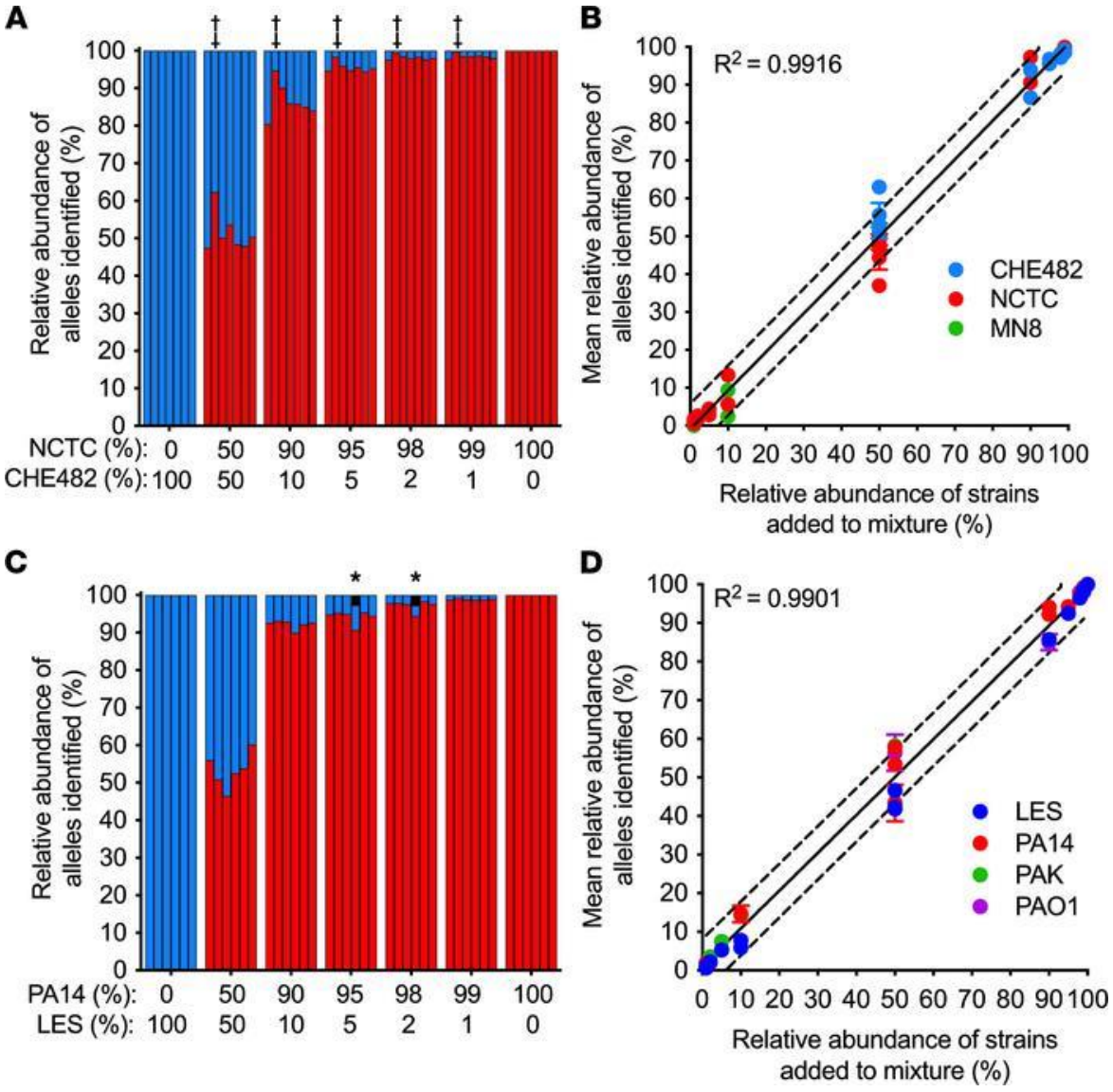

Figure 3. PopMLST measures strain relative abundance. **(A and C)** DNA from two *Sa* **(A)** and *Pa* **(C)** strains with different MLST types were mixed at indicated ratios. Red bars indicate reads that PopMLST called as alleles from *Sa* NCTC8325 **(A)** and *Pa* PA14 **(C)**; blue bars indicate reads called as alleles from *Sa* CHE482 **(A)** and *Pa* LES (C). **(B and D)** Mean loci relative abundance and SEM corresponding to the indicated MLST type from 21 independent two-strain *Sa* mixtures **(B)** including NCTC8325 (red) with CHE482 (blue) or MN8 (green); and 20 independent two-strain *Pa* mixtures **(D)** including PA14 (red) and LES (blue) or PAK (green), or PAO1 (purple) and LES (blue). Data for individual allele measurements can be found in Figure S2 and S3. Some error bars (SEM) were smaller than symbols; solid line indicates expected result, dashed lines indicate +/- 10%. Bars in **(A)** show relative abundance of *arc, aro, glp, gmk,*

pta, tpi, and *yqi* (in order). Bars in **(C)** show relative abundance of *acs, gua, mut, nuo, pps,* and *trp* (in order). MLST alleles identified but not present in the mixtures (likely sequencing error), are indicated in black and those detected at >1%, are indicated with *. ‡ indicates PCR bias as evidenced by one allele being consistently under or overrepresented.

We also tested PopMLST's ability to measure strain relative abundance in three and four strain mixtures (Figure 4). PopMLST measurements of strain relative abundance in mixtures containing equal ratios of three *Sa* strains reported an average strain relative abundance of 33.7% (SEM 7.9%), and measurements of equal-ratio four-strain *Sa* mixtures reported average strain relative abundance of 24.9% (SEM 5.57%) (Figure 4A). In equal-ratio *Pa* three-strain mixtures, PopMLST reported average strain relative abundance of 33.2% (SEM 9.5%). In equal-ratio four-strain *Pa* mixtures PopMLST reported average strain relative abundance of 24.6% (SEM 6.0%) (Figure 4B).

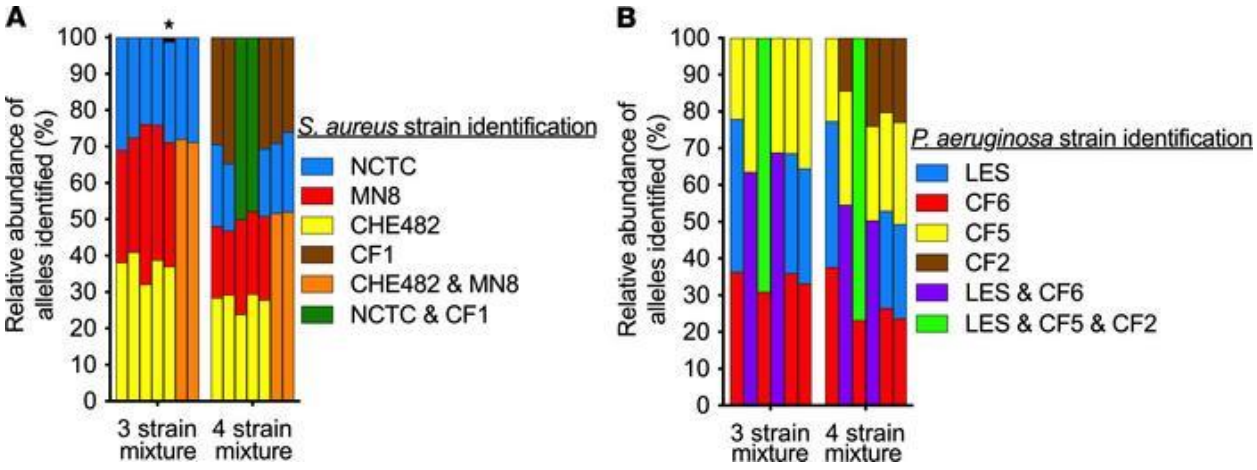

Figure 4. PopMLST can identify at least 4 unique MLST types in a mixture. Equimolar mixtures of DNA from three or 4 strains were analyzed by PopMLST. Unique MLST loci alleles of the four strains present in the mixtures are shown as blue, red, yellow, and brown. Alleles shared between strains added to the mixture cannot be assigned to a particular strain, and are therefore colored as follows (alleles common to strains indicated with red & blue were indicated with purple; alleles common to strains indicated with yellow & red were indicated with orange; alleles common to strains indicated with blue & brown were indicated with green **(A)** and alleles common to strains indicated with blue & yellow & brown were indicated with green **(B)**). Bars in **(A)** show relative abundance of *Sa* MLST alleles *arc, aro, glp, gmk, pta, tpi,* and *yqi* (in order). Bars in **(B)** show relative abundance of *Pa* MLST alleles *acs, gua, mut, nuo, pps,* and *trp* (in order). MLST alleles identified but not present in the mixtures (likely sequencing error), are indicated in black and those detected at >1%, are indicated with *.

Despite use of triplicate PCR reactions, a single locus type was occasionally detected at higher-than-expected abundance (Figures 3 and S2-S3). These finding are likely due to PCR bias (indicated by ‡ in Figures 3 and S2-S3) or jackpot amplifications (indicated by # in Figures S3). PCR bias and jackpots also occur in 16S rRNA gene measurements (177) which likewise uses amplicon sequencing. However, because PopMLST averages data from 6 or 7 independently amplified loci (unlike 16S sequencing which relies on a single locus), the effect of error in any given loci is dampened. Furthermore, loci that appear to be outliers can be interpreted in context of others to estimate strain relative abundance. Because of these advantages, PCR bias and jackpot amplifications had little effect on strain relative abundance measurements in the experimental mixtures we tested (Figure 3B and 3D, Figure S2-S3).

PopMLST has a low frequency of false positive strain calls. Error inherent to PCR and Illumina sequencing could cause PopMLST to artificially report strains that are not present. We examined control experiments containing between 1-4 strains of known composition (n=38 for *Pa* and n=41 for *Sa*) to examine the effect of using different abundance thresholds to make strain presence and absence calls.

As shown in Table 2, using the criterion that single variant locus be present at ≥1% relative abundance falsely registered the presence of a new strain in 9/49 (18%) of control experiments with *Pa*, and 7/41 (17%) of control experiments with *Sa*. Using the criterion that two or more loci be present at ≥1%, or raising the relative abundance threshold for a single allele to ≥4% produced accurate calls in all 49 *Pa*, and all 41 *Sa* experiments. We conclude that using a threshold for defining detection of a single variant locus at greater that 4% relative abundance or two variant loci at >1% relative abundance results in a low likelihood of erroneously interpreting sequencing error as strain presence. Moreover, because the false positive calls we detected tended to be sequencing run-specific (Table S2), their impact on PopMLST's accuracy could be decreased by repeated sequencing of samples.

Table 2. Frequency of false positive calls depending on criteria used to call MLST type presence.

Accuracy is shown as function of the abundance and number of loci used to make calls.

Abundance of loci used to call MLST type presence	*P. aeruginosa*		*S. aureus*	
	1 locus used to call MLST type presence	2 loci used to call MLST type presence	1 locus used to call MLST type presence	2 loci used to call MLST type presence
	# experiments with false positive (%)	# experiments with false positive (%)	# experiments with false positive (%))	# experiments with false positive (%)
5%	0/38 (0%)	0/38 (0%)	0/41 (0%)	0/41 (0%)
4%	0/38 (0%)	0/38 (0%)	0/41 (0%)	0/41 (0%)
3%	0/38 (0%)	0/38 (0%)	2/41 (5%)	0/41 (0%)
2%	3/38 (8%)	0/38 (0%)	5/41 (12%)	0/41 (0%)
1%	4/38 (11%)	0/38 (0%)	7/41 (17%)	0/41 (0%)
0.50%	5/38 (13%)	1/38 (3%)	7/41 (17%)	0/41 (0%)
0.25%	6/38 (16%)	1/38 (3%)	8/41 (20%)	0/41 (0%)
0.10%	9/38 (23%)	2/38 (5%)	10/41 (24%)	2/41 (5%)
0.01%	14/38 (37%)	7/38 (18%)	10/41 (24%)	2/41 (5%)
0%	14/38 (37%)	7/38 (18%)	10/41 (24%)	2/41 (5%)

PopMLST can detect specific MLST types with high sensitivity. In certain settings, clinicians and researchers need to detect specific strains with known MLST types. Examples include superinfections with virulent *Pa* epidemic strains in people with CF already colonized by *Pa*, or infection control surveillance during outbreaks. Theoretically, known MLST types should be detectable with higher sensitivity than unknown types, as it is extremely unlikely that the chance occurrence of errors would report the presence of the specific MLST loci of interest.

To test this, we measured PopMLST's sensitivity to detect targeted low abundance MLST alleles in complex mixtures. As shown in Table 3 and Table 4, targeted low abundance alleles were detected in all experiments when present at 5% relative abundance or greater, and in almost all experiments when present at 2%, 1% and 0.1% relative abundance. These findings suggest that PopMLST could be used for early detection of known strains with high transmissibility or virulence, or to investigate efficacy of infection control measures.

Table 3. PopMLST's sensitivity for detecting known *Sa* MLST types

% low abundance MLST type	MLST Loci: *arc* # times loci detected* (range)	*aro* # times loci detected* (range)	*glp* # times loci detected* (range)	*gmk* # times loci detected* (range)	*pta* # times loci detected* (range)	*tpi* # times loci detected* (range)	*yqi* # times loci detected* (range)
10%	4/4 (19.5-2.8)	4/4 (6.0-1.8)	4/4 (10.6-1.9)	4/4 (14.0-2.8)	4/4 (14.1-2.3)	4/4 (14.9-2.4)	4/4 (16.0-2.3)
5%	4/4 (5.3-3.8)	4/4 (3.2-1.6)	4/4 (6.1-1.8)	4/4 (5.2-2.7)	4/4 (4.6-3.0)	4/4 (5.5-3.4)	4/4 (4.7-3.9)
2%	4/4 (2.4-1.7)	4/4 (1.2-0.6)	4/4 (3.4-0.7)	4/4 (11.1-2.0)	3/4 (1.7-0)	4/4 (2.3-1.4)	3/4 (1.9-0)
1%	3/4 (2.2-0)	4/4 (1.1-0.1)	3/4 (1.5-0)	4/4 (1.5-0.2)	2/4 (1.4-0)	3/4 (1.5-0)	3/4 (2.0-0)
0.1%	2/3 (0.4-0)	3/3 (0.3-0.1)	2/3 (0.3-0)	3/3 (1.5-0.2)	0/3 (0-0)	3/3 (0.3-0.2)	1/3 (0.2-0)

* Each replicate experiment was performed three or four independent times. The number of replicate experiments analyzed is indicated by the denominator.

Table 4. PopMLST's sensitivity for detecting known *Pa* MLST types

% low abundance MLST type	MLST loci: *acs* # times loci detected* (range)		*gua* # times loci detected* (range)		*mut* # times loci detected* (range)		*nuo* # times loci detected* (range)		*pps* # times loci detected* (range)		*trp* # times loci detected* (range)	
10%	4/4	(13.5-6.2)	3/3	(24.8-4.1)	4/4	(14.9-6.9)	3/3	(13.3-8.2)	4/4	(14.8-3.9)	4/4	(15.2-6.0)
5%	3/3	(7.0-4.6)	2/2	(6.6-4.8)	3/3	(7.7-2.4)	1/2	(6.6-1)	3/3	(7.6-4.6)	3/3	(7.7-2.8)
2%	3/3	(3.18-1.7)	2/2	(2.3-2.1)	3/3	(3.2-1.4)	2/2	(2.8-1.9)	3/3	(4.2-1.7)	3/3	(3.5-2.0)
1%	4/4	(1.6-0.7)	3/3	(4.0-0.4)	4/4	(2.1-0.7)	3/3	(1.6-1.1)	4/4	(2.7-0.5)	4/4	(1.8-0.7)
0.1%	3/3	(0.3-0.1)	2/3	(0.5-0)	3/3	(0.1-0.06)	1/3	(0.4-0)	3/3	(0.3-0.08)	3/3	(0.2-0.08)

* Each replicate experiment was performed three or four independent times. The number of replicate experiments analyzed is indicated by the denominator. Two of the strains used for in one replicate experiment (for the 10%, 5%, 2%, and 1% low abundance MLST type) shared alleles for the *gua* and *nuo* loci, because the two strains could not be differentiated at these loci, they were eliminated from analysis for these loci thereby decreasing the denominator only at the *gua* and *nuo* loci.

PopMLST works in the presence of excess human or non-target bacterial DNA. Clinical samples can contain vast amounts of human and non-target bacterial DNA. For example, despite high pathogen density (*Pa* can reach 10^8-10^9 CFU/ml in CF sputum), 95-99% of CF sputum DNA is human (178), and DNA from other pathogens or oral bacteria can also be highly abundant.

We investigated the effects of contaminating DNA on PopMLST two ways. First, we performed PCR on human and non-target bacterial DNA (including closely related species) using *Sa* and *Pa* PopMLST primers. Amplicon yields and the number of reads mapped to *Sa* and *Pa* MLST loci in these experiments were similar to no-template controls (Figure 5 A-D). Second, we tested the ability of PopMLST to detect strains in the presence of 95% human DNA, and found that the vast excess of human DNA did not compromise detection, even when strains were present at as low as 1% relative abundance (Figure 5E and F).

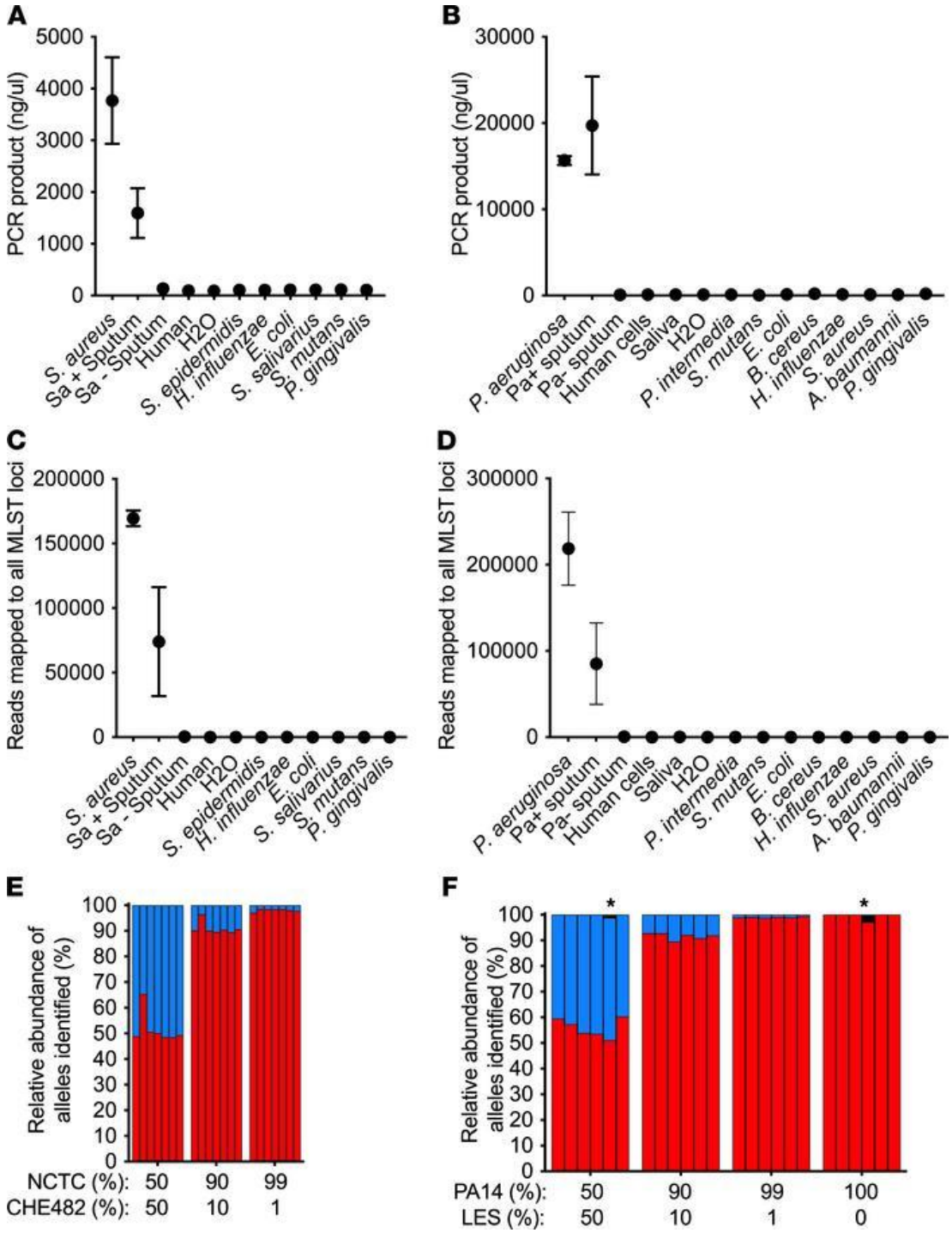

Figure 5. Heterologous DNA does not interfere with PopMLST. (A and B) The average concentration of PCR product from the seven or six amplified loci after PCR using PopMLST primers for *Sa* **(A)** and *Pa* **(B)** on DNA from the indicated sources. 'Human' indicates DNA extracted from tissue culture cells; 'H2O' indicates ultrapure water; '*Sa*+ sputum' and '*Pa*+ sputum' indicates sputum from three CF subjects

culture-positive for *Sa* and *Pa* respectively; and '*Sa*- sputum' and '*Pa*- sputum' indicates sputum from a CF subject culture-negative for *Sa* and *Pa* respectively. **(C and D)** The sum of sequence reads produced by PopMLST that mapped to seven *Sa* **(C)** or six *Pa* **(D)** MLST loci are shown for samples containing target and non-target DNA from PCR reactions shown in A and B. Mixtures of *Sa* NCTC8325/CHE482 were used as positive control in A and C, and mixtures of PA14/PAO1 were used in B and D. For samples with negligible PCR amplification, >2X volume of sample was used for Illumina sequencing than was used for other samples The average and SEM of 3 separate samples are shown for *Sa*, *Sa*+ sputum, *Pa*, and *Pa*+ sputum in A and D. **(E and F)** 95% human DNA from tissue culture cells was added to the same mixtures of two control strains from Figure 2C. Bars in **(E)** show relative abundance of *arc, aro, glp, gmk, pta, tpi,* and *yqi* matching the MLST type of NCTC8325 (red) or CHE482 (blue). Bars in (**F**)show relative abundance of *acs, gua, mut, nuo, pps,* and *trp* (in order) matching the MLST type of PA14 (red) or LES (blue). * indicates the presence of an unexpected loci type (black), likely due to sequencing error.

PopMLST measures strain abundance in clinical samples. Encouraging results with experimental strain mixtures led us to perform proof-of-principle tests of PopMLST on clinical samples. In the first test, we cultured sputum from seven *Sa*-infected CF subjects, and performed PopMLST on DNA prepared from ~100 colonies that grew from each sample (scraped *en masse* from culture plates). PopMLST reported that three of seven samples contained two *Sa* MLST types (Figures 6A and S4, Table S3). We verified the presence of two strains in these samples by Sanger sequencing a distinguishing MLST locus in 20-30 individual colonies from each sample, and found MLST types at a similar relative abundance as that determined by PopMLST (R^2 = 0.9247; slope = 0.9296 [95% CI: 0.5612-1.298]) (Figure 6A-B).

Second, we tested PopMLST's ability to resolve strains in CF sputum by mixing sputum samples that each contained a single strain as determined by PopMLST (>99% of reads from each loci reporting a single allele) at varying ratios. When samples were combined, MLST types were identified close to the expected ratios (Figure 6C, Table S1).

Finally, we analyzed sputum samples from 5 subjects that were all known to harbor two *Sa* strains each. We performed PopMLST on DNA prepared directly from sputum and from several hundred *Sa* isolates from each sample scraped *en masse* from culture plates. As shown in Figure 6D, PopMLST detected the same MLST loci types in sputum DNA and culture scrapes from all 5 subjects. Conventional MLST typing of representative isolates confirmed the dominant and secondary sequence types detected by PopMLST (6D and Table S3). In subjects 11 and 12, strain relative abundance differed in sputum as compared to the culture scrapes ($p < 0.001$ by multiple t-test), and in subject 9 a third MLST locus type was detected in sputum that was not present in *ex vivo* culture. These findings could be due to differential growth capacity of strains in *ex vivo* culture conditions.

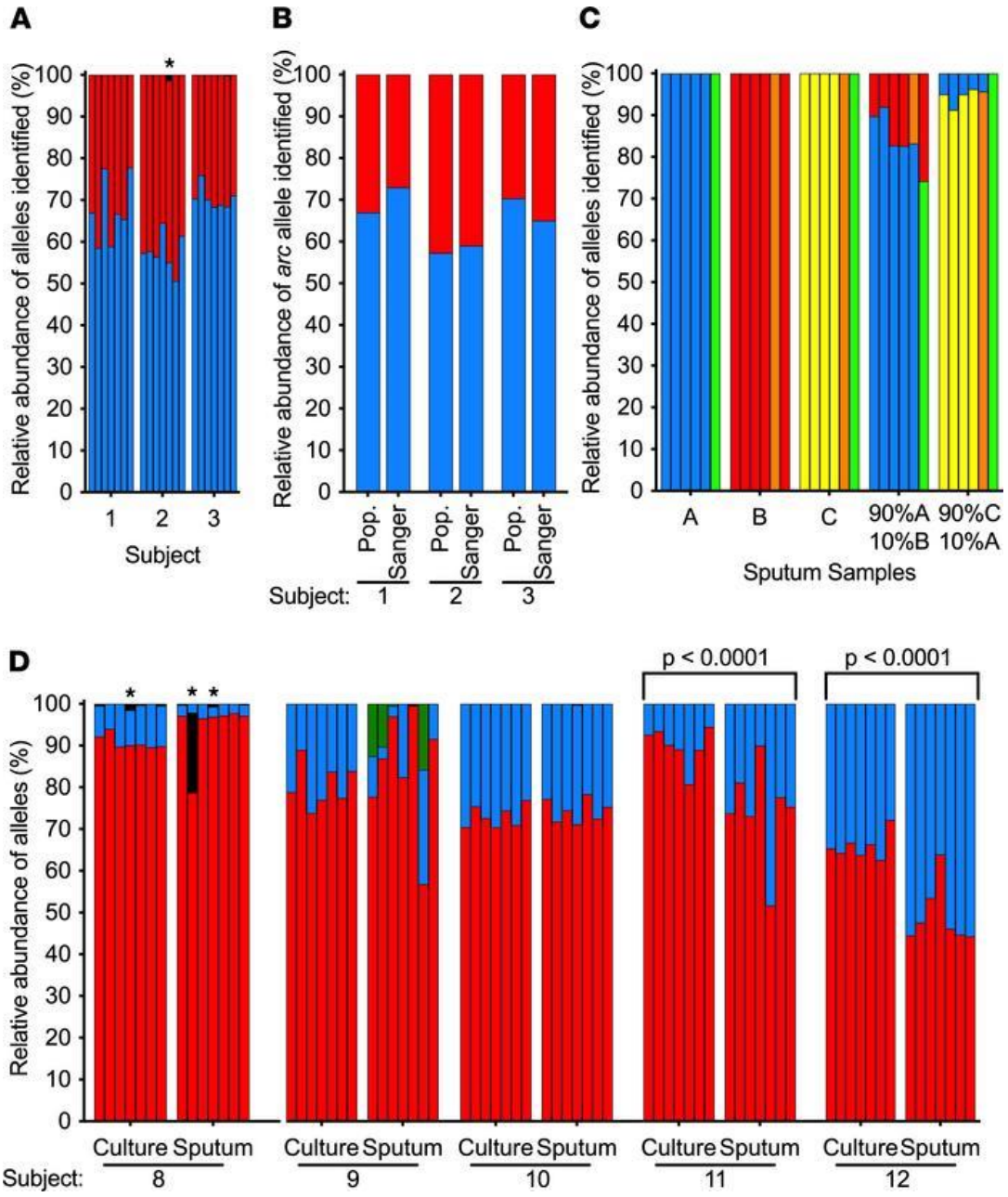

Figure 6. PopMLST on clinical samples. **(A and B)**. PopMLST results from 3 of 7 CF subjects in whom PopMLST detected 2 *Sa* strains (see Fig S4 for the 4 of 7 subjects in whom one strain was detected). **(A)** PopMLST results from DNA pooled from 90-95 cultured *Sa* isolates. Blue and red bars indicate different MLST loci alleles for each subject (Table S3). Bars for each sample show relative abundance of *arc, aro, glp, gmk, pta, tpi,* and *yqi*. A third *pta* allele (black bar and indicated with *) differed at a single nucleotide from the allele indicated in red, likely representing sequencing error or mutation. (**B**). Relative abundance of *arc* locus as measured by PopMLST (Pop) and by individually Sanger sequencing (Sanger) 20-30

isolates from each sample from **(A)**. **(C)** PopMLST performed directly on DNA isolated from 3 sputum samples (A, B, C) and from mixtures of these samples. Red, blue, and yellow bars indicate the abundance of MLST alleles corresponding to sample A, B, and C respectively, green bars indicate an allele shared between A and C and orange bars indicate an allele shared between B and C (see Table S1). Control experiments examining >100 *Pa* isolates cultured from sputum A, B, and C showed each contained a single *Pa* MLST type. **(D)** PopMLST of DNA pooled from >100 *Sa* cultured colonies (culture) and directly from sputum (sputum). Red and blue indicate different MLST types, which were confirmed by Sanger sequencing individual isolates (Table S1). Subject 9's sputum contained three loci from an additional allele, likely indicating a third MLST type (green) that was not detected in culture. Indicated significant differences were determined by the multiple t-test of minor allele abundance. Black bar indicated with * indicates the presence of a third allele, likely due to mutation or sequencing error.

Discussion

Infecting bacteria can exhibit heritable diversity at the species, strain, and intra-strain level. While recent findings and new methods have accelerated work on species diversity (179–187) and diversification within individual strains (92, 134, 148–150, 175, 176), studies of strain-level diversity have lagged. A major factor limiting progress is that established methods to detect strains must generally be performed on one cultured isolate at a time (140, 156–159). Thus, non-dominant strains are difficult to detect.

PopMLST addresses this problem, as it can estimate the relative abundance of strains in pools of tens to hundreds of isolates that have been cultured *en masse* from infected sites, and can be used on DNA extracted directly from clinical specimens without prior culture. Other advantages include technical approaches to minimize PCR and sequencing error, its robustness when human or other bacterial DNA is in vast excess (Figure 5), its ability to detect targeted strains at low relative abundance (Table 3 and 4), and a capacity to detect strains with *ex vivo* growth defects when the method is used on DNA prepared directly from clinical specimens. Furthermore, the method is accurate even when intra-strain genetic diversity has evolved (Figure 2, Table S1), likely because MLST loci are within conserved “housekeeping” genes that may be less variable than elements involved in Spa typing (131), RAPD (random amplified polymorphic DNA), or PFGE (140, 156). Finally, MLST databases are in widespread use and exist for over 100 bacterial species (170), so PopMLST can be easily be adapted for use for many organisms and results are comparable between laboratories.

PopMLST also has limitations. First, several circumstance can limit PopMLST’s ability to enumerate and identify strains. These include the presence of unrelated strains having the same MLST sequence type, *Pa* strain mixtures in which the *aro* locus is the only distinguishing locus (see Figure S1), strain mixtures in which most MLST alleles are shared between strains, or cases where evolved diversity substantially alters MLST loci. However, these circumstances will be relatively rare as many MLST types have been identified for most pathogens. For example, ~3,500 *Pa* and ~ 5,500 *Sa* MLST types have been described to date (170), so strain distinguishing power is generally robust. Moreover, MLST loci are generally

conserved, and our control experiments showed PopMLST remained accurately identified mutator strains that had genetically diversified (Figure 2) *in vivo*.

Second, while PCR and Illumina sequencing enable the method to be used on complex mixtures containing multiple strains and abundant non-target DNA, these techniques are subject to errors and biases. We reduce, but cannot entirely eliminate, the effect of these problems using replicate PCR, adaptive trimming, and statistical methods.

Third, PopMLST does not identify which MLST loci are linked in individual isolates. While this limitation does not compromise strain enumeration and relative abundance measurements under most circumstances, it can complicate identification of the strain types present in complex mixtures. Finally, we have not yet performed head-to-head test comparing PopMLST's resolution with other available methods for strain enumeration.

Despite these limitations, we think that PopMLST could provide useful strain-level information. One key area is in infection control, as PopMLST's ability to detect strains of interest at low relative abundance improves on existing methods, particularly in settings where the strain being tracked belongs to a commonly encountered species. PopMLST performed serially on clinical samples could also detect episodes of strain gain or loss in individual patients. Strain changes could herald important variation in the host environment (e.g changes in host defenses or treatment that select for new strains), or mutational changes in existing strains that compromise strain persistence *in vivo*. An additional advantage is that PopMLST can detect strains with *ex vivo* growth defects.

PopMLST could also be used for early detection of superinfections with highly virulent or antibiotic resistant strains. A notorious example is the Liverpool Epidemic *Pa* strain, which can displace existing *Pa* strains that infect the lungs of people with CF, and cause increased morbidity and treatment resistance (188). Since discovery of the Liverpool strain, other epidemic strains have been identified at disparate locations worldwide (147). Early detection of such strains is difficult in already-colonized subjects as

clinical microbiology analyses only report the species present, and detecting epidemic strains when they are at low relative abundance would require tests on tens or hundreds of cultured isolates using conventional colony-by-colony assays (like MLST).

Finally, PopMLST could be used to investigate strain changes not associated with epidemic strains. Patients with chronic bacterial infections frequently experience highly variable disease manifestations, antibiotic responses, and rates of progression. The acquisition of different strains of a given species or changes in strain relative abundance could account for some of this variation (189). PopMLST will enable new hypotheses that explore the effects of strain-level diversity on human infection to be tested.

Methods

Patient samples. *Sa* was isolated after sputolysin diluted sputum was cultured on Mannitol Salts Agar (Difco). Populations were scraped from plates containing >100 colonies by flooding the plate with 2 ml of LB and using a L-spreader to resuspend the bacteria. *Pa* was isolated after sputolysin diluted sputum was cultured on MacConkey (Difco). All cultures were stored at -80^{o}C in 15% glycerol prior to analysis. Sputum samples analyzed directly were diluted with sputolysin as above and stored at -80^{o}C until DNA isolation could be performed.

DNA isolation. *Pa* DNA was isolated from 100 ul of resuspended culture using the DNeasy Blood and Tissue kit (Qiagen) using the protocol for gram-negative bacteria. Due to the difficulty of lysing gram-positive bacteria, all *Sa* and sputum samples were extracted using methods with increased lysis efficacy. DNA extraction of *Sa* and sputum samples was performed using the DNeasy Power Soil Kit (Qiagen) with the following modifications: samples were incubated with 2.9 mg lysozyme and 0.14mg lysostaphin prior to lysis with 0.1 mm beads using bead beater (Mini-Beadbeater-16; Biospec), a method validated previously by our laboratory for efficient *Pa* and *Sa* lysis from sputum (164); or using the DNeasy Powersoil Pro kit for Qiacube automated extraction system (Qiacube) which results in comparable lysis of *Sa* and *Pa* from sputum in our laboratory. Lysis method used depended on availability of the extraction method at time of sample collection. All samples were eluted in EB buffer (Qiagen) regardless of extraction method.

Control mixtures. Control strains (Table S4 and Table S5) were streaked from freezer stocks and grown overnight prior to DNA isolation. *Sa* and *Pa* strains were from the Singh lab as well as donated by Matthew Parsek (University of Washington, Seattle, WA) and Lucas Hoffman (University of Washington, Seattle, WA). Cultured HELA or HEK293 cells (donated by Joseph Mougous, University of Washington, Seattle, WA) were pelleted and DNA was isolated as above. Isolated DNA was quantified by Qubit and mixed at ratios described in the figures. MLST types of control strains were based on the MLST database and confirmed by MLST typing of single isolates if necessary (Table S4 and Table S5). PAO1-lacZ:PA14

mixtures were pre-mixed at designated ratios and plated on LB+xGal to confirm the ratio. Growth from the plate was scraped and subjected to DNA isolation as above.

PopMLST amplification and sequencing methods. 5 ng/ul DNA from cultured bacteria, 20 ng/ul of sputum DNA, or 20 ng/ul of bacterial DNA mixed with human DNA was amplified by PCR using published MLST primers for *Sa* and *Pa* (168, 169) with Illumina adapters on the 5' ends to enable next generation sequencing of MLST loci (Table S6). PCR amplification of each of the seven MLST loci was performed in triplicate to reduce chances of random PCR bias using reagents listed in Table S7. Triplicate reactions were pooled after PCR and amplified DNA was visualized by agarose gel electrophoresis and quantified by Pico green (Thermo Fisher). After cleaning with Ampure beads (Beckman Coulter), the seven MLST loci for each sample were pooled in equimolar amounts and barcoded with Illumina Nextera XT indexes. PCR amplification, indexing, and cleanup was performed as described in the 16S Metagenomic Sequencing Library Preparation guide (Illumina). Indexed MLST loci were cleaned with Ampure beads (Beckman Coulter) prior to pooling and sequenced on the Illumina MiSeq to produce 2 x 300 bp paired-end reads.

Bioinformatic analysis. Methods outlined below for PopMLST are available at https://github.com/marade/PopMLST (commit ID 0de7f83). Because DADA2 is designed for one amplicon locus (typically 16S) at a time, reads were deconvolved based on their locus-specific primer sequence using Python tre, with approximate matching to MLST loci allowing for up to a 25% mismatch (https://github.com/laurikari/tre/) prior to analysis. Due to a significant number of paired-end reads failing to merge for some loci, we developed a dynamic read-trimming method using a binary search algorithm which iteratively trims the 3' end of the reverse read and re-tests merging until it maximizes the number of merged reads of the correct size. Trimmed reads for all MLST loci, except *yqi*, were merged using VSEARCH 2.13.4 fastq_mergepairs. Two basepairs of the sequence in the *yqi* locus beyond the 3' ends of read 1 and 2 (due to the length of this amplicon) were artificially supplied (these bases are conserved according to the MLST database (170)). *yqi* reads were joined using VSEARCH 2.13.4 fastq_join. Merged

reads, with their adaptors trimmed using Cutadapt 2.3, were then processed using the remaining DADA2 pipeline steps to generate amplicon sequence variants (ASVs) for each locus.

To determine the identity and quantify the relative abundance of each MLST locus, the ASVs were queried against the PubMLST database (https://pubmlst.org/saureus/ and https://pubmlst.org/paeruginosa/) (170) for the appropriate species using BLAST+ BLASTN (190). The matching sequence with the highest identity and longest length (less than or equal to the maximum locus length present in the database) was used to label each ASV by locus type, with less than 100% identity matches being marked as potential novel alleles. The resulting output table includes each MLST loci type identified, the ASV, and the number of reads assigned to each type, much like a classic 16S operational taxonomic unit table.

Statistics. The abundance of MLST types was reported as the average relative abundance of 7 corresponding *Sa* MLST loci or 6 corresponding *Pa* MLST loci, and standard error of the mean was reported. When strain type(s) were known (Figures 2 and 3 and Table 1), the relative abundances of the alleles matching that strain type were used. When strain types were unknown, alleles with similar relative abundances were assumed to be from the same strain. Linear regression of the average relative abundance was used to determine the accuracy of measuring strain abundance (Figure 3, B and D). R^2 values were reported in text. Multiple t tests were used to compare relative abundance of individual loci from sputum with those from bacterial culture (Figure 6D). P values more than 0.05 were determined to be not significant and were not reported. All statistical analyses were performed in GraphPad Prism.

Study approval. Sputum samples were collected in accordance with University of Washington Institutional Review Board (protocols numbers 06-4469 and STUDY00011983), and the Research Ethics Committee, St. Vincent's Hospital, Dublin, Ireland (RS20-048). Patients provided written informed consent prior to collection of samples.

Supplemental information

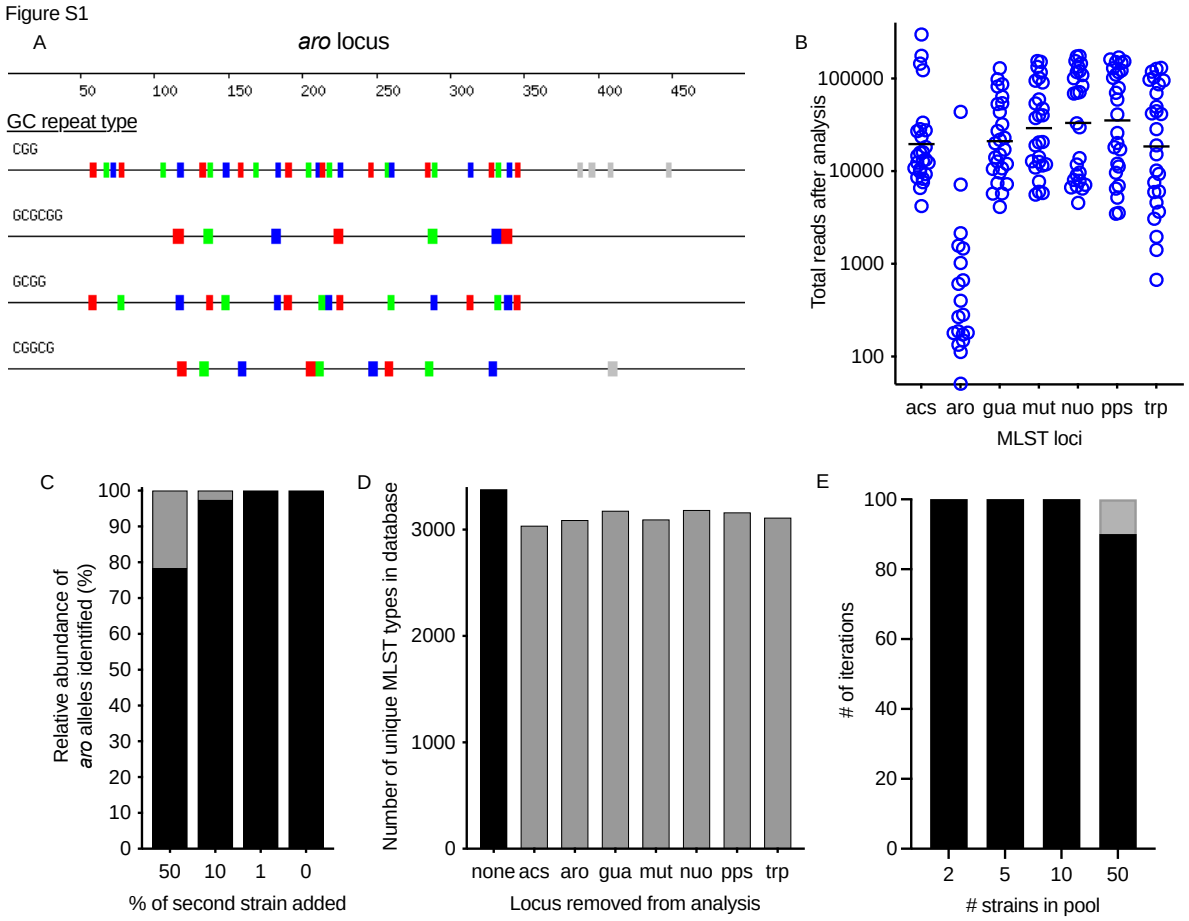

Figure S1. *Pa aro* MLST loci are underrepresented by PopMLST. A. Schematic representation of high GC repeats in the *aro* MLST locus with each box showing the location of repeats identified by Geneious Prime 2020.1.1 (https://www.geneious.com). **B.** The number of reads recovered from *aro* are more than a log lower than other loci despite four-times higher levels of DNA used as input for Illumina sequencing. **C.** Despite the low number of reads as shown in B, the *aro* reads detected were in ratios are similar to the expected ratios of the strains and the ratios of the other loci shown in Figure 3C. **D.** Analysis of the 3391 MLST types in the *Pa* MLST database shows that omitting any one of the seven MSLT loci (indicated on the x-axis) still enables most MLST types to be identified. The number of unique combinations of MLST allele types when all seven alleles were utilized is indicated in black. The alleles for a given locus were removed and the analysis for unique combinations of allele types using the remaining six loci were determined (grey bars). **E.** Sets of two, five, ten, or 50 MLST types were randomly selected from the

MLST database (https://pubmlst.org/organisms/pseudomonas-aeruginosa/) and assessed to determine if the variation in the other six loci was sufficient to distinguish between the strains in the set. This analysis was repeated 100 times. Sets for which all MLST types could be distinguished without *aro* are shown in black. Sets for which *aro* was required for differentiation between MLST types in the set are in grey.

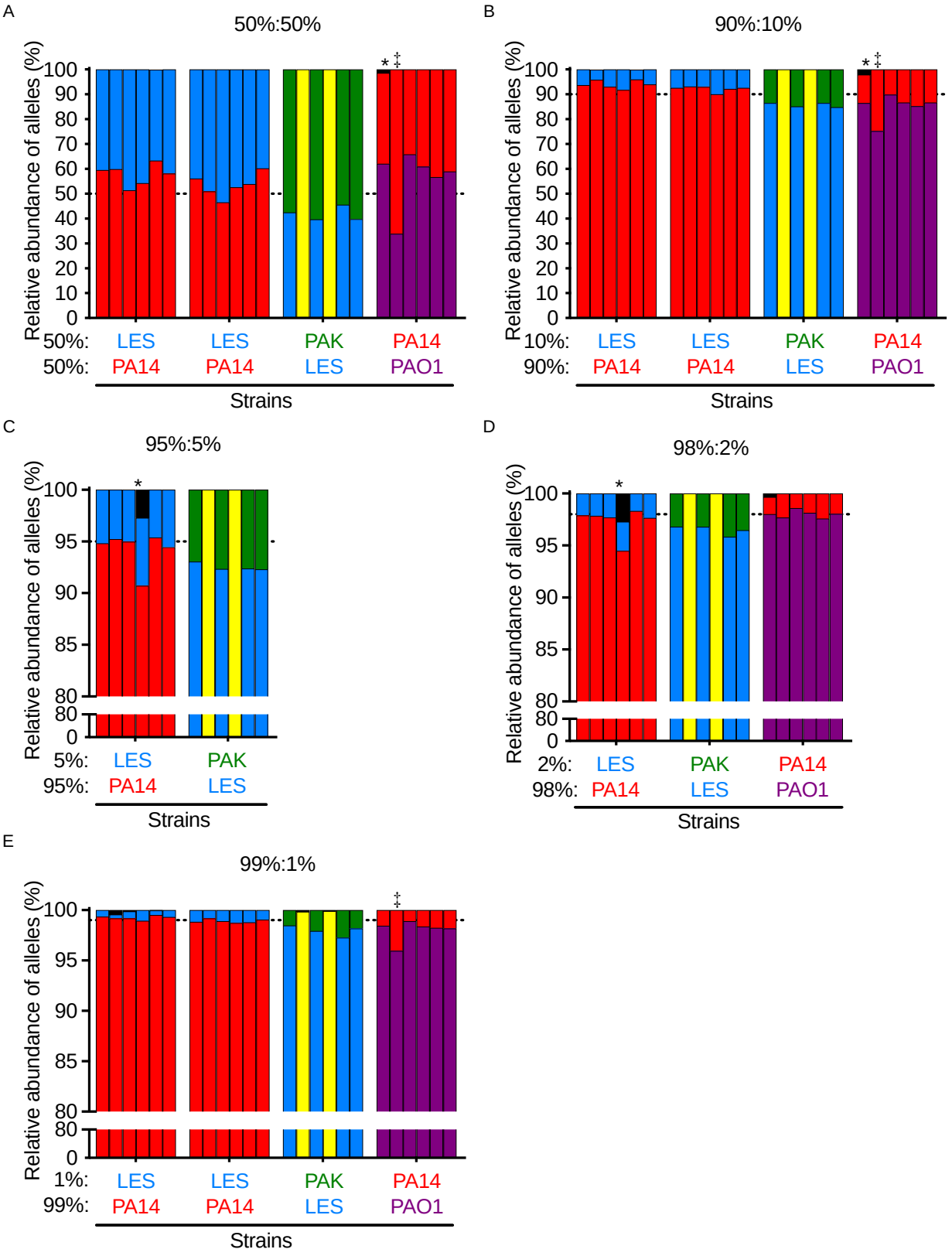
A
50%:50%
Relative abundance of alleles (%)
100
90
80
70
60
50
40
30
20
10
0
* ‡
50%: LES LES PAK PA14
50%: PA14 PA14 LES PAO1
Strains
B
90%:10%
Relative abundance of alleles (%)
* ‡
10%: LES LES PAK PA14
90%: PA14 PA14 LES PAO1
Strains
C
95%:5%
Relative abundance of alleles (%)
100
95
90
85
80
80
0
*
5%: LES PAK
95%: PA14 LES
Strains
D
98%:2%
Relative abundance of alleles (%)
*
2%: LES PAK PA14
98%: PA14 LES PAO1
Strains
E
99%:1%
Relative abundance of alleles (%)
‡
1%: LES LES PAK PA14
99%: PA14 PA14 LES PAO1
Strains

Figure S2. PopMLST on mixtures of *Pa* laboratory strains reproducibly identifies the relative abundance of each strain. We tested pairwise combinations of four *Pa* strains with different MLST types across a range of ratios. In all cases, the two strains were identified in ratios close to expected. Each strain is represented by a different color (PAO1=purple, PA14=blue, LES=red, and PAK=green). PA14 and PAK have the same sequence for two loci indicated in yellow. PopMLST was performed on mixtures of cultured colonies for the PAO1:LES experiments, all others were performed on mixtures of DNA. Each set of bars represents an independent experiment. MLST alleles identified but not present in the mixtures, likely due to sequencing error, are indicated in black and those detected at >1%, are indicated with *. ‡ indicates PCR bias as evidenced by one allele being consistently under or overrepresented.

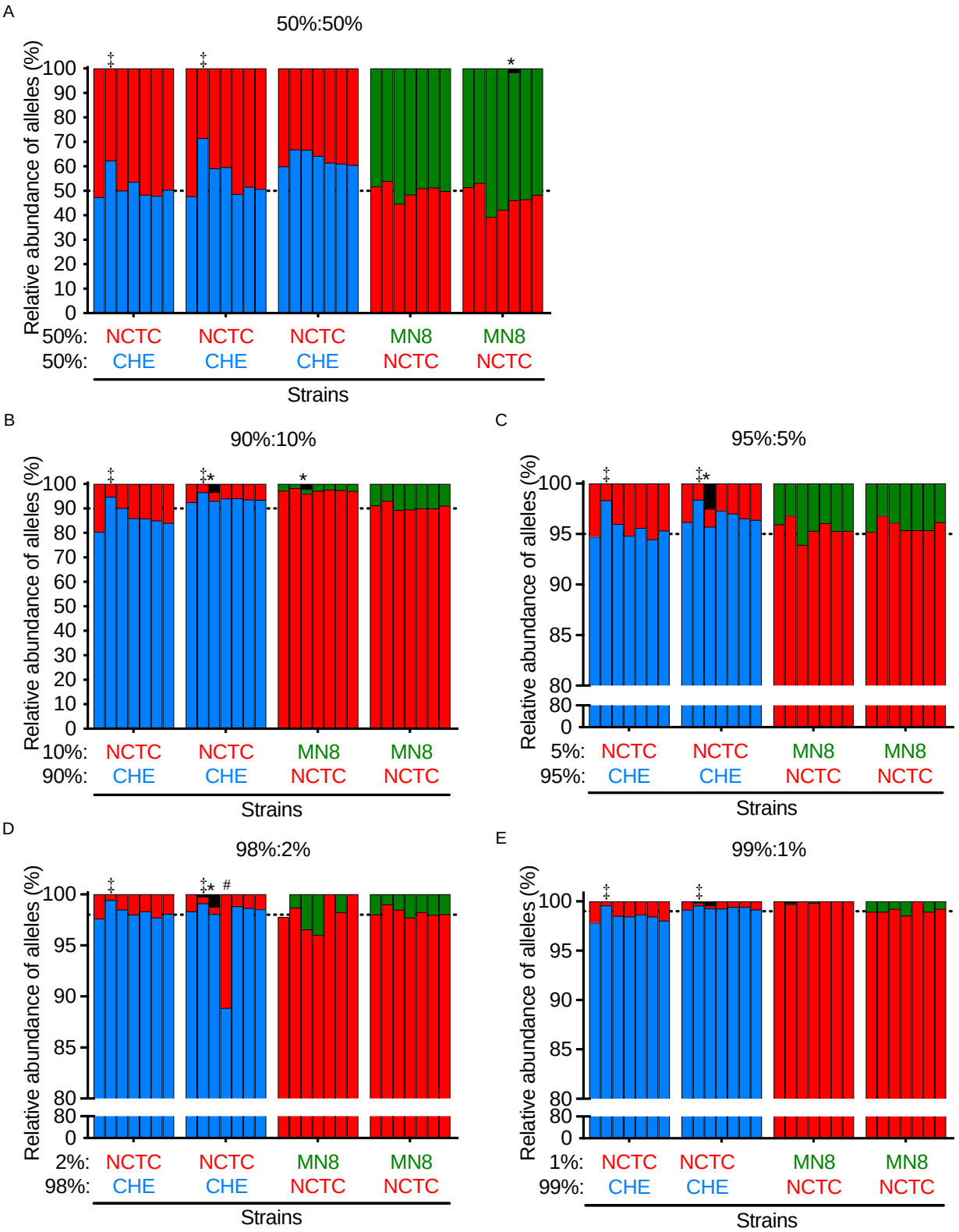
A
50%:50%
Relative abundance of alleles (%)
100
90
80
70
60
50
40
30
20
10
0
50%:
50%:
NCTC
CHE
NCTC
CHE
NCTC
CHE
MN8
NCTC
MN8
NCTC
Strains
B
90%:10%
Relative abundance of alleles (%)
10%:
90%:
NCTC
CHE
NCTC
CHE
MN8
NCTC
MN8
NCTC
Strains
C
95%:5%
Relative abundance of alleles (%)
95
85
80
5%:
95%:
NCTC
CHE
NCTC
CHE
MN8
NCTC
MN8
NCTC
Strains
D
98%:2%
Relative abundance of alleles (%)
2%:
98%:
NCTC
CHE
NCTC
CHE
MN8
NCTC
MN8
NCTC
Strains
E
99%:1%
Relative abundance of alleles (%)
1%:
99%:
NCTC
CHE
NCTC
CHE
MN8
NCTC
MN8
NCTC
Strains

Figure S3. PopMLST on mixtures of *Sa* laboratory strains reproducibly identifies the relative abundance of each strain. We tested pairwise combinations of three *Sa* strains with ratios close to expected. Each strain is represented by a different color (NCTC8325=red, CHE=blue, MN8=green). Each set of bars represents an independent experiment. Black indicates the presence of a third allele. MLST alleles identified but not present in the mixtures, likely due to sequencing error, are indicated in black and those detected at >1%, are indicated with *. ‡ indicates PCR bias as evidenced by one allele being consistently under or overrepresented. # indicates non-systemic under/over representation of an allele, possibly due to jackpot amplifications.

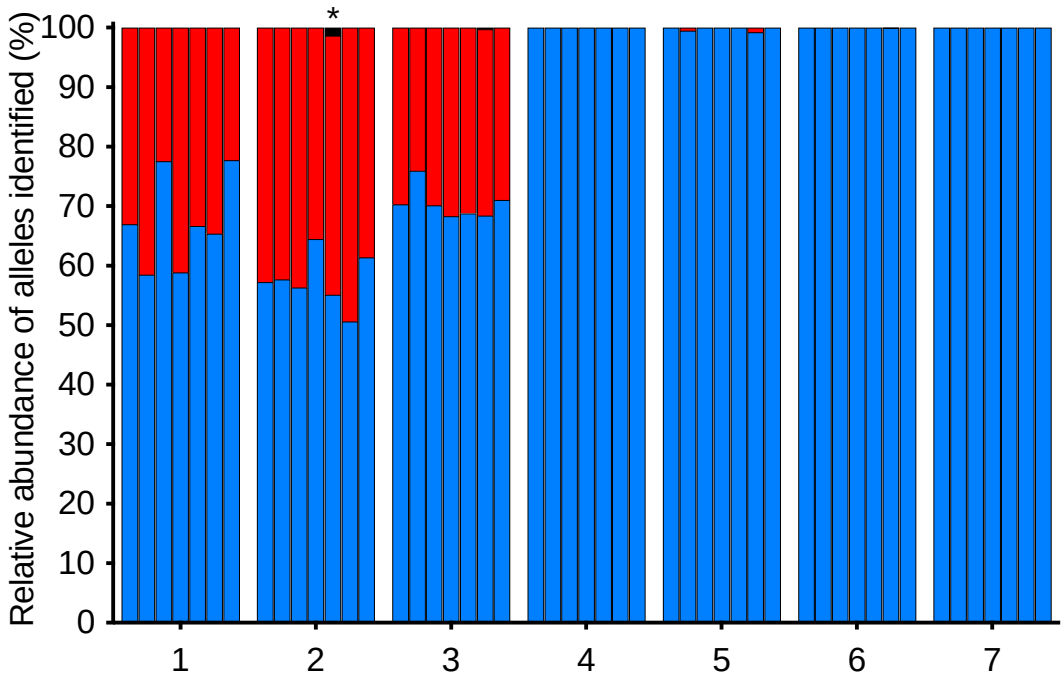

Figure S4. Detection of multiple MLST loci types from isolates from sputum. ~95 *Sa* isolates cultured on MSA from sputum were selected from each subject. Growth from all ~95 isolates was pooled and PopMLST performed. Blue indicates the predominant MLST loci type by abundance, and red indicates any secondary alleles detected. Subjects 1-3 are shown in figure 6. Bars for each sample show relative abundance for *arc, aro, glp, gmk, pta, tpi,* and *yqi* (in order). * indicates an additional MSLT type detected, with a single SNP, likely due to sequencing error.

Table S1. *Pa* clinical sample MLST types.

subject [a]	*acs*	*gua*	*mut*	*nuo*	*pps*	*trp*
1	36	28	3	4	13	7
2	6	5	3	4*	15	7
3	28	22	18*	3	15	7
A	11	1	7	9	4	7
B	17	5	3	4	15	26
C	28	22	18	3	15	7

[a] Subject number corresponds to subjects in Figures 2 and 6C

* Number indicated is the closest allele type to loci alleles in the MLST database

Table S2. False positive detection of MLST loci is eliminated if PopMLST is repeated. Sequencing errors leading to false-positive calls of a *Sa* or *Pa* MLST locus (i.e calling a locus not present in the experimental mixture) were not detected when PopMLST was repeated a second and third time.

			Proportion of samples in which false positive locus was detected (at > 1%).		
Strain mixtures tested	Expected loci type	False loci type detected (at > 1%)	In run that false positive was detected	In repeat sequencing run #1	In repeat sequencing run #2
Sa NCTC+ *Sa* CHE	glp_8 glp_1	glp_23	3/7	0/5	0/2
Sa MN8 + *Sa* NCTC	glp_1 glp_2	glp_6x	1/5	0/6	0/2
	pta_4 pta_6	pta_495	3/5	0/6	0/2
Pa PA14+ *Pa* LES	nuo_1 nuo_4	nuo_23	2/5	0/4	0/3

* Mixtures of the same two strains at any ratio were grouped for this analysis.

Table S3. *Sa* clinical sample MLST types.

subject [a]	*arc*	*aro*	*glp*	*gmk*	*pta*	*tpi*	*yqi*	MLST[b]
1	3	35	19	2	20	26	39	398
	1	1	1	1	1	1	1	1
2	2	2	2	2	6	3	2	30
	3	3	1	1	1	1	10	9
3	2	2	2	2	2	2	2	39
4	2	2	2	2	6	3	2	30
	5	4	1	4	4	6	3	7
5	13	13	1	1	12	11	13	15
6	10	14	8	6	10	3	2	45
7	4	1	4	1	5	5	4	25
8	3	3	1	1	4	4	3	8
	2	2	2	2	6	3	2	30
9	1	4	1	4	12	1	10	5
	2*	2	2	2	6	3	2	-
10	1	4	1	4	12	1	10	5
	10	14	8	6	10	37	2	256
11	1	4	1	4	6	1	10	-
	2	2	2	2	12	3	10	-
12	10	14	8	6	10	3	2	45
	1	4	1	4	12	1	28	105

[a] Subject number corresponds to subjects in Figures 6A, 6D, and S4.

[b] When two strains are present, MLST type determined by relative abundance of alleles and confirmed by sanger sequencing of individual isolates. – indicates this MLST type is not in the database.

* number indicated is the closest allele type to loci alleles in the MLST database

Table S4. *Sa* strains and MLST types

Strain	*arc*	*aro*	*glp*	*gmk*	*pta*	*tpi*	*yqi*	MLST type
NCTC8325	3	3	1	1	4	4	3	8
CHE482	10	14	8	6	10	3	2	45
MN8	2	2	2	2	6	3	2	30
CF*	13	13	1	1	12	11	13	15

* Clinical isolate from patient with Cystic Fibrosis

Table S5. *Pa* strains and MLST types

Strain	acs	aro	gua	mut	nuo	pps	trp	MLST type
PA14	4	4	16	12	1	6	3	253
LES	6	5	11	3	4	23	1	146
PAO1	7	5	12	3	4	1	7	549
PAK	11	5	11	11	4	4	14	693
CF5*	28	5	30	3	3	4	14	1538
CF6*	40	5	11	5	4	38	37	167
CF2*	11	76	5	3	61	14	3	485

* Clinical isolate from patient with Cystic Fibrosis

Table S6. Primers used for PopMLST

MLST loci	Published MLST primer	PopMLST primer
SaarcF	TTGATTCACCAGCGCGTATTGTC	TCGTCGGCAGCGTCAGATGTGTATAAGAGACAGCCGTTGATTCACCAGCGCGTATTGTC
SaarcR	AGGTATCTGCTTCAATCAGCG	GTCTCGTGGGCTCGGAGATGTGTATAAGAGACAGGCTAGGTATCTGCTTCAATCAGCG
SaaroF	ATCGGAAATCCTATTTCACATTC	TCGTCGGCAGCGTCAGATGTGTATAAGAGACAGCCGATCGGAAATCCTATTTCACATTC
SaaroR	GGTGTTGTATTAATAACGATATC	GTCTCGTGGGCTCGGAGATGTGTATAAGAGACAGGCTGGTGTTGTATTAATAACGATATC
SaglpF	CTAGGAACTGCAATCTTAATCC	TCGTCGGCAGCGTCAGATGTGTATAAGAGACAGCCGCTAGGAACTGCAATCTTAATCC
SaglpR	TGGTAAAATCGCATGTCCAATTC	GTCTCGTGGGCTCGGAGATGTGTATAAGAGACAGGCTTGGTAAAATCGCATGTCCAATTC
SagmkF	ATCGTTTTATCGGGACCATC	TCGTCGGCAGCGTCAGATGTGTATAAGAGACAGCCGATCGTTTTATCGGGACCATC
SagmkR	TCATTAACTACAACGTAATCGTA	GTCTCGTGGGCTCGGAGATGTGTATAAGAGACAGGCTTCATTAACTACAACGTAATCGTA
SaptaF	GTTAAAATCGTATTACCTGAAGG	TCGTCGGCAGCGTCAGATGTGTATAAGAGACAGCCGGTTAAAATCGTATTACCTGAAGG
SaptaR	GACCCTTTTGTTGAAAAGCTTAA	GTCTCGTGGGCTCGGAGATGTGTATAAGAGACAGGCTGACCCTTTTGTTGAAAAGCTTAA
SatpiF	TCGTTCATTCTGAACGTCGTGAA	TCGTCGGCAGCGTCAGATGTGTATAAGAGACAGCCGTCGTTCATTCTGAACGTCGTGAA
SatpiR	TTTGCACCTTCTAACAATTGTAC	GTCTCGTGGGCTCGGAGATGTGTATAAGAGACAGGCTTTTGCACCTTCTAACAATTGTAC
SayqiF	CAGCATACAGGACACCTATTGGC	TCGTCGGCAGCGTCAGATGTGTATAAGAGACAGCCGCAGCATACAGGACACCTATTGGC
SayqiR	CGTTGAGGAATCGATACTGGAAC	GTCTCGTGGGCTCGGAGATGTGTATAAGAGACAGGCTCGTTGAGGAATCGATACTGGAAC
PaacsF	GCCACACCTACATCGTCTAT	TCGTCGGCAGCGTCAGATGTGTATAAGAGACAGCCGGCCACACCTACATCGTCTAT
PaacsR	AGGTTGCCGAGGTTGTCCAC	GTCTCGTGGGCTCGGAGATGTGTATAAGAGACAGAGGTTGCCGAGGTTGTCCAC
PaaroF	ATGTCACCGTGCCGTTCAAG	TCGTCGGCAGCGTCAGATGTGTATAAGAGACAGCCAATGTCACCGTGCCGTTCAAG
PaaroR	GTTCCTTGGCTGACGGAAGT	GTCTCGTGGGCTCGGAGATGTGTATAAGAGACAGGGTTGAAGGCAGTCGGTTCCTTG
PaguaF	AGGTCGGTTCCTCCAAGGTC	TCGTCGGCAGCGTCAGATGTGTATAAGAGACAGCCAGGTCGGTTCCTCCAAGGTC
PaguaR	GACGTTGTGGTGCGACTTGA	GTCTCGTGGGCTCGGAGATGTGTATAAGAGACAGCGACGTTGTGGTGCGACTTGA
PamutF	AGAAGACCGAGTTCGACCAT	TCGTCGGCAGCGTCAGATGTGTATAAGAGACAGCCGAGAAGACCGAGTTCGACCAT
PamutR	GGTGCCATAGAGGAAGTCAT	GTCTCGTGGGCTCGGAGATGTGTATAAGAGACAGGCAGGGTGCCATAGAGGAAGTCAT

PanuoF	ACGGCGAGAACGAGGACTAC	TCGTCGGCAGCGTCAGATGTGTATAAGAGACAGCCACGGCGAGAACGAGGACTAC
PanuoR	TGGCGGTCGGTGAAGGTGAA	GTCTCGTGGGCTCGGAGATGTGTATAAGAGACAGTGGCGGTCGGTGAAGGTGAA
PappsF	GGTGACGACGGCAAGCTGTA	TCGTCGGCAGCGTCAGATGTGTATAAGAGACAGGGTGACGACGGCAAGCTGTAC
PappsR	GTATCGCCTTCGGCACAGGA	GTCTCGTGGGCTCGGAGATGTGTATAAGAGACAGGGTATCGCCTTCGGCACAGGA
PatrpF	TTCAACTTCGGCGACTTCCA	TCGTCGGCAGCGTCAGATGTGTATAAGAGACAGCTTTTCAACTTCGGCGACTTCCATGT
PatrpR	GGTGTCCATGTTGCCGTTCC	GTCTCGTGGGCTCGGAGATGTGTATAAGAGACAGCGGTGTCCATGTTGCCGTTCC

Table S7. PCR conditions

Loci	PCR reagent	Ta
Sa		
arc	Q5 (NEB)	61
aro	Q5 (NEB)	56
glp	Q5 (NEB)	56
gmk	Phusion (NEB)	56
pta	Q5 (NEB)	61
tpi	Q5 (NEB)	61
yqi	Q5 (NEB)	61
Pa		
arc	Kapa (Roche)	59
gua	Kapa (Roche)	59
mut	Q5 + GC buffer (NEB)	55
nuo	Kapa (Roche)	62
pps	Q5 + GC buffer (NEB)	67
trp	Q5 + GC buffer (NEB)	67

CHAPTER 3: Combining Ivacaftor and Intensive Antibiotics Achieves Limited Clearance of Cystic Fibrosis Infections

Published as: Samantha L. Durfey, Sudhakar Pipavath, Anna Li, Anh T. Vo, Anina Ratjen, Suzanne Carter, Sarah J. Morgan, Matthew C. Radey, Brenda Grogan, Stephen J. Salipante, Michael J. Welsh, David A. Stoltz, Christopher H. Goss, Edward F. McKone*, & Pradeep K. Singh*. mBio. 2021 Dec 21;12(6):e0314821. doi: 10.1128/mbio.03148-21.

Author contributions: Concept and design: S.L.D., S.C., M.J.W., D.A.S., C.H.G., E.F.M., and P.K.S. Acquisition of data, analysis, and interpretation: S.L.D., S.P., A.L., A.T.V., A.R., S.C., S.J.M., M.C.R., B.G., S.J.S., M.J.W., C.H.G., E.F.M., and P.K.S. Drafting the manuscript: S.L.D. and P.K.S. All authors reviewed the manuscript. E.F.M and P.K.S. contributed equally as senior authors.

Abstract

Drugs called CFTR modulators improve the physiologic defect underlying cystic fibrosis (CF) and alleviate many disease manifestations. However, studies to date indicate that chronic lung infections that are responsible for most disease-related mortality generally persist. Here we investigated whether combining the CFTR modulator ivacaftor with an intensive 3.5-month antibiotic course could clear chronic *Pseudomonas aeruginosa* or *Staphylococcus aureus* lung infections in subjects with *R117H-CFTR,* who are highly ivacaftor-responsive. Ivacaftor alone improved CFTR activity, and lung function and inflammation within 48 hours, and reduced *P. aeruginosa* and *S. aureus* pathogen density by ~10-fold within a week. Antibiotics produced an additional ~10-fold reduction in pathogen density, but this reduction was transient in subjects who remained infected. Only 1/5 *P. aeruginosa*-infected and 1/7 *S. aureus*-infected subjects became persistently culture-negative after the combined treatment. Subjects appearing to clear infection did not have particularly favorable baseline lung function or inflammation, pathogen density or antibiotic susceptibility, or bronchiectasis scores on CT scans, but they did have remarkably low sweat chloride values before and after ivacaftor. All persistently *P. aeruginosa*-positive subjects remained infected by their pretreatment strain, whereas subjects persistently *S. aureus*-positive frequently lost and gained strains. This work suggests chronic CF infections may resist eradication despite marked and rapid modulator-induced improvements in lung infection and inflammation parameters and aggressive antibiotic treatment.

Importance: Recent work shows that people with cystic fibrosis (CF) and chronic lung infections generally remain persistently infected after treatment with drugs that target the CF physiological defect (called “CFTR modulators”). However, changes produced by modulators could increase antibiotic efficacy. We tested the approach of combining modulators and intensive antibiotics in rapid succession and found that while few subjects cleared their infections, combined treatment appeared most effective in subjects with the highest CFTR activity. These findings increase understanding of the challenges that remain to improve the health of people with cystic fibrosis.

Introduction

The genetic disease cystic fibrosis (CF) has been transformed by drugs that act on the basic CF defect, impaired anion conductance of the cystic fibrosis transmembrane conductance regulator (CFTR) channel (191). Studies of ivacaftor, the first highly effective drug of this kind (called CFTR modulators), showed that treatment improved subjects' lung function, nutritional status, and reduced pulmonary exacerbations (192).

A remarkable finding from studies of ivacaftor was that treatment had only modest effects on a cardinal manifestation of CF, chronic lung infections caused by *Pseudomonas aeruginosa (Pa), Staphylococcus aureus (Sa),* and other pathogens. For example, work using culture-based methods showed that ivacaftor produced rapid reductions in sputum *Pa* density in chronically infected subjects and reduced lung inflammation (164). However, *Pa* density rebounded after ~1 year and *Pa* strains present pretreatment were found to persist for ~6 years of follow up (116). Epidemiological studies analyzing patient registry data (108, 118–120, 193), and studies using DNA-based methods (108, 121, 122) also indicate that chronic infections usually persist in modulator-treated patients. Persistent infection is likely to be detrimental, so strategies that eradicate infections in modulator-treated patients could markedly increase the health benefits from these drugs.

Antibiotics generally have only modest and transient effects in chronic CF infections (22, 194–197). However, several findings raise the possibility that antibiotic efficacy could be increased following treatment with modulators. First, studies in CF pigs and humans indicate that improved CFTR function increases the activity of lung antimicrobials by raising airway pH (62, 198). Innate antimicrobials can be synergistic with antibiotics (199), so combining modulators and antibiotics could amplify the infection-reducing effects of each. Second, modulator-mediated reductions in bacterial density (as seen in (164)) could increase antibiotic efficacy by the inoculum effect, a phenomenon wherein reduced bacterial density markedly increases antibiotic susceptibility (200, 201).

Third, modulators could reduce the stress-tolerant phenotype of infecting pathogens that causes resistance to killing. The tolerance phenotype is postulated to be due in part to nutrient and oxygen limitation in airway mucus (202–204), where pathogens mostly live (205, 206). Modulators reduce airway obstruction and increase mucociliary clearance (108), and these effects along with decreased pathogen density may diminish tolerance. Finally, reduced pathogen density could decrease intra-strain genetic diversity that is known to evolve during CF infections (92, 149, 207, 208). This effect could increase antibiotic efficacy, if the abundance of drug-resistant variants were reduced as a consequence (209).

Together these ideas led us to hypothesize that combining highly effective modulators with intensive antibiotic treatment might eradicate some *Pa* and *Sa* infections in chronically infected people with CF. Here we test this hypothesis, and we also present long-term follow up data on the effects of modulators on infection and inflammation in treated subjects.

Results

Study design and subjects. The rationale for combined treatment was the finding that chronic CF infections generally persist after ivacaftor. When this fact became known (108, 164), most ivacaftor-eligible subjects world-wide were already treated, and effective modulators for more common mutations did not exist. These points led us to seek out subjects with the rare ivacaftor-responsive *R117H-CFTR* mutation (210) who were not yet treated. Dublin, Ireland has among the highest worldwide prevalence of *R117H-CFTR* subjects (allele frequency 3% vs 1.04% in Europe and 0.7% world-wide) (211, 212), and the St. Vincent's University Hospital in Dublin is a CF referral center with robust research capabilities. Thus, we were able to test combined treatment in a cohort of chronically infected subjects with at least one copy of *R117H-CFTR* at this center.

Combined treatment could utilize antibiotics or modulators first, or both simultaneously. We decided to use modulators alone for one week and then start antibiotics (Figure 1) for three reasons. First, previous work showed that 1 week of ivacaftor reduced sputum *Pa* density in subjects with a *CFTR* gating mutation (*G551D-CFTR*) by ~10 fold (164). Reductions in this range are known to increase antibiotic activity via the inoculum effect (200, 201). Second, we thought there could be an advantage in starting ivacaftor and antibiotics in rapid succession to reduce time for bacterial adaptation. Third, the ivacaftor-alone period enabled us to repeat observations on modulators' acute effects.

After ethics approval and informed consent, we prospectively studied 10 adults (aged 25-64) with CF and ≥1 *R117H-CFTR* allele. Average forced expiratory volume in 1 second percent predicted (FEV_1pp) was 65%. Three subjects were chronically infected with *Pa*, 5 were chronically infected with *Sa*, and 2 were infected with both. See Table 1 for additional subject characteristics and Table S1 for inclusion and exclusion criteria. We used aggressive antibiotic regimens (Table 1). The 5 *Pa*-infected subjects were treated for 14 days with 2 antipseudomonal antibiotics administered concurrently by IV, followed immediately by 3 months of oral ciprofloxacin and inhaled colistin administered together (Figure 1). The 7 *Sa*-infected subjects were treated with 3.5 months of oral flucloxacillin, the drug of choice locally for *Sa* (Figure 1).

Table 1. Subject characteristics and antibiotics prescribed.

Subject ID*	CFTR Genotype: *R117H/*	Baseline FEV_1 [*L (% Predicted)*]	Age at Entry	Gender	Pathogens cultured at entry^	IV anti-biotic	Oral anti-biotic	Inhaled anti-biotic
1	*ΔF508*	3.80 (108%)	45	Male	*Sa*	none	Flu	none
2	*ΔF508*	3.75 (96%)	40	Male	*Sa*	none	Flu	none
3	*ΔF508*	2.44 (87%)	41	Female	*Sa*	none	Flu	none
7	*ΔF508*	2.39 (69%)	52	Male	*Pa, Sa*	Cef, tob	Flu, cip	Col
8	*M156R*	1.37 (43%)	42	Female	*Pa*	Mer, col	Cip	Col
9	*M156R*	1.49 (35%)	40	Male	*Pa, Sa*	Cef, col	Flu, cip	Col
10	*2622+1G→A*	3.41 (75%)	25	Male	*Sa*	none	Flu	none
11	*ΔF508*	1.90 (62%)	46	Female	*Pa*	Cef, tob	Cip	Col
12	*ΔF508*	1.93 (57%)	53	Male	*Sa*	none	Flu	none
13	*3849+4A→G*	0.99 (57%)	64	Female	*Pa*	Mer, col	Cip	Col

*There is no subject 6. Subjects 4 and 5 were excluded as they were culture negative for all pathogens at trial entry, despite a history of culture positivity.

^Fungal colonization is presented in Table S2.

CFTR = cystic fibrosis transmembrane conductance regulator; FEV_1 = forced expiratory volume in one second; *Sa* = *Staphylococcus aureus*; *Pa* = *Pseudomonas aeruginosa*; flu = flucloxacillin; cip = ciprofloxacin; col = colistin; cef = ceftazidime; mer = meropenem; tob = tobramycin.

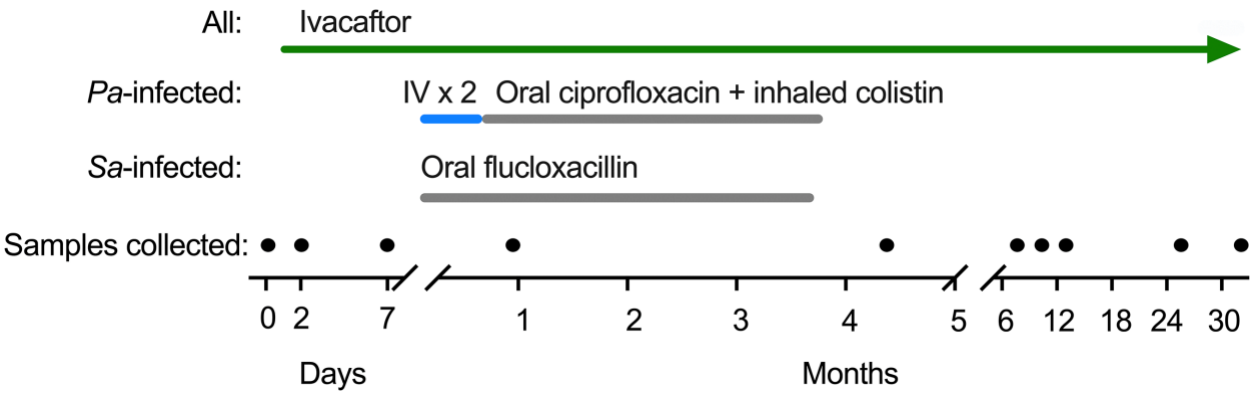

Figure 1. Study design. Subjects received ivacaftor for 1 week before initiating antibiotics. *P. aeruginosa* (*Pa*)-infected subjects received 2 weeks of 2 intravenous (IV) antibiotics simultaneously (including meropenem, tobramycin, colistin, or ceftazidime), followed by 3 months of oral ciprofloxacin and inhaled colistin simultaneously (see Table 1). *S. aureus* (*Sa*)-infected subjects received 3.5 months of oral flucloxacillin. We collected the first post-antibiotic samples after a 1-month antibiotic-free washout period, and subjects were followed for 31 months in total; the filled circles indicate sample collection times.

Ivacaftor improved sweat chloride, lung function, and inflammation within 48 hours. After 48 hours of ivacaftor-alone treatment, average sweat chloride decreased from 80.4 to 50.3 mM (95% CI: -41.7 to -18.5; p=0.0002) (Table 2 reports means, multiple-comparison adjusted p-values, and 95% CIs for all measurements) and did not decrease further by day 7 (Figure 2A). Average FEV_1pp improved from 65.0% to 68.9% after 48 hours (95% CI: 0.35 to 7.4; p=0.03), with additional improvement to 72.0% at day 7 (95% CI: 1.7 to 12.3%; p=0.01) (Figure 2B and C). Sputum neutrophil elastase levels declined from 1.8 to 1.5 $\log_{10}$ ug/mL after 48 hours (95% CI: -1.1 to 0.6; p=0.86), then declined further to 1.1 $\log_{10}$ ug/mL at day 7 (95% CI: -1.4 to -0.003; p=0.049) (Figure 2D). IL-1β, IL-8 and BMI did not change appreciably (Figure S1). These responses are similar to *G551D-CFTR* subjects previously studied (164).

Table 2. Effects of ivacaftor on clinical parameters and inflammation.

			Change from baseline		
	Mean	**N**	**Mean**	**95% CI**	**P value (adj)**
Sweat chloride (mM)					
Baseline	80.44	9	-	-	-
2 days	50.33	9	-30.11	(-41.70 to -18.53)	0.0002
7 days	55.88	8	-24.57	(-35.99 to -13.14)	0.0008
2.5 years	42.13	8	-38.32	(-62.61 to -14.03)	0.0050
FEV_1 (% predicted)					
Baseline	64.98	10	-	-	-
2 days	68.87	10	3.88	(0.35 to 7.41)	0.03
7 days	71.98	10	7.00	(1.68 to 12.33)	0.01
2.5 years	71.14	8	6.16	(-1.34 to 13.66)	0.11
Neutrophil elastase (log_{10} ug/mL)					
Baseline	1.76	10	-	-	-
2 days	1.51	10	-0.25	(-1.12 to 0.60)	0.86
7 days	1.07	9	-0.69	(-1.39 to -0.003)	0.049
2.5 years	1.04	7	-0.72	(-2.17 to 0.72)	0.38
IL-1β (log_{10} pg/mL)					
Baseline	3.69	10	-	-	-
2 days	3.66	10	-0.03	(-0.92 to 0.85)	0.99
7 days	3.38	9	-0.31	(-1.21 to 0.60)	0.79
2.5 years	2.60	7	-1.09	(-2.63 to 0.44)	0.17
IL-8 (log_{10} pg/mL)					
Baseline	4.68	10	-	-	-
2 days	4.70	10	0.02	(-0.71 to 0.75)	>0.99
7 days	4.50	9	-0.19	(-1.08 to 0.71)	0.97
2.5 years	4.16	7	-0.52	(-1.64 to 0.60)	0.48
MacConkey (log_{10} CFU/mL) (presumptive *Pa*)					
Baseline	6.62	5	-	-	-
2 days	6.26	5	-0.37	(-2.50 to 1.77)	0.96
7 days	5.61	4	-1.02	(-3.59 to 1.56)	0.41
2.5 years	3.34	3	-3.28	(-8.42 to 1.85)	0.12
MSA (log_{10} CFU/mL) (presumptive *Sa*)					
Baseline	5.31	7	-	-	-
2 days	4.98	7	-0.33	(-2.35 to 1.69)	0.99
7 days	4.19	6	-1.11	(-2.11 to -0.12)	0.03
2.5 years	3.49	4	-1.82	(-6.33 to 2.68)	0.40

CI = confidence interval; adj = adjusted for multiple comparisons; FEV1 = forced expiratory volume in 1 second; IL = interleukin; *Pa* = *Pseudomonas aeruginosa*; MSA = mannitol salt agar; *Sa* = *Staphylococcus aureus*.

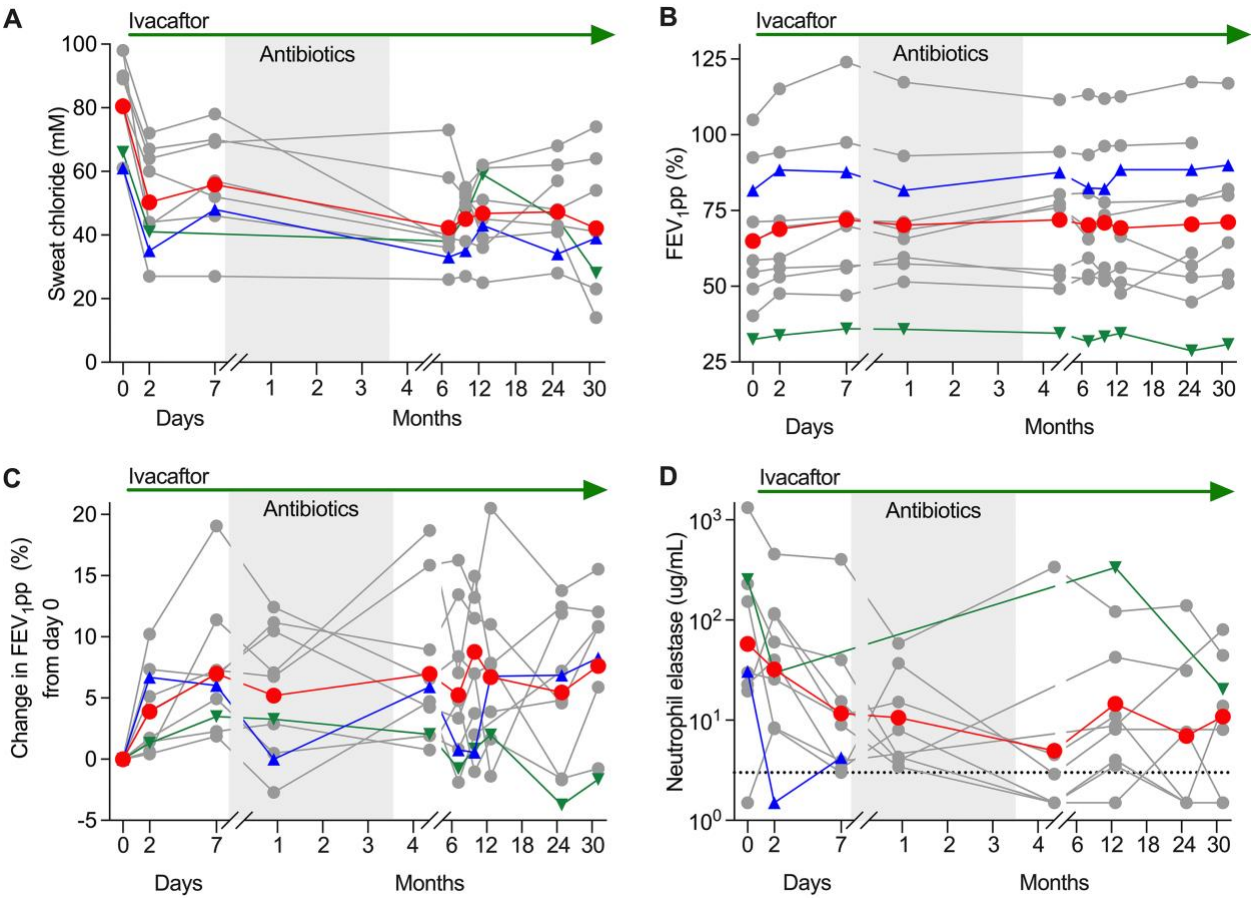

Figure 2. Ivacaftor rapidly improved CFTR and lung function, and lung inflammation. (A to D) Gray lines represent individuals, the red line represents the mean (A, B, C) or geometric mean (D), blue triangles represent subject 3, green triangles represent subject 9, ivacaftor treatment is indicated at the top, and the shaded region represents the on-antibiotic period. Subjects 3 and 9 are graphed differently because they became culture negative (see Results). Data with each line labeled by subject number are available in Fig. S2. (A) Sweat chloride. (B) Lung function as measured by forced expiratory volume in 1 second percent predicted (FEV_1pp). (C) Change in FEV_1pp from day 0. (D) Neutrophil elastase per mL sputum. The dashed line represents the limit of detection.

Ivacaftor rapidly reduced sputum *Pa* and *Sa* density. We measured *Pa* and *Sa* density after the week of ivacaftor-alone treatment and found both decreased by ~10-fold (*Pa* mean change: -1.0 $\log_{10}$ CFU/mL (95% CI: -3.6 to 1.6, p=0.41); *Sa* mean change: -1.1 $\log_{10}$ CFU/mL (95% CI: -2.1 to -0.12; p=0.03) (Figure 3). Changes were corroborated by PCR and sequencing analysis (Figure S4) and similar to *G551D-CFTR* subjects previously studied (164). Importantly, ~10-fold reduction in bacterial density (as achieved here) can markedly increase antibiotic efficacy by the inoculum effect (200, 201).

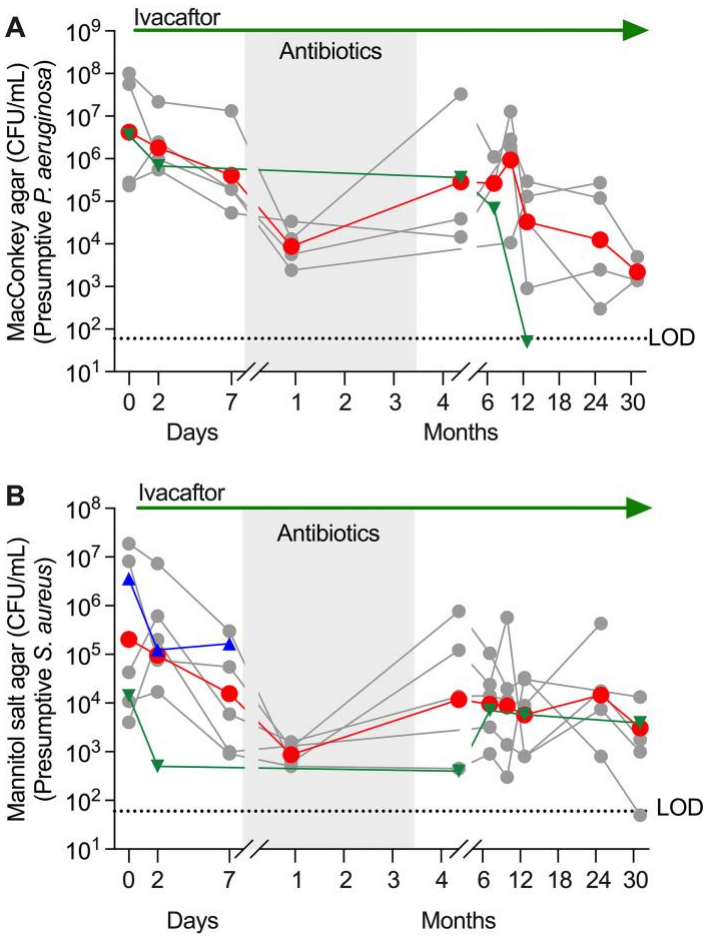

Figure 3. Ivacaftor rapidly improved sputum pathogen density. Gray lines represent individuals, the red line represents the geometric mean, blue triangles represent subject 3, green triangles represent subject 9, ivacaftor treatment is indicated at the top, the shaded region represents the on-antibiotic period, and the dotted line represents the limit of detection (LOD). Data with each line labeled by subject number are available in Fig. S3. (A) CFU per mL of sputum growing on MacConkey agar (presumptive *Pseudomonas aeruginosa*). (B) CFU per mL of sputum growing on mannitol salt agar (presumptive *Staphylococcus aureus*). See Fig. S4 for DNA-based measurements of pathogen density.

Antibiotics further reduced pathogen density, but the decrease was transient. *Pa* and *Sa* density were reduced by an additional ~10-fold after 3 weeks of antibiotics. *Pa* decreased by 1.7 $\log_{10}$ CFU/mL (95% CI: -5.0 to 1.7; p=0.23); *Sa* decreased by 1.3 $\log_{10}$ CFU/mL (95% CI: -4.0 to 1.5; p=0.32) (Figures 3 and S4).

We initially assayed for infection clearance 1 month after the 3.5-month antibiotic course had finished (and after 4.75 months of ivacaftor) to avoid residual antibiotic effects. Antibiotic-induced *Pa* and *Sa* reductions were transient in most subjects as pathogen density rebounded soon after antibiotics were stopped (Figure 3) (see subsequent sections). However, one *Sa*-infected subject and one *Pa*-infected subject became consistently culture-negative (discussed immediately below).

One subject with chronic *Sa* infection became culture negative. Subject 3 was infected with *Sa* for at least 15 years prior to the study (Table S3). Sputum cultures were *Sa*-positive on days 2 and 7 while on ivacaftor alone (Figure 4A). However, the subject became non-productive for sputum after antibiotics (i.e. from day 7 to study end at month 31) (Figure 4A).

We anticipated that subjects could stop producing sputum, so we collected swabs from the posterior pharynx after forced coughing at every study visit. Control experiments indicated that swabs reliably reported *Sa* but not *Pa* sputum culture positivity (Figure S5). Swabs collected from Subject 3 on days 0, 2, and 7 (when sputum was *Sa* positive) were *Sa* culture positive, whereas all swabs after antibiotics were negative (Figure 4A). In addition, we made 3 attempts to collect induced sputum after inhalation of 7% saline. Only one attempt (month 23) yielded sputum, and it was *Sa* culture negative (Figure 4A). These data suggest that the subject's chronic *Sa* infection likely cleared.

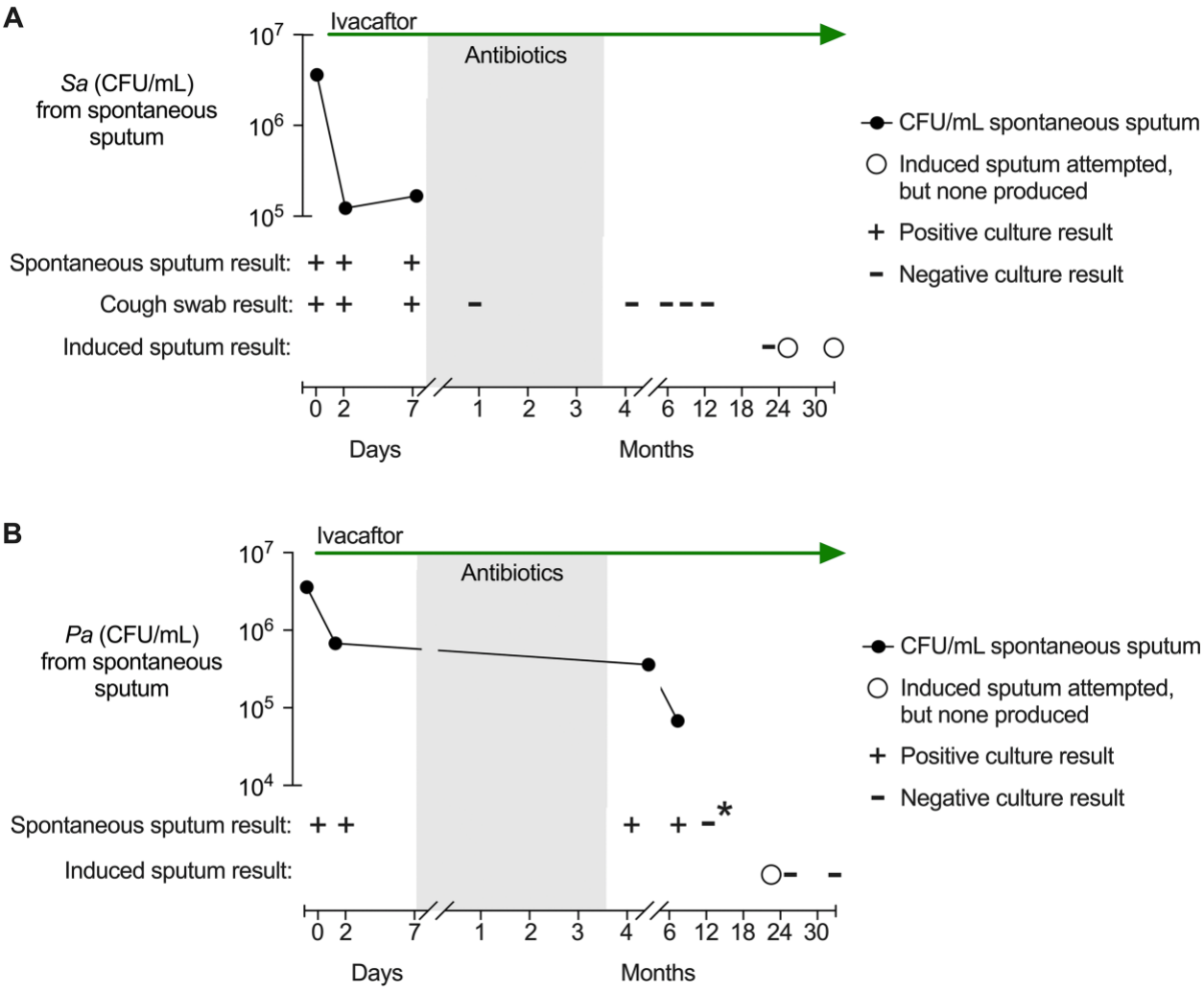

Figure 4. Ivacaftor and antibiotics reduced pathogen density below detectable levels in two subjects. Black lines represent CFU per mL in spontaneous sputum samples; pluses and minuses indicate culture results from each spontaneous sputum, induced sputum, or cough swab sample; and circles indicate times when induced sputum was attempted but unsuccessful. Ivacaftor is indicated at the top, and the shaded region represents the on-antibiotic period. (A) *Staphylococcus aureus* (*Sa*) culture results from subject 3. (B) *Pseudomonas aeruginosa* (*Pa*) culture results from subject 9. The asterisk (*) indicates that the culture result was confirmed with species-specific qPCR.

One subject with *Pa* infection became culture negative. Subject 9 had a complicated infection history (Table S3). The subject became *Pa* positive ~1 year before treatment started and had *Pa* positive cultures on day 0 and day 2 during ivacaftor-alone treatment (Figure 4B).

Sputum cultures at months 4 and 7 were also *Pa*-positive before the subject's sputum became persistently *Pa* negative after month 7 (Figure 4B). The subject spontaneously produced sputum at month 13 that was *Pa* culture and *Pa* qPCR negative (Figure 4B), and then became non-productive. We made 3 attempts to collect induced sputum (after inhalation of 7% saline). Two attempts yielded sputum (months 26 and 31) and were *Pa* negative (Figure 4B). Notably, Subject 9's sputum was consistently *Sa*-positive (even after *Pa* was no longer detected), and the subject suffered an exacerbation at month 26. Sputum before, during, and after the exacerbation were *Pa*-negative (Figure 4B). Repeated negative cultures suggest that *Pa* infection cleared.

Subjects clearing infection did not harbor particularly sensitive isolates. We investigated whether subjects becoming culture-negative were outliers in some way as this might suggest traits predisposing to infection clearance. We began by testing isolates' baseline (i.e. before ivacaftor treatment) antibiotic sensitivities. *Pa* isolates were tested against all agents used for IV, oral, and inhaled treatment (Table 1); *Sa* isolates were tested against flucloxacillin. Because pathogens can genetically diversify during infections, we tested the inhibitory concentration (IC) of 35-96 isolates from each subject, and examined three parameters derived from the ICs of these populations of isolates. These included the median IC of the population from each subject, the IC defining the most resistant quartile of the population, and the IC of the most resistant isolate from the tested population, as we thought these could affect infection clearance.

Sa isolates from Subject 3 (who became *Sa*-negative) were actually the most flucloxacillin resistant in the *Sa* cohort as measured by 2 of the 3 parameters (median and most resistant quartile) (Figure 5A). *Pa* isolates from subject 9 (who became culture negative for *Pa*) were the most ciprofloxacin sensitive of the *Pa* cohort by all three criteria (all *Pa*-infected subjects received ciprofloxacin), but were not particularly

sensitive to the IV or inhaled antibiotics this subject received (Table 1 and Figure 5B-F). Moreover, persistently infected subjects also harbored unusually sensitive isolates (Subject 13's isolates were most sensitive to colistin and Subjects 7 and 11's isolates were most sensitive to ceftazidime) (Figure 5C and E). Thus, unusual antibiotic sensitivity (as measured *ex vivo* on cultured isolates) did not appear to account for infection clearance. However, we note that laboratory tests of antibiotic sensitivity may not reflect *in vivo* treatment efficacy.

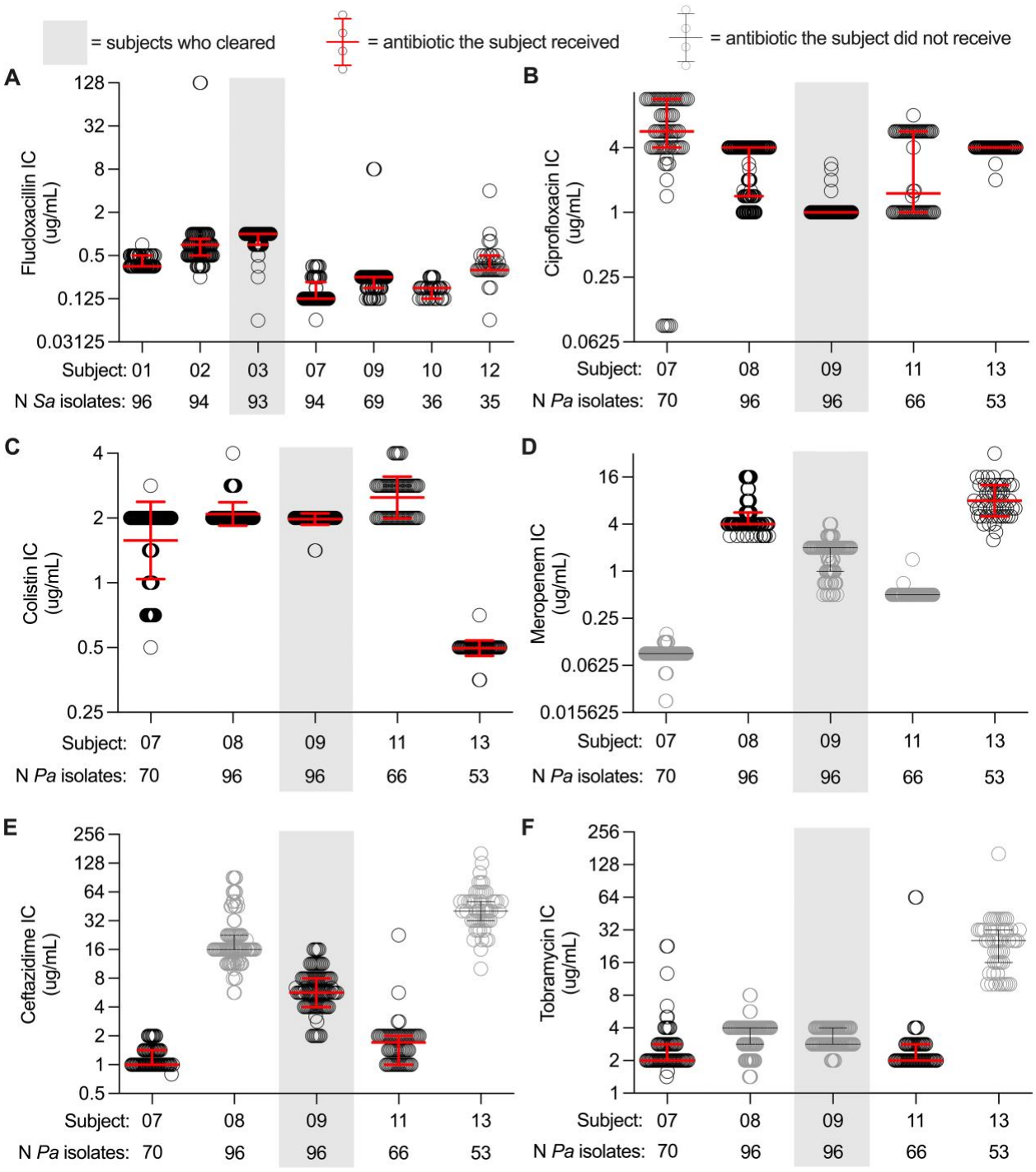

Figure 5. Subjects 3 and 9 do not harbor particularly sensitive bacteria. Each circle indicates the inhibitory concentration (IC) for each tested isolate (n = 35 to 96 per subject), and the error bars represent the median and interquartile range (IQR) calculated from the population of isolates. Results from antibiotics used to treat the respective subjects are reported using black circles with red error bars; results from antibiotics not used to treat the respective subjects are reported using gray circles with black error

bars, and the shading indicates the subjects that cleared infection (3 and 9). (A) *Staphylococcus aureus* (*Sa*) flucloxacillin ICs. (B to F) *Pseudomonas aeruginosa* (*Pa*). (B) Ciprofloxacin ICs. (C) Colistin ICs. (D) Meropenem ICs. (E) Ceftazidime ICs. (F) Tobramycin ICs.

Subjects clearing infection had low baseline and ivacaftor-induced sweat chloride. We also examined other characteristics of subjects who did and did not clear infection. Subjects clearing infection were not in the upper quartile of lung function or BMI. Nor were they in the lower quartile of age; lung injury on chest CT scans; baseline *Pa* or *Sa* sputum densities; or sputum neutrophil elastase, IL-1β or IL-8 (Figure 6A-J). Moreover, 16S rRNA sequencing indicated that subjects becoming culture-negative had similar baseline sputum taxa relative abundance profiles (Figure S6) and diversity (Figure 6K) as persistently infected subjects.

However, Subjects 3 and 9 (who cleared *Sa* and *Pa,* respectively) had among the lowest baseline sweat chloride values (61 and 66, versus average of 80 mM for others), and achieved among the lowest values after ivacaftor (35 and 41 at 2 days, versus average of 50 mM for others) (Figure 7). These findings raise the possibility that infection clearance may depend in part on the amount of CFTR activity achieved (see discussion).

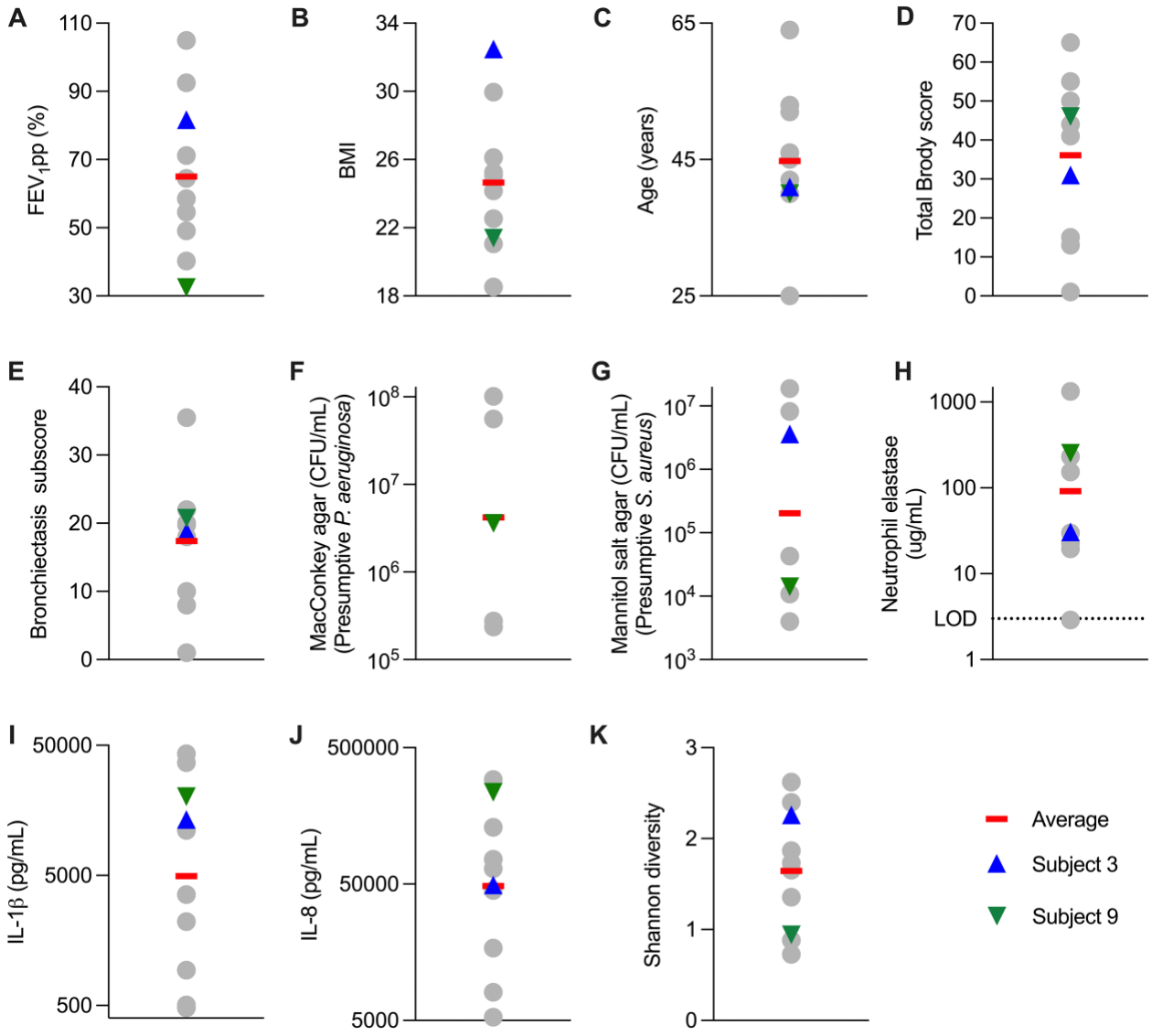

Figure 6. Subjects 3 and 9 clinical characteristics. Gray circles indicate individual subjects; the red line is the average (A to E, K, and L) or geometric mean (F to J), blue triangles indicate subject 3 (cleared S. aureus) and green triangles indicate subject 9 (cleared P. aeruginosa). All data are from baseline (day 0). (A) FEV_1 percent predicted. (B) BMI. (C) Age. (D) Total Brody CT score. (E) Brody CT bronchiectasis subscore. (F) CFU per mL of sputum growing on MacConkey agar (presumptive *Pseudomonas aeruginosa*). (G) CFU per mL of sputum growing on mannitol salt agar (presumptive *Staphylococcus aureus*). (H) Neutrophil elastase per mL sputum. The dotted line indicates the limit of detection (LOD). (I) IL-1β per mL sputum. (J) IL-8 per ml sputum. (K) Shannon alpha diversity of sputum.

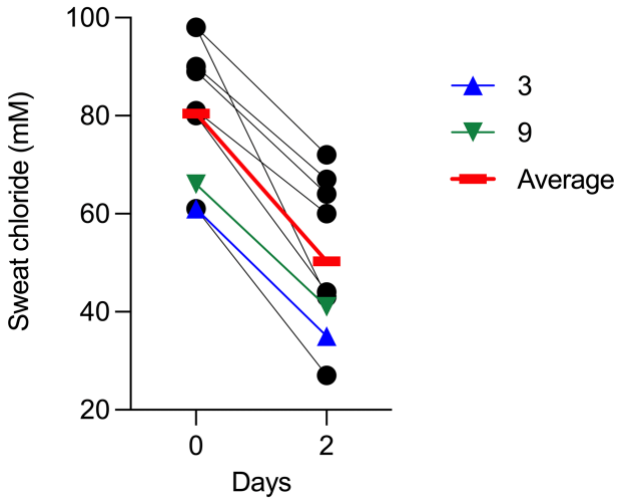

Figure 7. Subjects 3 and 9 had low baseline and ivacaftor-induced sweat chloride. Black lines represent individuals, the red line represents the mean, blue triangles represent subject 3 (cleared *S. aureus*), and green triangles represent subject 9 (cleared *P. aeruginosa*).

Sweat chloride, lung function, and inflammation improved little after first week. Little data exist about modulators' long-term effects, so we tracked key clinical parameters over 2.5 years (Table 2; Figure 2). Notably, the acute sweat chloride and lung function improvements were sustained but did not increase. Average sweat chloride decreased by 30.1 mM from baseline to 48 hours, and 38.3 mM from baseline to 2.5 years (95% CI: -62.6 to -14.0; p=0.005); average FEV_1pp increased by 7.0% from baseline to 1 week, and 6.2% from baseline to 2.5 years (95% CI: -1.3 to 13.7; p=0.11). Sputum neutrophil elastase followed a similar pattern with the first weeks' improvements persisting over 2.5 years of follow up; average neutrophil elastase decreased by 0.7 $\log_{10}$ ug/mL from baseline to one week, and 0.7 $\log_{10}$ ug/mL from baseline to 2.5 years (95% CI: -2.2 to 0.7; p=0.38).

We also examined long-term trends in pathogen density (Figure 3). Between the end of the antibiotic wash-out (month 4.75) and the study's end (2.5 years), average *Pa* density decreased by 2.1 $\log_{10}$ CFU/mL but variability was high, so interpretation is difficult (95% CI: -9.3 to 5.1; p=0.41). Average *Sa* density changed little during this time (95% CI: -7.9 to 6.7; p=0.96).

Subjects with persistent *Pa* infection retained pre-treatment strains, but *Sa* strains frequently switched. While pathogen density rebounded ~1 month after antibiotics, during combined treatment it was ~100-fold lower than baseline (Figures 3 and S4) and much lower than typical in CF. These marked reductions raised the possibility that pre-treatment *Pa* or *Sa* lineages were partially or completely replaced by new strains. We examined this possibility using PopMLST (213), a method that detects gain or loss of strains with high resolution by testing tens to hundreds of isolates per sample.

PopMLST performed on ~95 *Pa* isolates cultured from each timepoint showed that all cultured isolates from persistently infected subjects belonged to the single MLST type detected before treatment (Figure 8A). These findings suggest that a single *Pa* strain was dominant prior to treatment in all study subjects and persisted through 2.5 years.

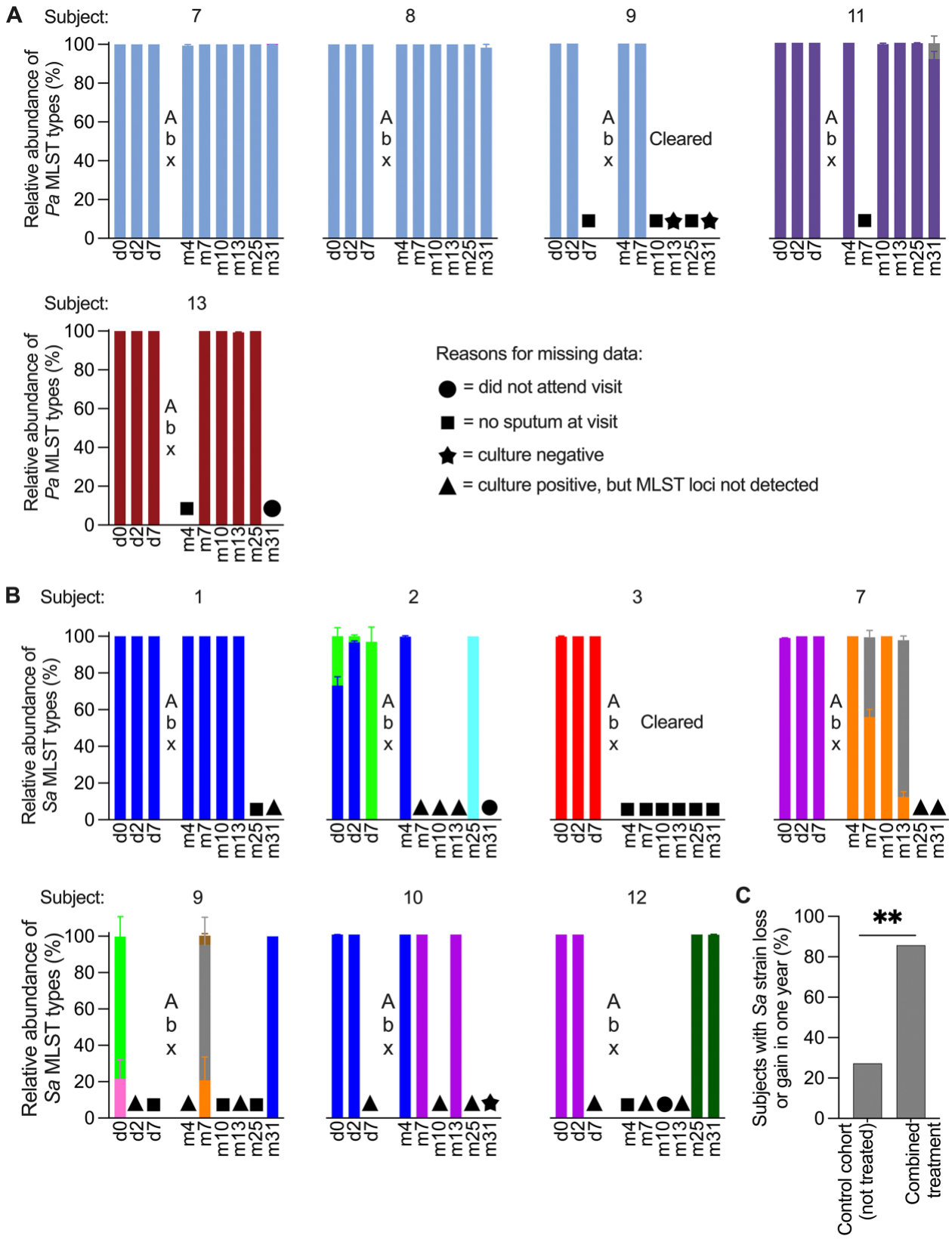
A
Subject: 7
8
9
11
Relative abundance of Pa MLST types (%)
Abx
Cleared
d0 d2 d7 m4 m7 m10 m13 m25 m31
Subject: 13
Reasons for missing data:
= did not attend visit
= no sputum at visit
= culture negative
= culture positive, but MLST loci not detected
B
Subject: 1
2
3
7
Relative abundance of Sa MLST types (%)
9
10
12
C
Subjects with Sa strain loss or gain in one year (%)
**
Control cohort (not treated)
Combined treatment

Figure 8. The relative abundance of MLST types recovered from subjects' sputum. Each color represents a unique MLST type and is consistent across subjects; d, day; m, month; Abx, antibiotic period. MLST type abundances were determined using PopMLST (see Chapter 2) and represent the average relative abundance of alleles from 6 *P. aeruginosa* (*Pa*) or 7 *S. aureus* (*Sa*) MLST loci inferred to originate from a single strain. Where total relative abundance does not equal 100%, less than one-half the MLST loci exhibited a secondary allele, likely due to sequencing error. Symbols differentiate reasons for missing data (see key). (A) Relative abundance of *P. aeruginosa* MLST types. (B) Relative abundance of *S. aureus* MLST types. (C) Percentage of subjects who experienced at least one *S. aureus* strain gain or loss in 1 year for the control cohort (CF subjects not receiving combined ivacaftor + antibiotic treatment [$n = 11$]) and the combined treatment cohort (this clinical trial of ivacaftor + antibiotics [$n = 7$]) (**, $P = 0.0022$).

In contrast, *Sa* infections exhibited more strain diversity and switching. Baseline samples from 5/7 subjects contained 1 strain type, and 2/7 subjects were infected with 2 strains (Figure 8B). Importantly, 6 of 7 (86%) of subjects either lost an existing *Sa* strain or acquired a new *Sa* strain during the first year of ivacaftor with most strain switches becoming apparent at the first or second sputum sample obtained after antibiotics. For a comparison group, we examined banked samples from 11 additional *Sa*-infected CF subjects who were not treated with modulators and intensive antibiotics. Over a comparable time period (11.5-14 months), only 3 of 11 (27%) experienced *Sa* strain loss or gain ($p=0.002$ as compared to treatment group). These data and previous work showing that *Sa* strains generally persist for long time periods (130, 135, 214) suggest that modulators, antibiotics or the combination compromised the stability of infecting *Sa* strains.

Discussion

Chronic lung infections are among the most consequential manifestations of CF, and studies to date indicate they generally persist after the basic CF defect is pharmacologically improved (108, 118, 119, 121, 164, 193, 215). We tested an approach to improve outcomes by combining intensive antibiotics with modulators and studied the long-term effects of modulators in subjects with chronic infections.

We made four main findings. First, despite using intensive antibiotics in highly responsive subjects receiving highly effective modulators, only 1/5 *Pa*-infected and 1/7 *Sa*-infected individuals cleared infection. Second, subjects clearing infection had particularly low baseline and post-ivacaftor sweat chloride levels, but we were not able to identify other distinguishing characteristics of these subjects. Third, subjects persistently infected with *Pa* retained their pre-treatment strains for 2.5 years of follow up, but frequent strain switching was observed in *Sa*-infected subjects. Fourth, sweat chloride, lung function, and sputum neutrophil elastase markedly improved after one week of ivacaftor, but showed minimal additional change over 2.5 years.

Mechanisms that could explain infection persistence. One explanation for persistent infection is that treated subjects could have significant residual lung host defense defects. Such defects could arise from at least three mechanisms. First, modulators produce incomplete restoration of CFTR function. This is the case in well-vascularized and uninflamed sweat glands (192), thus lung cells in chronically infected subjects almost certainly have residual (and perhaps significant) CFTR dysfunction. Second, injury to lung epithelia and immune cells in regions with structural lung disease could restrict the beneficial effects of CFTR-targeting therapies to lung regions without such damage. Third, the continual presence of pathogens for years or decades could restrict improvements in innate antimicrobial activity due to immune tolerance mechanisms (216), even after CFTR function is restored.

A second explanation is that established chronic infections become autonomous or independent of CF host defense defects and would persist even if host defenses completely normalized. Lung defenses typically encounter a low density of inhaled or aspirated bacteria from environmental sources and clear

these effectively. In contrast, modulator-corrected lung defenses must contend with high-density populations of pathogens that have genetically adapted and diversified over time (92, 133, 149, 207, 208, 217). In addition, CF pathogens exhibit phenotypes that produce tolerance to killing including low metabolic activity (218), an aggregated growth mode (205), and constitutive activity of stress responses (219, 220). These factors could make infection eradication challenging even if CFTR-dependent host defenses were normalized.

***Pa* strains persist, but *Sa* strains are transient.** It was interesting that *Pa* lineages persisted, but *Sa* lineages were frequently gained and lost. The persistence of pre-treatment *Pa* strains could be due to specific pathogenic capabilities such as tolerance to antimicrobials (221, 222) or resistance to mechanical and phagocytic clearance (223, 224). Pathogen density may also contribute, as baseline average *Pa* density was ~10 fold higher that of *Sa*.

Our finding that almost all *Sa*-infected subjects receiving combined treatment gained or lost *Sa* strains during the first year of treatment was unexpected. Subjects studied in the pre-modulator era (130, 135, 214), and our control cohort not receiving combined treatment exhibited much lower rates of strain switching. This finding suggests that modulators, antibiotics, or the combination might destabilize existing *Sa* strains, but not improve host defenses enough to prevent reinfection with new *Sa* strains. The ability of new *Sa* strains to infect after modulator treatment could be related to *Sa*'s ability to act as both a pathogen and commensal, as commensals can colonize sites in the absence of severe host defense defects. It is also possible that acquired *Sa* strains are inherently more capable in CFTR-corrected lungs than those that disappeared. If so, comparative genomics or phenotyping could identify differences.

Persistently infected subjects exhibit most improvement in the first treatment week. It was notable that sweat chloride, lung function, and neutrophil elastase improved in the first week with minimal additional improvements in the subsequent 2.5 years. *Pa* and *Sa* density also showed 10-fold declines in the first week, with additional changes difficult to discern. These findings are consistent with previous observations (164) and suggest that benefits produced by improving lung defenses, inflammation, and

physiology may not amplify each other over time to produce continual improvement. The mechanisms that limit improvement to the period immediately after drug initiation are unclear, but pathogen persistence and structural lung disease could be factors. Future work comparing lung function and inflammation responses in subjects with and without chronic infection would be informative.

Study limitations. Our study had several important limitations. First was the small study size. Several factors severely reduced subject availability. For example, we thought that the best test of an infection clearance regimen would target chronically infected subjects with highly responsive *CFTR* mutations, and that starting modulators and antibiotics in rapid succession might reduce time for bacterial adaptation. These considerations limited us to subjects with the rare *R117H-CFTR* mutation as most subjects with *G551D-CFTR* were already receiving ivacaftor, and modulators for subjects with other *CFTR* mutation classes were not yet available. Furthermore, the study was burdensome and difficult to expand beyond a single center as it required 3.5 months of IV, oral and inhaled antibiotic treatment, immediate on-site sample processing, and close follow-up. Together these factors restricted subject availability and may limit generalizability of the findings. The small study size also limited our ability to identify parameters (like the extent of sweat chloride improvement) associated with infection clearance outcomes, and to determine how infection clearance affects lung function (or other health outcomes). However, we do note that many study outcomes achieved statistical significance ($p \leq 0.05$ with multiple comparison testing) including changes in sweat chloride, FEV_1pp, neutrophil elastase, and *Sa* density.

Second, definitively proving that lung infections have been eradicated is challenging. Even the gold standard approach using bronchoscopy (which was not performed here) interrogates at most a few lung regions, and the sputum sampling used here may be less sensitive. However, repeated throat swabbing and spontaneous and induced sputum sampling in the two subjects that became culture-negative support the conclusion that infection was cleared.

Third, the lack of a control group treated with ivacaftor but not antibiotics is a limitation. Prior studies indicate that chronic infections generally persist after modulator treatment and antibiotics when each are

used alone (108, 118–122, 164, 193, 225). While this suggests that combined treatment could have caused infection clearance in the two cases, the absence of a control group makes this postulate tentative. Importantly, the lack of a control group does not compromise our central conclusion that chronic CF infections are difficult to clear even after aggressive use of antibiotics and modulators.

Finally, sampling issues somewhat limit the conclusions we can draw from the observation of *Sa* strain switching. For example, *Sa*'s ability to colonize upper airway tissues raises the possibility that the presence of some *Sa* strains in sputum arises from contamination from upper airway secretions, rather than originating from subjects' lungs. In addition, no samples were banked from before treatment was initiated, so we were unable to determine how long pre-treatment *Sa* strains were present before strain switching occurred.

This study highlights opportunities and challenges in treating chronic CF lung infections in the post-modulator era. It was encouraging that modulators produced rapid reductions in sputum pathogen density and inflammation markers, and improved lung function. Our finding that infection clearance may be associated with low sweat chloride raises the possibility that infection clearance rates might be increased if CFTR function could be improved further. Studies of more effective modulators could test this idea. In addition, the high rate of strain *Sa* switching suggests that modulators may destabilize existing *Sa* strains, and this might be exploited therapeutically.

On the other hand, our finding that most subjects remained infected by *Pa* and *Sa* despite highly effective modulators and intensive antibiotics points to challenges ahead. Future work will be needed to determine the extent to which persistent infection compromises health in modulator-treated subjects, and to devise new strategies to eradicate chronic CF infections so that the full health benefits of CFTR modulators can be realized.

Methods

Cohort characteristics. This clinical trial of CFTR modulators plus antibiotics (EudraCT: 2016-001785-29) was performed at the National Referral Center for Adult Cystic Fibrosis at St. Vincent's University Hospital in Dublin, Ireland. Subjects provided written informed consent prior to collection of samples. Subjects were people diagnosed with CF and heterozygous for the *CFTR-R117H* mutation. Individual subject characteristics are summarized in Table 1.

Sweat chloride measurements. Sweat was collected with the Macroduct® collection system (Wescor, Logan UT), and sweat chloride was measured using standard laboratory techniques.

Spirometry. Measurements were obtained using American Thoracic Society Standards (226). FEV_1pp is based on GLI 2012 values for adults (227).

Computed tomography scans and scoring. Images were obtained using 64-slice CT (Sensation 64, Siemens, Erlangen, Germany) with patients in the supine position. Inspiratory images were obtained in suspended deep inspiration with 1mm slice thickness every 10 mm from the apices to the costophrenic angles. Expiratory images were obtained in full expiration at five levels: the top of the aortic arch, the carina, pulmonary veins, between level 3 and 5 and 2 cm above the diaphragm. Scanning parameters were 80–120 kVp and 50–120 mA with images reconstructed using a high spatial frequency bone algorithm and a 512×512 matrix. Lung windows with a width of 1,500 and level of −700 houndsfield units were applied. Scans were reconstructed with filtered back projection and standard kernel, and they were de-identified prior to transfer to the University of Washington for analysis. For scoring, the 5 parameters of the Brody score (bronchiectasis, peri-bronchial wall thickening, mucous plugging, parenchymal damage, and air trapping) were measured in each of the 6 lobes of the lung (RUL, RML, RLL, LUL, Lingula, and LLL), and the sum of all scores was registered as the total Brody score (228, 229).

Sputum processing for quantitation of bacterial concentration and inflammatory biomarkers, and culturing of *Pa* and *Sa*. Sputum specimens were homogenized with cold 0.1% dithiothreitol (DTT). One

aliquot of homogenized sputum was serially diluted and plated on MacConkey agar (Difco) and mannitol salt agar (MSA; Difco) to quantify *Pa* and *Sa* concentration, respectively. Up to 96 *Pa* and *Sa* isolates were picked and made into freezer stocks.

Quantification of sputum inflammatory biomarkers. Homogenized sputum was processed according to the CF Therapeutics Development Network Coordinating Center standard operating procedure (164). IL-8 and IL-1β [Luminex Multiplex Bead, R&D Systems; Abingdon, Oxon, UK] and free neutrophil elastase activity [Spectrophotometric assay, Sigma Diagnostics; St. Louis, MO] were analyzed.

Bacterial DNA extraction. DNA was extracted from DTT-treated sputum using Qiagen's DNeasy PowerSoil Kit with modifications (164).

Bacterial quantification. Bacteria were quantified in duplicate with 16S rRNA qPCR primers and probe ("All bacteria" in (164)) with Luna Universal Probe qPCR master mix (NEB) with a CFX96 Touch Real-Time PCR Detection System (Biorad). Genomic DNA from *P. aeruginosa* PAO1 was used to generate a standard curve, which included a negative control (no template) and was run with every experiment.

Bacterial 16S rRNA gene sequencing and analyses. The V3-V5 variable region of the 16S rRNA gene was amplified with primers containing Illumina adapter sequences (Illumina 16S Metagenomic Sequencing Library Preparation). De-multiplexed sequencing reads were assigned to amplicon sequence variants (ASVs) using DADA2 pipeline (171) (version 1.18). Shannon diversity was calculated in R (version 4.0.3) using the Vegan package (https://github.com/vegandevs/vegan) and scripts adapted from Foster and Grunwald (230). ASVs were quantified by multiplying the total bacterial abundance determined by 16S rRNA gene qPCR by the relative abundances of each ASV determined by bacterial 16S rRNA gene sequencing, as in (42).

Population-based multi-locus sequence typing (PopMLST). Detailed methods reported in (213). The frozen *Pa* or *Sa* isolates were inoculated into LB (for *Pa*) or BHI (for *Sa*) broth and grown overnight, then

stamped onto LB or BHI plates using a 96-pin microplate replicator and grown overnight at 37°C. All isolates were scraped together using 1x PBS, pelleted, and frozen for future DNA extraction with the Qiagen DNeasy PowerSoil kit, with modifications (164). See Table S4 for number of isolates analyzed.

We amplified the seven species-specific MLST loci using primers modified with the Illumina adapter sequence (213). We sequenced the amplicons on a 2x300 cycle cartridge (Illumina). Sequencing reads were processed using PopMLST software (https://github.com/marade/PopMLST). Briefly, reads were deconvolved based on their loci-specific primers and then amplicon sequence variants (ASVs) were inferred using DADA2. To identify each allele, ASVs were queried against the PubMLST database (https://pubmlst.org/saureus/ and https://pubmlst.org/paeruginosa/) (170).

Cough swab culture. Due to limitations inherent in performing the study overseas, we froze the cough swabs in a glycerol-based transport medium (231). Thawed media was serially diluted and plated onto MSA, Baird-Parker (Difco), MacConkey, and *Pseudomonas* isolation agar (PIA; Difco). *Pa* positivity was defined as growth of at least one colony on MacConkey or PIA. *Sa* positivity was defined by phenotypes of growth on Baird-Parker and MSA, because both media also permit growth of *Staphylococcus epidermidis*.

Antibiotic inhibitory concentration. Briefly, the frozen isolates (day 0) were grown overnight in LB (*Pa*), or BHI (*Sa*), stamped onto each plate with a 96-pin replicator, and grown at 37°C for 20-24 hours. Each plate contained a different antibiotic concentration on a 2-log scale in LB. The inhibitory concentration (IC) of each isolate was recorded as the lowest concentration of antibiotic where the isolate did not grow, i.e. if an isolate grew at 2 ug/mL but not at 4 ug/mL, the IC was recorded as 4 ug/mL. *Pa* isolates were tested on meropenem (obtained from clinic), tobramycin (RPI), ceftazidime (clinic), colistin (clinic), and ciprofloxacin (RPI). *Sa* isolates were tested on flucloxacillin (Sigma-Aldrich). All tests were done in duplicate, unless there was a >2-fold discrepancy.

Control cohort for *Sa* strain switching. Sputum samples were collected in accordance with University of Washington Institutional Review Board (protocol number 06-4469) from the adult CF clinic at University of Washington. Patients provided written informed consent prior to collection of samples. Samples were selected based on 2 criteria: 1) no history of CFTR modulator use and 2) ≥2 banked *Sa* samples collected ≥1 year apart. Sputolysin treated sputum was cultured on MSA. Populations were scraped from plates containing >100 colonies with LB. All cultures were stored at -80^{o}C in 15% glycerol prior to analysis. About 100uL of the glycerol-preserved sample was DNA extracted using the DNeasy PowersoilPro kit (Qiagen) for Qiacube (Qiagen). DNA was subjected to PopMLST as described above.

Statistical analyses. Repeated measures analysis of variance (assuming gaussian distribution with a mixed model adjustment for missing data) was used to test FEV_1pp, sweat chloride, culture, and inflammatory marker data. Where data were nonnormally distributed, they were first log-transformed. All p-values are corrected for multiple comparisons, using Dunnett for comparisons to baseline and Šídák for comparisons between followup visits. A two-tailed p-value of ≤ 0.05 was considered significant. To compare *Sa* strains switching, the control group was used as the expected and the combined treatment group was compared to this expected using a binomial test. Prism version 9.1 was used to perform all statistics and produce graphs.

Supplemental information

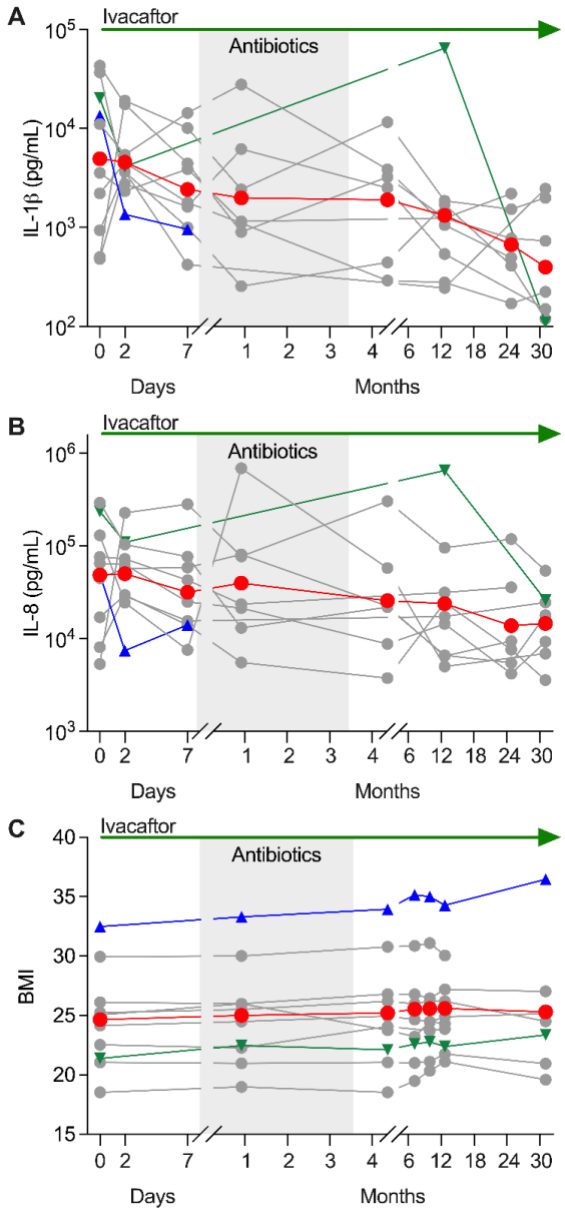

Figure S1. Ivacaftor's effects on lung inflammation and body mass index (BMI). Gray lines represent individuals, red line represents geometric mean (A, B) or mean (C), (▲) represents Subject 3, (▼) represents Subject 9, ivacaftor treatment is indicated at top, and shaded region represents on-antibiotic period. (A) IL-1β per mL of sputum. (B) IL-8 per mL of sputum. (C) BMI.

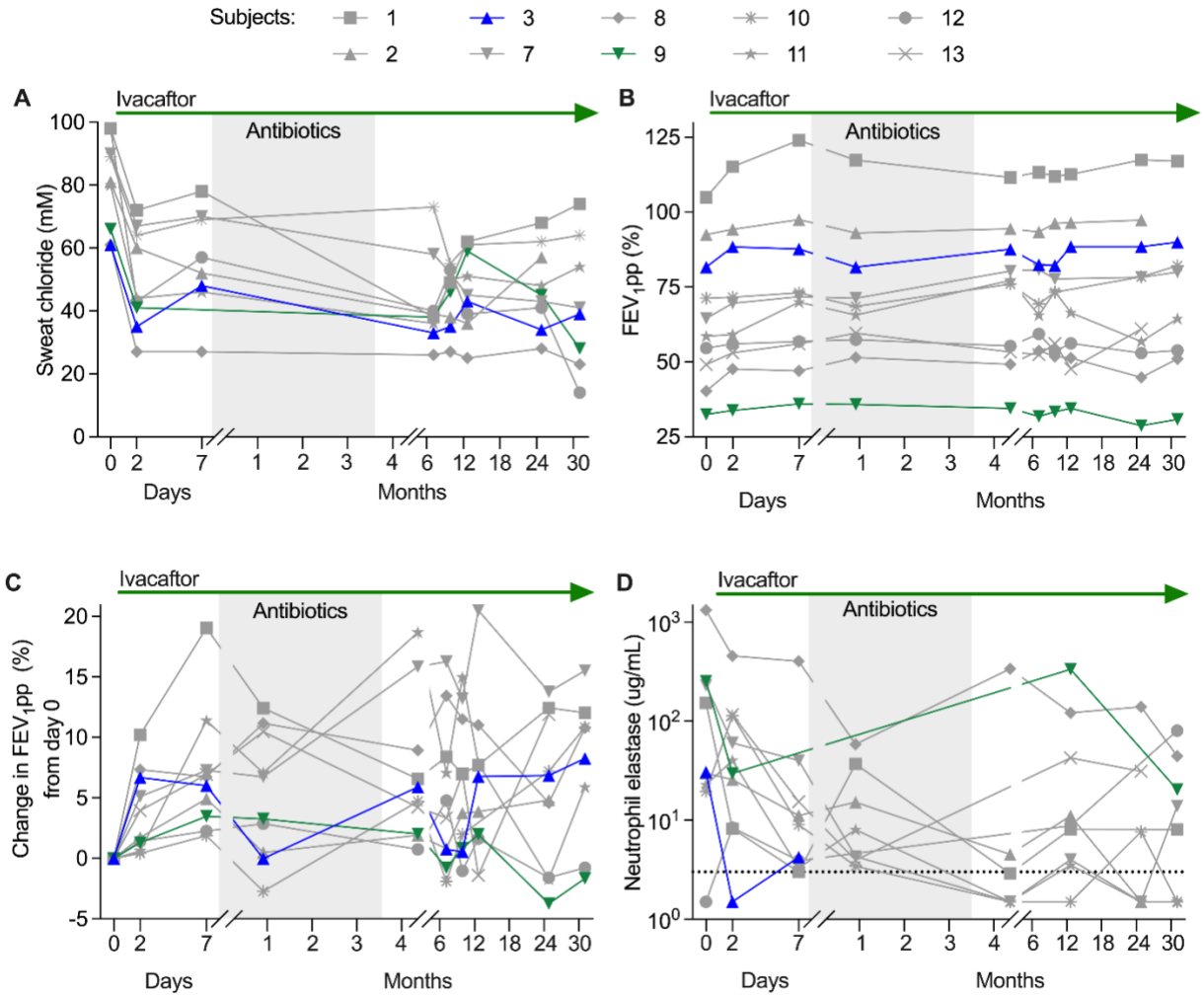

Figure S2. Individual subjects' data for sweat chloride, lung function, and neutrophil elastase. Each line represents an individual and each individual is identified with a unique shape and color combination, ivacaftor treatment is indicated at top, and shaded region represents on-antibiotic period. (A) Sweat chloride. (B) Lung function as measured by forced expiratory volume in one second percent predicted (FEV_1pp). (C) Change in FEV_1pp from day 0. (D) Neutrophil elastase per mL sputum. Dashed line represents limit of detection.

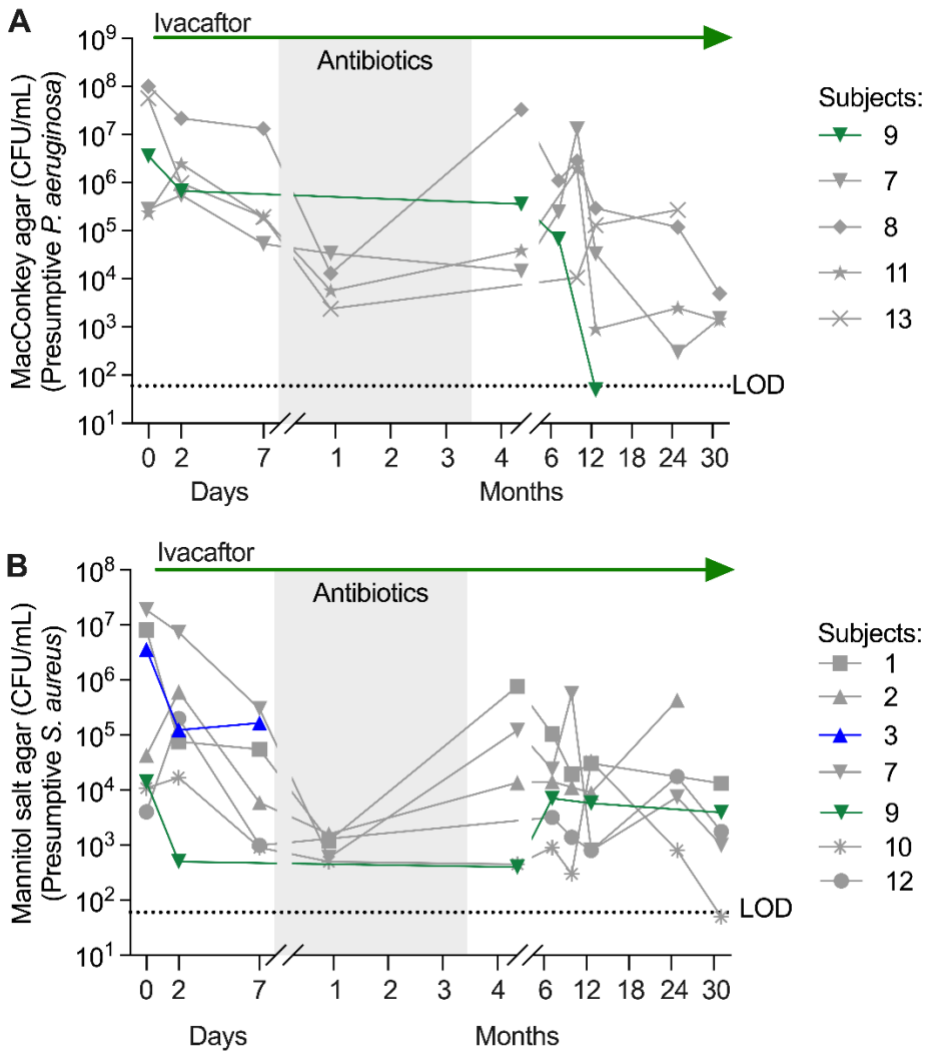

Figure S3. Individual subjects' data for *Pa* and *Sa* density. Each line represents an individual and each individual is identified with a unique shape and color combination, ivacaftor treatment is indicated at top, shaded region represents on-antibiotic period, and dotted line represents limit of detection (LOD). (A) CFU per mL of sputum growing on MacConkey agar (presumptive *Pseudomonas aeruginosa* (*Pa*)). (B) CFU per mL of sputum growing on mannitol salt agar (presumptive *Staphylococcus aureus* (*Sa*)). See Fig S4 for DNA-based measurements of pathogen density.

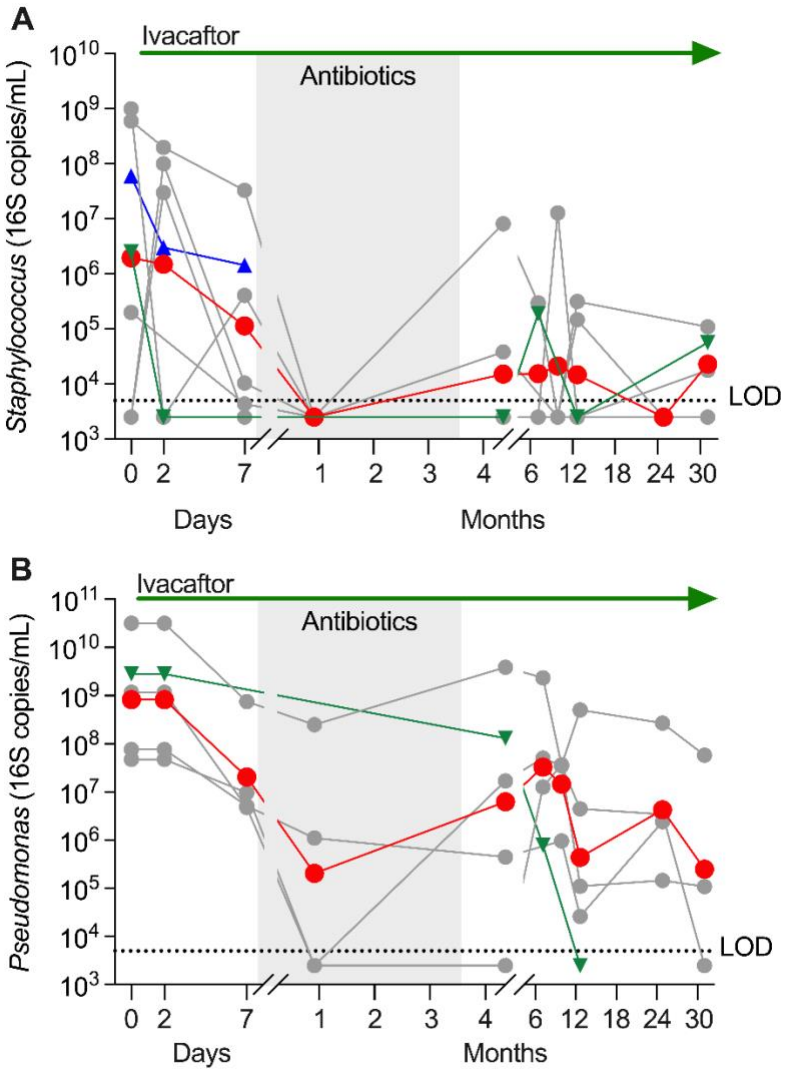

Figure S4. Calculated absolute abundance of pathogens corroborates CFU counts (see Figure 3). Gray lines represent individuals, red line represents geometric mean, (▲) represents Subject 3, (▼) represents Subject 9, ivacaftor treatment is indicated at top, and the shaded region indicates on-antibiotic period. Absolute abundance was calculated by multiplying the total bacterial abundance determined by 16S rRNA gene qPCR by the relative abundances of each amplicon sequence variant (ASV) determined by bacterial 16S rRNA gene sequencing. (A) *Staphylococcus* 16S copies per mL sputum. (B) *Pseudomonas* 16S copies per mL sputum.

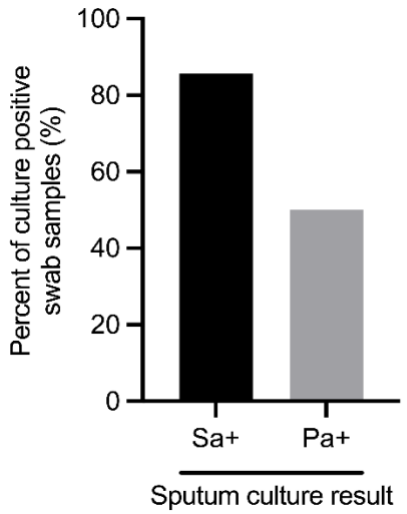

Figure S5. Cough swab concordance with concurrently collected sputum samples. We tested the accuracy of cough swabs by culturing swabs that were collected concurrently with sputum. When the sputum sample was *Sa* culture positive (n=7), 85% of cough swabs were *Sa* culture positive. However, when sputum samples were *Pa* culture positive (n=4), only 50% of swabs were *Pa* culture positive.

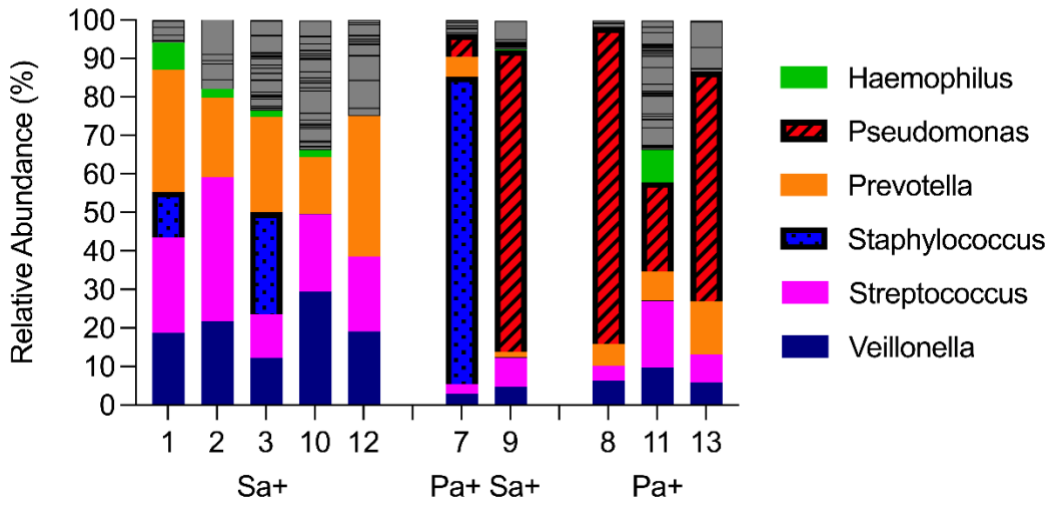

Figure S6. Relative abundance of genera detected by 16S sequencing of sputum collected at baseline (day 0). Only the top 6 genera are shown. Subjects are divided into groups by culture result.

Table S1. Inclusion and exclusion criteria.

Inclusion Criteria:

- Adult, greater or equal to 18 years of age.
- Documentation of a CF diagnosis with the *R117H-CFTR* mutation on at least 1 allele and any known or unknown second mutation other than *G551D-CFTR*. CF diagnosis is defined as evidenced by one or more clinical features consistent with the CF phenotype and one or more of the following criteria:
    a. Sweat chloride ≥60 mEq/liter by quantitative pilocarpine iontophoresis test (QPIT)
    b. Two well-characterized mutations in the cystic fibrosis transmembrane conductance regulator (CFTR) gene
    c. Abnormal nasal potential difference (change in NPD in response to a low chloride solution and isoproteronol of less than -5 mV)
- Prior chronic *Pa* or *Sa* in the sputum as defined by >50% of prior sputum cultures with each organism in the year prior to enrollment. Patients need a minimum of 2 prior cultures in the year.
- Able to expectorate sputum.
- Be clinically stable at the time of initiation of ivacaftor (day 0).
- Be off chronic inhaled or oral antibiotics (other than azithromycin) for 2 weeks prior to free enrollment
- Patients must be able to tolerate planned antibiotic regimen (anti-staphylococcal and anti-*Pseudomonas aeruginosa* regimens).
- Written informed consent and assent if indicated obtained from subject or subject's legal representative, able to communicate with the investigator and comply with the requirements of the protocol
- If female and of childbearing potential, must have a negative pregnancy test on Day 1(Start of Treatment) prior to receiving study drug.
- If female and of childbearing potential, is willing to use adequate contraception for the duration of the study and for 1 month following the study, as determined by the investigator.
- If male and able to father a child, is willing to use adequate contraception for the duration of the study and for 1 month following the study, as determined by the investigator.

Exclusion Criteria:

- Participation in the VX-770-105, VX-770-106, VX-770-108, VX-770-109, VX-770- 110, VX-770-111, VX-770-112, or VX-770-113 study, VX-770 Extended Access Program, VX-661-108, or use of ivacaftor within 6 months prior to day 0.
- Any upper or lower respiratory symptoms requiring treatment with oral, inhaled or IV antibiotics within the 2 weeks prior to day 0.
- History of solid organ transplantation.
- Presence of a condition or abnormality that in the opinion of the investigator would compromise the safety of the patient or the quality of the data.
- History of massive hemoptysis (>240 mL) within 72 hours of day 7.
- Inability to produce sputum.
- Females who have a positive pregnancy test at day 2, are lactating, or are not practicing (or willing to practice) a medically acceptable form of contraception (acceptable forms of contraception: hormonal birth control, intrauterine device, barrier method plus a spermicidal agent or abstinence) from day 2 through month 10 unless surgically sterilized or postmenopausal.

Table S2. Fungi colonization at trial entry.

Subject	Cultured fungi at entry
1	Candida
2	Candida
3	none
7	none
8	none
9	none
10	Candida
11	Candida
12	none
13	Candida

Culture was performed by the clinical diagnostic lab.

Samples collected ~2 weeks before day 0.

Table S3. Infection histories of Subjects 3 and 9.

Date	*S. aureus*	*P. aeruginosa*
	Subject 3	
06/2001	+++	Not tested
10/2008	+	-
03/2011	+	-
10/2011	+++	-
12/2013	++	-
12/2014	+++	-
02/2015	+++	-
12/2015	++	-
10/2016	+++	-
	Subject 9	
12/2000	+	++ (mucoid)
05/2001		+ (mucoid)
12/2001		+ (mucoid)
05/2002	+	+
06/2002	-	++ (mucoid)
11/2003	++	++ (mucoid)
02/2005	+	
03/2006	+	
09/2007	-	-
10/2007	-	-
11/2007	-	-
11/2008	+	-
08/2009		-
01/2012	+	-
09/2012	+++	-
02/2013	+++	-
03/2013	-	-
04/2015	+++	-
12/2015	-	+
02/2016	-	+
03/2016	-	+++
02/2017	+	+++

Culture was performed by the clinical diagnostic lab.

Table S4. Number of isolates tested for *Sa* and *Pa* by PopMLST.

Subject	Timepoint	Total isolates for *Staphylococcus auerus* popMLST	Total isolates for *Pseudomonas aeruginosa* popMLST
1	d0	96	
	d2	95	
	d7	95	
	m4	96	
	m7	95	
	m10	70	
	m13	94	
	m31	96	
2	d0	95	
	d2	95	
	d7	66	
	m4	96	
	m7	95	
	m10	8	
	m13	92	
	m25	69	
3	d0	94	
	d2	96	
	d7	95	
7	d0	94	95
	d2	95	93
	d7	95	95
	m4	96	91
	m7	95	94
	m10	81	95
	m13	26	96
	m25	94	12
	m31	40	32
9	d0	95	96
	d2	3	95
	m4	96	14
	m7	95	95
	m13	95	
	m31	95	
10	d0	87	
	d2	88	
	d7	2	
	m4	54	
	m7	32	
	m13	96	
	m25	35	
	m31	0	
11	d0		92
	d2		95
	d7		94
	m4		94
	m7		95
	m10		10
	m13		33
	m31		
12	d0	96	
	d2	95	
	d7	36	
	m7	80	
	m13	19	
	m25	90	
	m31	95	
13	d0		60
	d2		95
	d7		95
	m7		94
	m10		94
	m13		95
	m25		78

CHAPTER 4: Post-Modulator Cystic Fibrosis Infections Affect Mild and Severely Diseased Lung Regions and Pro-inflammatory Effects of Pathogens are Undiminished by Treatment

Anticipated to be published as: SL Durfey, SG Kapnadak, M Teresi, T Gambol, MM Willmering, R Villacreses, JD Godwin, L Boyken, M Stroik, AT Vo, SB Singh, C Steele, JC Woods, D Stoltz, T Pena, JP Clancy, ML Aitken, PK Singh

Author contributions: Concept and design: S.L.D., D.A.S., T.P., J.P.C., M.L.A., and P.K.S. Acquisition of data, analysis, and interpretation: S.L.D., S.G.K, M.T., T.G., M.M.W., R.V., J.D.G., L.B., M.S., A.T.V., S.B.S., C.S., J.C.W., D.A.S., T.P., M.L.A., and P.K.S. Drafting the manuscript: S.L.D. and P.K.S.

Introduction

The genetic disease cystic fibrosis (CF) has been transformed by drugs called modulators that act on the basic CF defect, impaired anion conductance of the cystic fibrosis transmembrane conductance regulator (CFTR) channel (191). Elexacaftor/tezacaftor/ivacaftor (ETI) is the most effective modulator to reach clinical use, and it improves lung function and nutritional status, and reduces disease flares (104, 232). However, modulators' effects on CF lung infections, a cardinal manifestation of the disease, are relatively modest. Two large epidemiological studies of an early-generation modulator (ivacaftor) showed that only a fraction of subjects become culture-negative for conventional pathogens after treatment (108, 118). Recent prospective studies of ETI found similar results (125). Only about ~1/3 of infected subjects become culture negative for *Pseudomonas aeruginosa* (*Pa*), and <1/4 of infected subjects become culture negative for *Staphylococcus aureus* (*Sa*) after ETI.

Persistent infection will likely degrade lung function over time due to pathogen-induced inflammation, and the direct effects of bacterially-produced toxins. In addition, bacterial variants able to evade host defenses or disrupt cells to acquire nutrients have been shown to emerge from populations replicating under host-applied selective pressure and accelerate future disease (233). Lung infections also cause systemic inflammation (234–239), which could disrupt metabolism (240, 241), aggravate CF-related diabetes (242), and worsen cardiovascular function (243). Thus, post-modulator lung infections will likely compromise patients' long-term health. Understanding the factors that affect infection outcomes after treatment is critical to designing effective approaches to eradicate CF infections and maximize the health of people with CF.

Infection outcomes after modulator treatment are likely determined by multiple factors acting at different scales, from patient-level determinants to individual lung region characteristics. These factors could include the magnitude of improvement in an individual's CFTR function, the conditions in lungs before treatment begins, and the capabilities of infecting bacteria to resist modulator-improved defenses. Some patient-level characteristics like systemic improvement in CFTR functioning are readily measured using sweat chloride values and other tests. In contrast, the lung conditions and pathogen characteristics

potentially most important for infection clearance are far more challenging to assess. This is in large part because of extensive region to region heterogeneity in these factors within CF lungs.

For example, some regions of an individual's lung can appear nearly normal by imaging and histology, while others can be denuded of epithelia, structurally destroyed, and highly inflamed (80–86). Modulator treatments may sufficiently enhance host defenses in regions with favorable host conditions leading to infection eradication, but insufficiently improve regions with more severe disease. Lung segments within individual patients can also differ in identity, density, and phenotypes of pathogens (42, 85–89, 91). Variation in microbial characteristics could also have profound effects on modulator outcomes.

Here we used bronchoscopy sampling of multiple lung regions in people with CF before and after starting ETI to investigate within-lung heterogeneity of structural damage, inflammation, and microbiology and regional disease outcomes after modulator treatment. We focused on four main research questions. First, we investigated the extent of heterogeneity in conditions before ETI was started. Second, we examined whether post-ETI lung infections were restricted to particular lung segments (e.g. those with severe damage) or were widespread throughout the lung. Third, we investigated the potential drivers of post-ETI inflammation. Finally, we begin exploring how pre-existing disease conditions affected regional responses to ETI.

Results

Study subject characteristics

All 9 subjects had been infected with *Pa* for a minimum of 1.25 years and 6 subjects were coinfected with *Sa* (based on positive clinical sputum cultures). At baseline, subjects' average age was 33.6 (range 26-39) years, mean lung function as measured by percent of predicted forced expiratory volume in one second (FEV_1pp) was 68.3% (range 58.2 – 80.6%), and average pre-ETI sweat chloride (based on medical records) was 95.6mM (range 68.0 – 131.0 mM) (Table 1). Seven of 9 subjects were homozygous for F508del *CFTR.* These 7 subjects were taking tezacaftor/ivacaftor prior to initiating ETI and the other two subjects had not taken modulators previously. All subjects were pancreatic insufficient, and additional comorbidities are summarized in Table 2. Subjects entered the study with different histories of suppressive antibiotic use; 3/9 were prescribed no maintenance antibiotics; 3/9 were prescribed alternating tobramycin and aztreonam; and the remaining 3 took only tobramycin or aztreonam.

Table 1. Subject characteristics at study baseline.

Subject	CFTR Genotype: *F508del/*	Baseline FEV_1 [*L (% Predicted)*]	Age (years)	Gender	Pathogens*	Sweat chloride (mM)	Prior modulator use
1	*F508del*	3.23 (72%)	29	Male	*Pa*, *Sa*	131	Tez/iva
2	*E60X*	2.17 (60%)	35	Female	*Pa*, *Sa*	Not available	None
3	*E542X*	2.44 (81%)	39	Female	*Pa*, *Sa*	126	None
4	*F508del*	3.26 (62%)	37	Male	*Pa*	84	Tez/iva
5	*F508del*	1.96 (73%)	32	Female	*Pa*	90	Tez/iva
6	*F508del*	1.92 (58%)	30	Female	*Pa*, *Sa*	71	Tez/iva
7	*F508del*	2.54 (78%)	26	Female	*Pa*, *Sa*	68	Tez/iva
8	*F508del*	2.2 (62%)	39	Female	*Pa*, *Sa*	109	Tez/iva
9	*F508del*	2.02 (69%)	35	Female	*Pa*	86	Tez/iva

*Pathogens are defined as any pathogen (bacterial or fungal) detected via clinical culture in the year prior to subjects starting ETI.

FEV_1 = forced expiratory volume in one second; *Pa* = *Pseudomonas aeruginosa*; *Sa* = *Staphylococcus aureus*

Table 2. Comorbidities.

Subject	PI	GERD	CFRD	ABPA	Smoking	Vaping	CF liver disease	Sinus disease	Sinus surgery	CF related bone disease
1	Yes	No	No	No	No	No	No	Yes	Yes	No
2	Yes	No	Yes	No	No	No	Yes	No	-	No
3	Yes	Yes	Yes	No	No	No	No	No	-	No
4	Yes	No	No	No	No	No	No	Yes	No	No
5	Yes	Yes	No	No	No	No	No	No	-	Unknown
6	Yes	Yes	Yes	Yes	No	No	No	Yes	Yes	No
7	Yes	Yes	No	No	Yes	No	Yes	Yes	No	No
8	Yes	No	No	No	No	No	No	Yes	No	No
9	Yes	Yes	Yes	No	No	No	No	Yes	No	Yes

All comorbidities should be read as “History of ___”.

PI = pancreatic insufficiency; GERD = gastroesophageal reflux disease; CFRD = cystic fibrosis related diabetes; ABPA = allergic bronchopulmonary aspergillosis.

Study design

To study regional lung responses to ETI, we performed bronchoscopy to sample 5 lung regions within each subject before and ~1.5 years after initiating ETI (Fig. 1). We used an extremes of phenotype design that targeted each subject's most and least structurally damaged lung regions for sampling. We stratified regions by this criterion, as CFTR modulators have been postulated to have less benefit in lung regions with structural lung damage. Thus, we reasoned that infection in the lowest and highest damaged lung regions may respond differently to ETI.

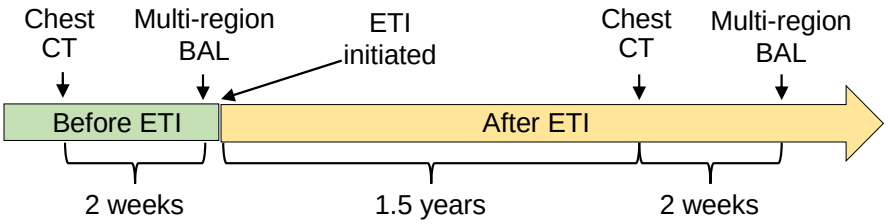

Figure 1. Study design. Chest CTs were collected <2 weeks before each multi-region bronchoscopy. Chest CT and bronchoscopy were repeated 1.5 years after subjects started ETI.

Regions were ranked by the extent of structural lung disease using high-resolution computed tomography (HRCT) scans performed within 2 weeks of the first bronchoscopy. An expert thoracic radiologist identified the 2 lung segments with the “highest” degree of disease and the 3 lung segments with the “lowest” amount of disease in each subject (collectively called “targeted segments” below), excluding the lower lobes due to concerns for low fluid return given that only 20mL of lavage fluid was used per sample (~100 mL total per subject) so as to avoid lung edema. Because of subject-to-subject variation in the location of mild and severe disease, subjects had different lung segments sampled (Fig. 2). However, the same 5 regions in each subject were sampled before and after ETI. We used a new disposable bronchoscope for each segment (i.e. 5 scopes per procedure) introduced via cuffed endotracheal tubes to reduce cross contamination between regions.

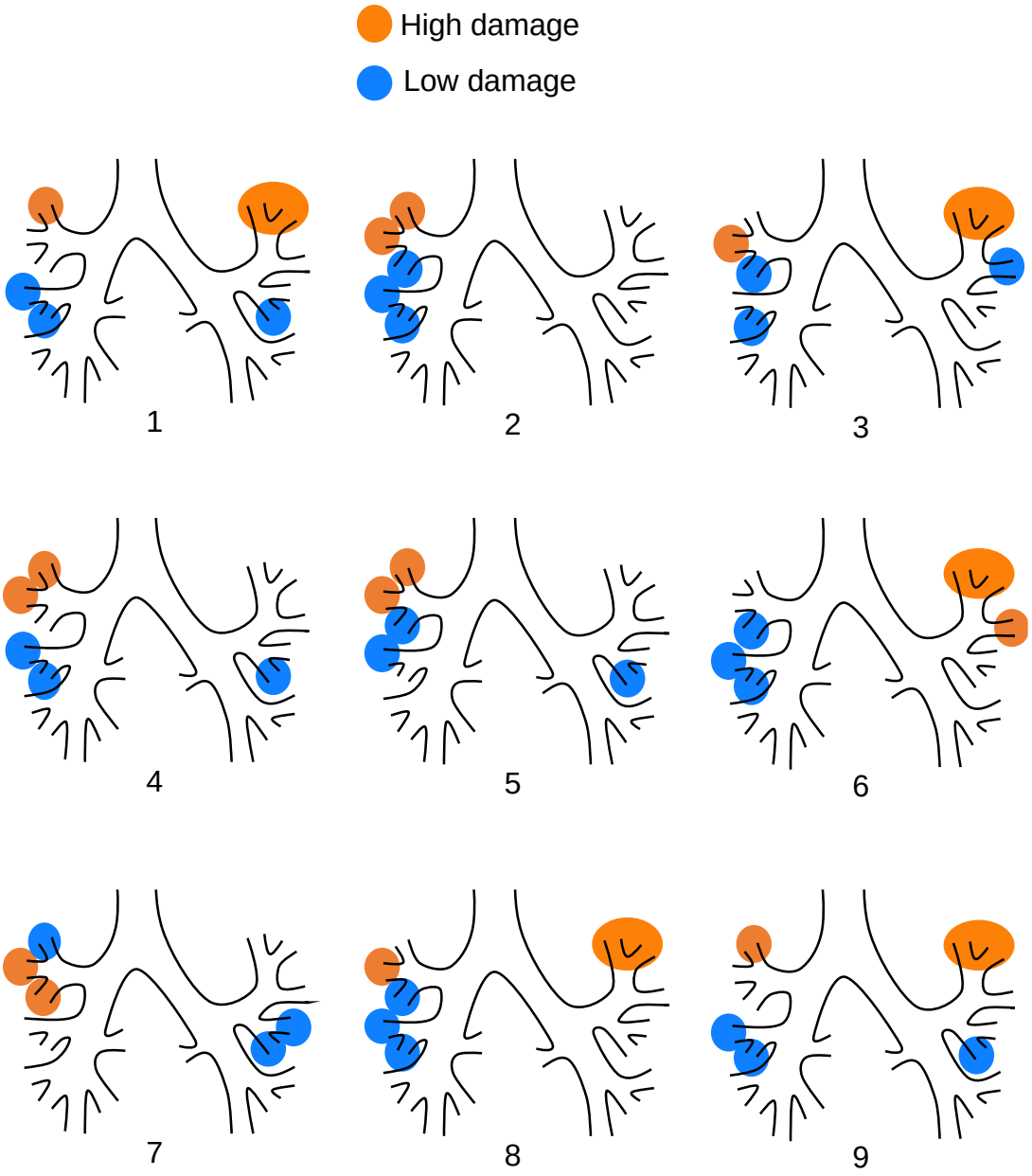

Figure 2. Lung regions sampled in each subject. Each lung drawing represents one subject. The lung segments that were selected as high damage are highlighted with orange. The lung segments that were selected as low damage are highlighted with blue. Each subject had unique segments sampled.

Quantitative culture was used to measure *Pa* density, and PCR was used to measure *Sa,* summed pathogen density (*Pa* + *Sa* genome copies/mL), and total bacterial load. We measured neutrophil elastase using an activity assay (Spectrophotometric assay; Sigma Diagnostics, St. Louis, MO) and CF Therapeutics Development Network Coordinating Center standard operating procedures (164). Structural lung disease of the targeted lung segments was assessed quantitatively using chest CT scans scored with the Brody system (see methods). The Brody score consists of 5 measures of CF-related lung pathologies visible on CT scans: bronchiectasis, peri-bronchial wall thickening, mucus plugging, parenchymal damage, and air trapping (229).

Bacterial density, inflammation, and damage differ markedly within lungs before ETI.

Lung imaging studies have consistently found heterogeneous disease, but little is known about region-to-region variation in microbiology and inflammation, and these factors could have a profound effect on infection outcomes after ETI. Thus, we measured segmental *Pa* density, *Sa* density, total bacterial load, neutrophil elastase, and Brody score in the targeted lung segments in each subject before ETI was initiated.

We began by measuring the extent of structural lung damage by the clinically validated Brody score that measures lung pathology characteristic of CF (229), and found that the five targeted segments in most subjects exhibited marked quantitative differences (Fig. 3A). The median difference between the highest and lowest scores of the targeted segments within individuals was 15.5 points (range: 4.3 – 26.5 out of 40 points). In all but 2 subjects (Subjects 5 and 7) Brody score measurements and the initial radiologist determination of “high” and “low” damage were concordant. These 2 subjects had the smallest differences in Brody score between their highest and lowest score segments (5.5 and 4.3 points, respectively).

We investigated the intra-patient heterogeneity in bacterial density using culture and PCR assays. We focused on *Pa* and *Sa* density as these pathogens have been linked to CF lung disease, and we also measured total bacterial load. The median observed difference between minimum and maximum density

among targeted segments from individual subjects was 2.9 $\log_{10}$ CFU/mL (range 0.5 – 6.0 $\log_{10}$ CFU/mL) for *Pa* (Fig. 3B), 2.1 $\log_{10}$ genomes/mL (range 1.3 – 2.7 $\log_{10}$ genomes/mL) for *Sa* (Fig. 3C); 2.3 $\log_{10}$ genomes/mL (range 0.2 – 5.1 $\log_{10}$ genomes/mL) for summed pathogen density (*Pa* + *Sa* genomes) (Fig. 3D); and 2.2 $\log_{10}$ genomes/mL (range 0.2 – 3.8 $\log_{10}$ genomes/mL) for total bacterial load (16S copies) (Fig. 3E). We assessed lung inflammation by measuring neutrophil elastase (NE), as NE is associated with clinical outcomes in CF and non-CF bronchiectasis (39, 244). The median observed difference in segmental NE level was 29.6-fold (range 2.8-150.1- fold; Fig. 3F).

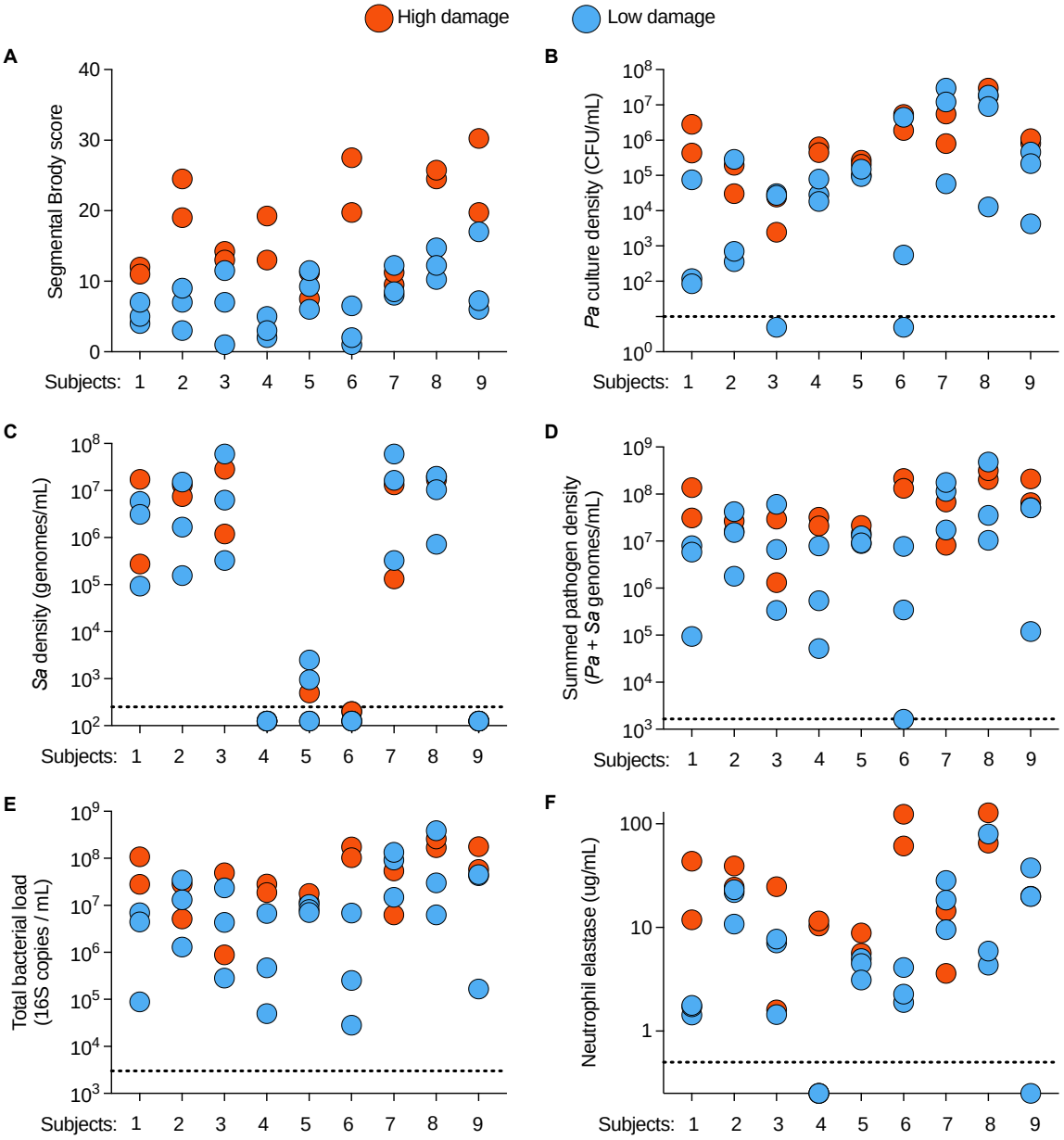

Figure 3. Pre-ETI intra-subject heterogeneity in structural lung damage, bacterial density, and inflammation. Each circle represents one lung segment within a subject. Orange circles indicate the 2 high damage segments. Blue circles indicate the 3 low damage segments. Each subject is shown individually along the x-axis. (A) Segmental Brody score. (B to F) Dashed lines indicate the limit of detection. Concentrations expressed per mL BAL fluid. (B) *Pa* per mL. (C) *Sa* per mL. (D) Summed pathogens (*Pa* + *Sa*) per mL. (E) Total bacterial load (16S copies) per mL. (F) Free neutrophil elastase per mL.

These data show that even in subjects without advanced lung disease (FEV1 in the cohort ranged from 58.2 – 80.6% predicted), lung regions differ markedly in structural damage, pathogen density, and lung inflammation. For example, observed median *Pa* density differences of 2-3 $\log_{10}$ between segments are comparable to or exceed the ~1 $\log_{10}$ CFU/mL change currently achieved by inhaled antibiotics (195), and the ~2 $\log_{10}$ CFU/mL change in sputum density after ETI (125). The ~30-fold within-lung differences in NE far exceed the 2-fold differences achievable by the most commonly used anti-inflammatory medicine used in CF (azithromycin) (245). Differences in lung conditions of this magnitude could affect ETI responses.

Bacterial density and inflammation are higher in more damaged segments before ETI.

We explored associations between structural lung disease, bacterial density, and inflammation in targeted segments. Segmental Brody scores were associated with *Pa* culture density ($r^2 = 0.27$; $p = 0.0003$), summed pathogen density ($r^2 = 0.33$; $p < 0.0001$), total bacterial load ($r^2 = 0.35$; $p < 0.0001$), and with NE ($r^2 = 0.42$; $p < 0.0001$) (Fig. 4A-D). Segmental Brody scores did not correlate with *Sa* density, even when the 3 *Sa*-negative subjects were excluded ($r^2 = 0.06$; $p = 0.19$) (Fig. 4E); however, this association may be complicated by co-infection with *Sa* and *Pa* in these subjects.

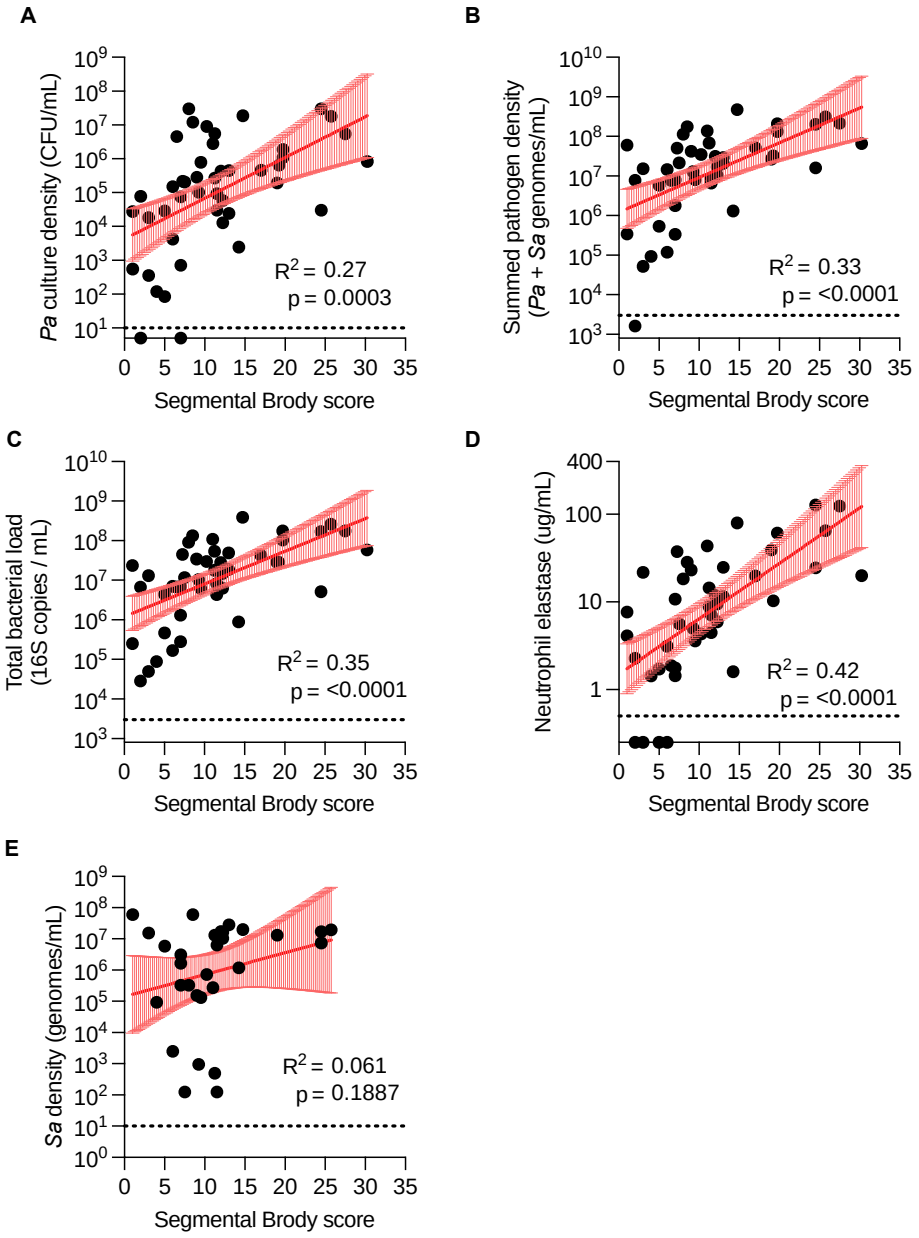

Figure 4. Associations between pre-ETI segmental damage and measures of bacterial density and inflammation. Black circles represent all lung segments across subjects. Red lines represent the line of best fit and 95% confidence intervals calculated with simple linear regression. Data with a lognormal distribution (all but segmental Brody score) were log transformed before the simple linear regression was calculated. Concentrations expressed per mL BAL fluid. Dashed lines represent the limit of detection. Associations between segmental Brody score and: (A) *Pa* culture density; (B) summed pathogen density; (C) total bacterial

load; (D) neutrophil elastase; and (E) *Sa* density. (E) Data from the 3 subjects who were *Sa*-negative pre-ETI are excluded.

Segmental neutrophil elastase was associated with 3 measures of bacterial density (Fig. 5A-C): *Pa* culture density ($r^2 = 0.28$; $p = 0.0002$), summed pathogen density (*Pa* + *Sa* genome copies) ($r^2 = 0.58$; $p < 0.0001$), and total bacterial load ($r^2 = 0.64$; $p < 0.0001$). Neutrophil elastase correlated weakly with *Sa* density when *Sa*-negative subjects were excluded ($r^2 = 0.16$; $p = 0.03$) (Fig. 5D), however this association may be complicated by co-infection with *Sa* and *Pa* in these subjects. These results show that Pa infection, inflammation, and damage are highly associated before ETI treatment, with lung regions with higher bacterial density and neutrophil elastase also showing more extensive structural lung disease.

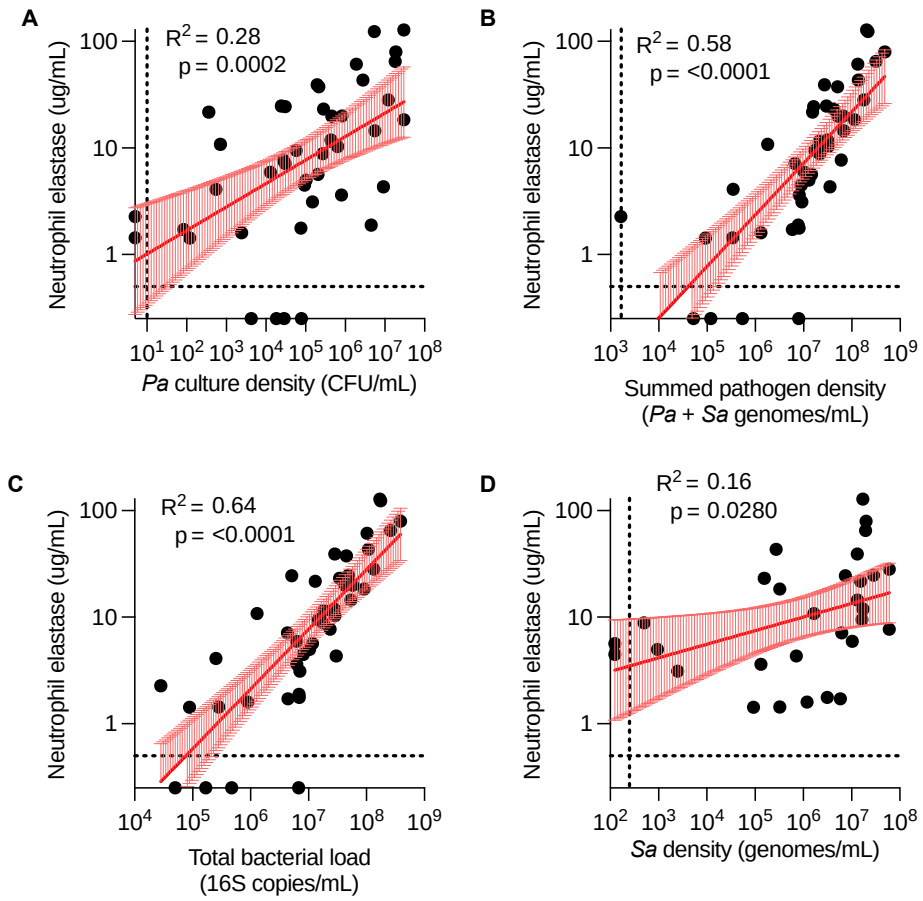

Figure 5. Associations between pre-ETI inflammation and measures of bacterial density. Black circles represent all lung segments across subjects. Red lines represent the line of best fit and 95% confidence intervals calculated with simple linear regression. All data were log transformed before the simple linear regression was calculated. Concentrations expressed per mL BAL fluid. Dashed lines represent the limit of detection. Associations between neutrophil elastase and: (A) *Pa* culture density; (B) summed pathogen density; (C) total bacterial load; and (D) *Sa* density. In (D), data from the 3 subjects who were *Sa*-negative pre-ETI are excluded.

Lung function and sweat chloride improve after subjects started ETI.

We measured lung function and sweat chloride responses to gauge clinical responses to ETI in the cohort. Average FEV_1pp improved from 68.2% (58.2 – 80.6%) to 84.4% (68.3 – 121.4%) (mean change +16.2%), and average sweat chloride decreased from 95.6 mM (68.0 – 131.0 mM) to 35.9 mM (16.5 – 72.0 mM) (mean change -59.7 mM). After ETI, all but 1 subject had sweat chloride values less than the diagnostic cutoff for CF (60 mM). These responses are comparable the those seen in large clinical studies of ETI's effects (104, 232).

Pathogen density and inflammation in lung segments decrease after ETI.

Previous work showed that modulators reduce sputum pathogen density, but responses have not been examined at the level of individual lung segments, so the effects of local conditions on infection responses could not be determined. In addition, less is known about modulators' effects on lung inflammation than on infection.

We began by examining all individual lung segments and found *Pa*, *Sa*, summed pathogens, total bacterial load, NE, and Brody scores all significantly declined after ETI (Fig 6). Average decrease in *Pa* was -2.3 $\log_{10}$ CFU/mL, in *Sa* was -3.0 $\log_{10}$ genomes/mL, in summed pathogens was -2.4 $\log_{10}$ genomes/mL, in total bacterial load was -1.9 $\log_{10}$ 16S copies/mL, in NE was -0.9 $\log_{10}$ ug/mL, and in Brody was -3.3 points. However, there was substantial heterogeneity in changes among the lung segments. For example, *Pa* CFU/mL changes in individual lung regions ranged from a 6.8 $\log_{10}$ reduction to a 2.6 $\log_{10}$ increase (Fig. 7A); neutrophil elastase $\log_{10}$ ug/mL changes ranged from a 2.7 $\log_{10}$ reduction to a 1.1 $\log_{10}$ increase (Fig. 7E); and segmental Brody score changes ranged from a 11- point reduction to 7- point increase (Fig. 7F).

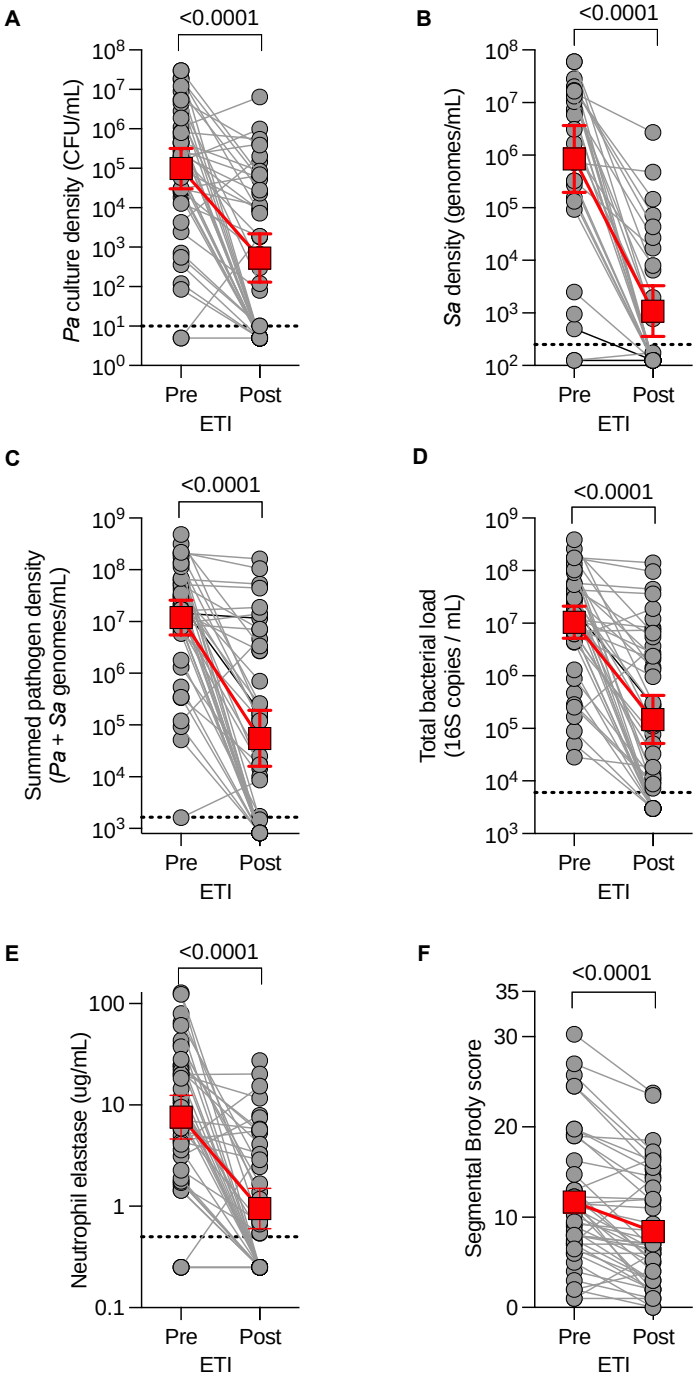

Figure 6. Bacterial density, inflammation, and structural lung damage decline after 1.5 years of ETI.

Red lines and squares indicate the geometric mean (A to E) or mean (F). Gray circles represent lung segments. Dotted lines represent the limit of detection. Concentrations expressed per mL of BAL fluid. (A) *Pa* culture density. (B) *Sa* density. Data from the 3 subjects who were *Sa*-negative pre-ETI are excluded. (C) Summed pathogen density. (D) Total bacterial load. (E) Neutrophil elastase. (F) Segmental Brody score.

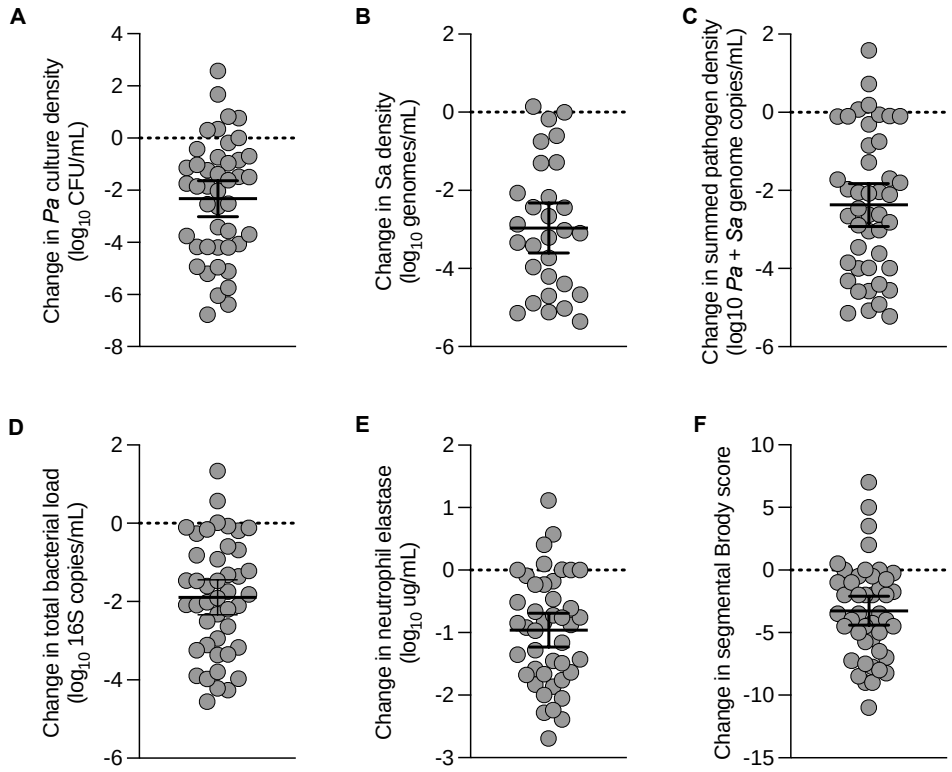

Figure 7. Lung segments exhibit marked heterogeneity in change in bacterial density, inflammation, and structural lung damage after ETI. Gray circles represent lung segments. Black lines and bars represent mean and 95% confidence intervals, respectively. Concentrations expressed per mL BAL fluid. Dashed lines represent no change. All changes were significant at $p < 0.0001$. Change in: (A) *Pa* culture density; (B) *Sa* density; (C) summed pathogen density; (D) total bacterial load; (E) neutrophil elastase; (F) segmental Brody score. (B) Data from the 3 subjects who were *Sa*-negative pre-ETI are excluded.

Subjects generally clear infection from all or none of their lung regions

We hypothesized that differential responses could be driven by characteristics inherent to individual subjects. For example, subjects could differ in improvement in CFTR activity, or innate or adaptive immune functioning. In addition, CF *Pa* strains can vary in pathogenesis phenotypes such as growth rate, resistance to host defenses, capacity for nutrient acquisition and other factors. Since the individuals in our study were infected by different *Pa* strains, “by subject” response variation includes “by strain” differences.

To examine the effect of subject-level factors on infection clearance, we plotted the changes in *Pa* and *Sa* densities by subject. Despite targeting regions representing the extremes of disease in each subject, we found a strong “by subject” pattern. In three of 9 subjects, *Pa* became undetectable after ETI in all targeted segments, including each of those subjects’ segments with the most severe disease (Fig. 8A). In the remaining 6 subjects, only 2 additional regions cleared. *Sa* followed a similar pattern (Fig. 8B). In 3 subjects, nearly all regions became negative by species-specific PCR. In the remaining 3 subjects who were *Sa*-positive pre-ETI, most regions remained *Sa*-positive. Notably, 2 of the 3 subjects who cleared *Sa* also cleared *Pa* (Subjects 1 and 7) while the remaining subject remained *Pa* positive in all 5 regions (Subject 5). Thus, subjects generally cleared both *Sa* and *Pa* infections from all or none of the targeted regions, and persistent infection in these ETI-treated subjects was not localized to particular lung regions.

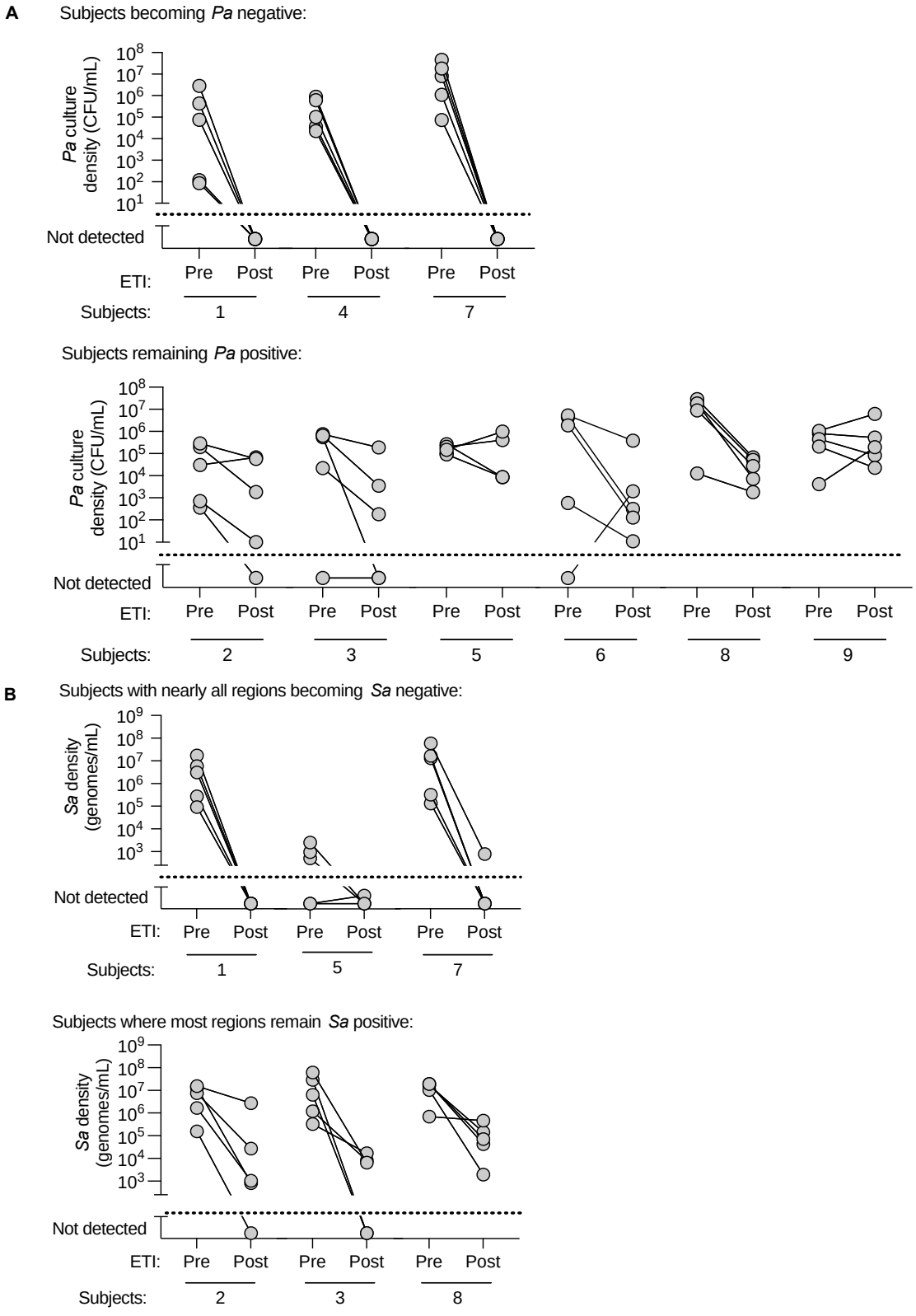

Figure 8. Subjects generally cleared *Pa* and *Sa* from all or none of their regions. Data is shown by subject. Each circle represents a lung segment. Dashed lines represent limit of detection. (A) *Pa* culture

density by subject. Top half of panel shows subjects who cleared *Pa* and bottom half panel shows subjects who remain infected. (B) *Sa* density by subject. Top half of panel shows subjects who cleared *Sa* and bottom half panel shows subjects who remain infected.

Subjects becoming *Pa* negative have lower pre-ETI total lung damage

We investigated whether subjects who became *Pa* culture negative in all targeted regions were outliers in any other characteristics, which could suggest traits predisposing to infection clearance. We compared subjects' sweat chlorides pre-ETI, post-ETI, and their ETI-mediated changes in sweat chloride (Fig. 9A-C). We also compared pre-ETI lung function, age, and BMI (Fig. 9D-F). The 3 subjects becoming *Pa*-negative were not outliers in any of these parameters.

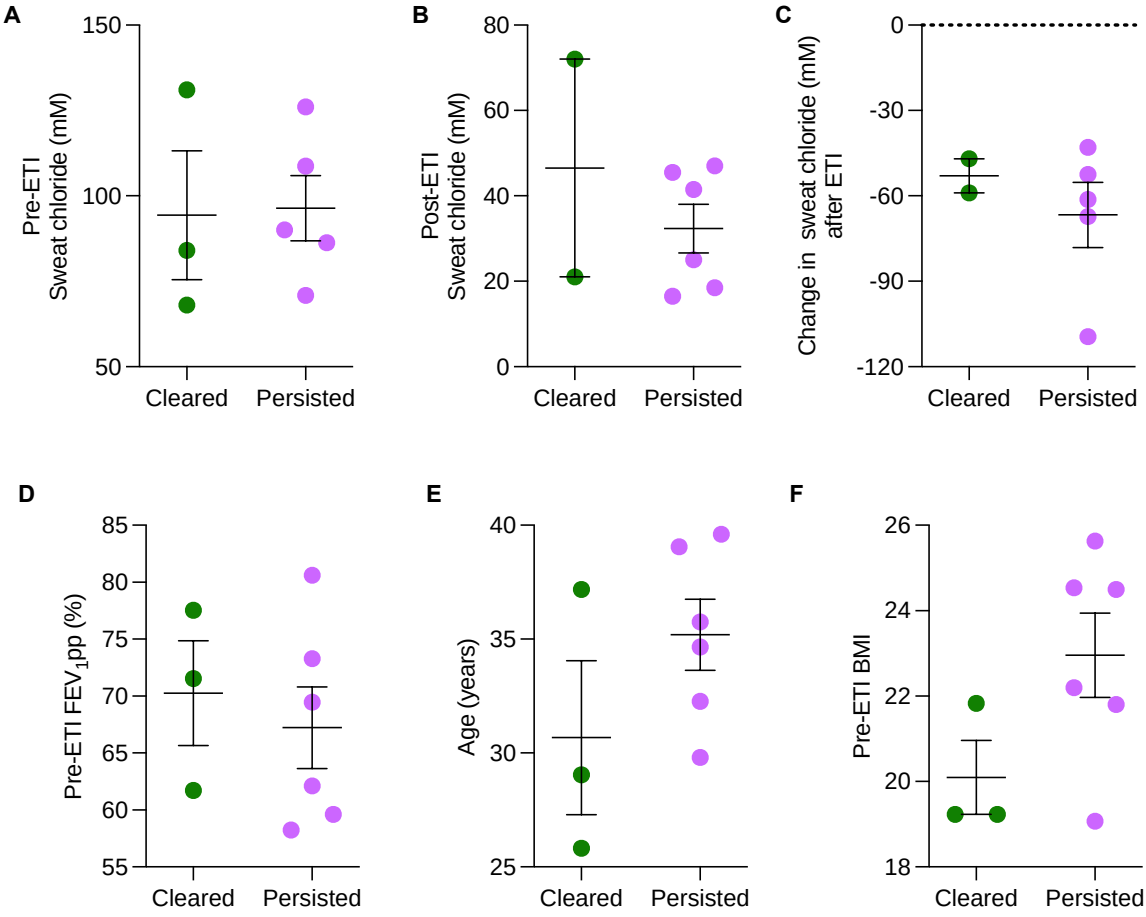

Figure 9. Clinical characteristics of subjects who cleared *Pa*. Circles indicate individual subjects; black lines and bars represent mean and standard error of the mean (SEM), respectively. (A) Pre-ETI sweat chloride. (B) Post-ETI sweat chloride. (C) Change in sweat chloride. (D) Pre-ETI FEV_1 percent predicted. (E) Age at study start. (F) Pre-ETI BMI.

However, subjects becoming *Pa*-negative had among the lowest pre-ETI total Brody scores, when the whole lung (as opposed to targeted segments) was analyzed. They also had lower pre-ETI Brody bronchiectasis sub-scores (Fig. 10A and B). Notably, these subjects did not experience a greater change in whole lung Brody score after ETI (Fig. 10C). These data suggest that subjects who cleared *Pa* had lower overall pre-existing lung damage.

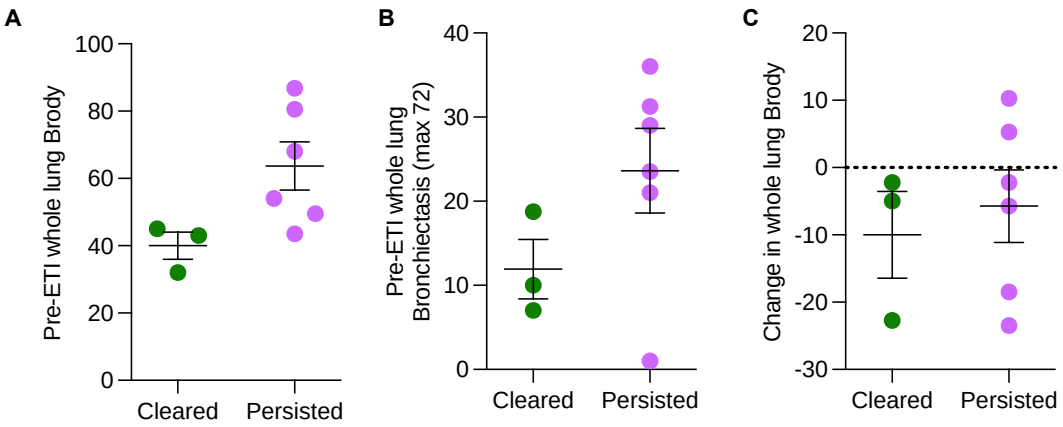

Figure 10. Subjects who cleared *Pa* had lower starting whole lung Brody scores. Circles indicate individual subjects; black lines and bars represent mean and standard error of the mean (SEM), respectively. (A) Pre-ETI whole lung Brody score. (B) Pre-ETI whole lung Brody bronchiectasis subscore. (C) Change in whole lung Brody score.

After ETI, inflammation is strongly associated with persistent infection

Lung inflammation that persists after ETI treatment will likely compromise subject's future health by causing local tissue damage and because of inflammation's systemic effects. NE is predictive of long-term outcomes in CF and in non-CF bronchiectasis (39, 244). We thus examined associations between segmental NE, bacterial density, and Brody score.

We first plotted changes in NE by subject, and found a strong "by subject" pattern that mirrored the infection clearance pattern. In subjects in whom *Pa* became undetectable throughout lungs (Subjects 1, 4, and 7), NE generally became undetectable as well. In contrast, NE remained elevated in subjects in whom *Pa* persisted. The one subject in whom *Sa* became undetectable but *Pa* persisted (Subject 5) exhibited NE changes that were comparable to the subjects who remained *Pa* positive.

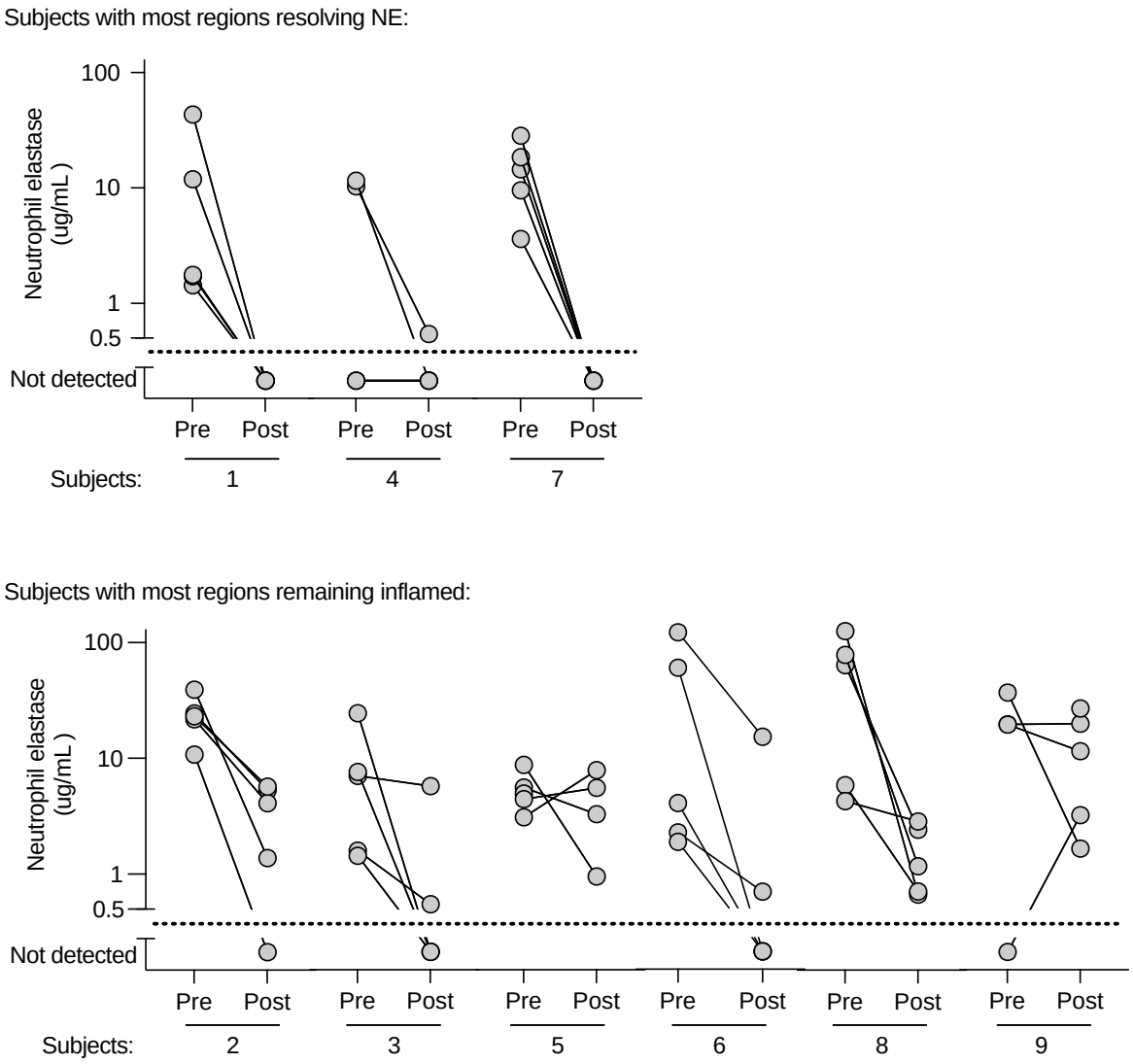

Figure 11. Subjects resolve inflammation in nearly all or few of their regions. Data is shown by subject. Each circle represents a lung segment. Dashed lines represent limit of detection. Top half of panel shows subjects who resolved NE in most regions and bottom half panel shows subjects with most regions remaining inflamed.

We then asked whether the bacterial density could explain inflammatory marker concentration. We found that *Pa* culture density ($r^2 = 0.76$; $p < 0.0001$), summed pathogen density ($r^2 = 0.85$; $p < 0.0001$), and total bacterial density ($r^2 = 0.72$; $p < 0.0001$) (Fig. 12A-C) were all strongly associated with segmental NE levels. NE also correlated with segmental Brody score, though less strongly ($r^2 = 0.30$; $p = 0.0001$; Fig. 12D). Notably, the slope of the linear regression between *Pa* culture density and NE was nearly identical before and after ETI (pre-ETI slope: 0.22; post-ETI slope: 0.28) indicating that the increase in NE per unit increase in *Pa* density is unchanged with ETI treatment. This suggests that ETI does not alter neutrophilic responses to *Pa*. These data suggest that pathogen density may be a key driver of inflammation in the post-ETI lung.

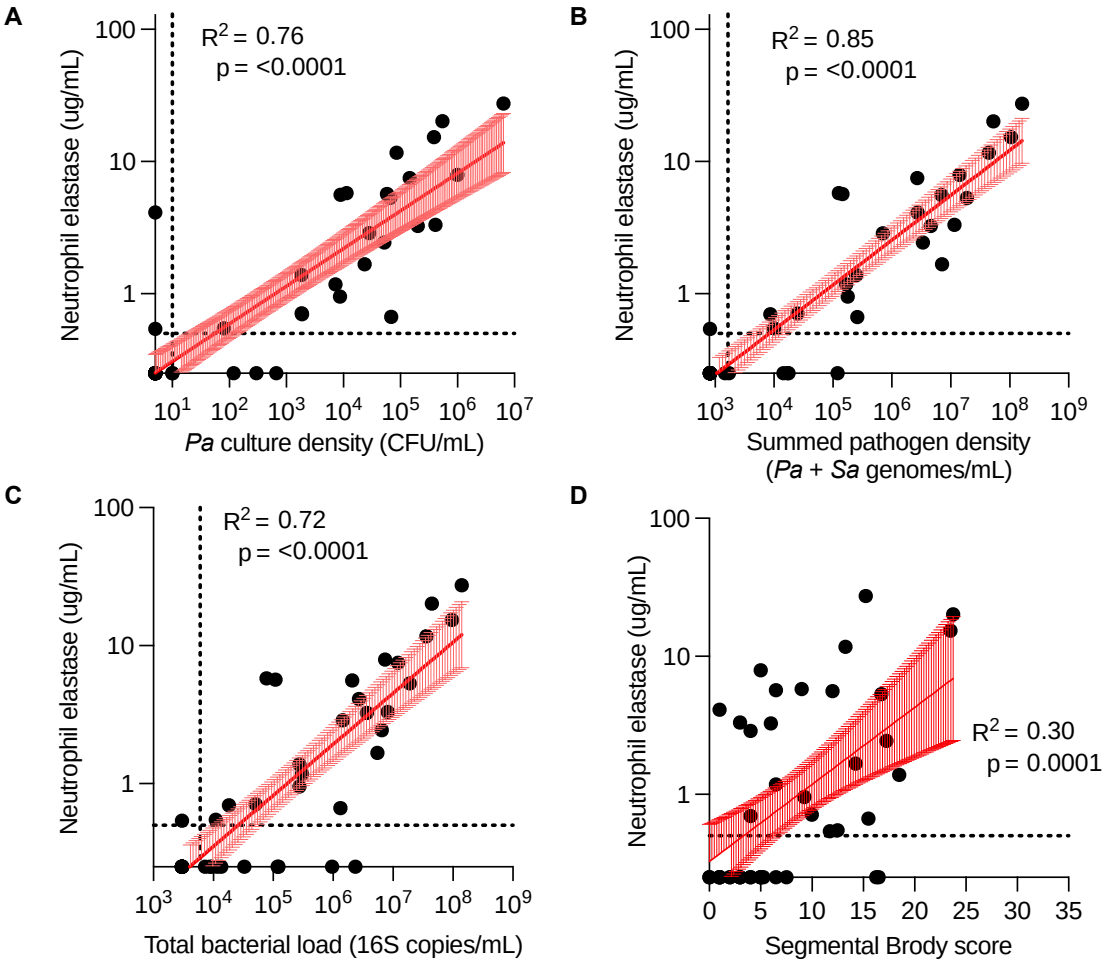

Figure 12. After ETI, neutrophil elastase is strongly associated with bacterial density. Black circles represent lung segments across all subjects. Red lines represent the line of best fit and 95% confidence intervals calculated with simple linear regression. Data with a lognormal distribution (all but segmental Brody score) were log transformed before linear regression was calculated. Concentrations expressed per mL BAL fluid. Dashed lines represent the limit of detection. Associations between neutrophil elastase and (A) *Pa* culture density; (B) summed pathogen density; (C) total bacterial load; and (D) segmental Brody score.

High and low damage regions within subjects respond similarly to ETI.

Finally, while infection clearance (as defined by *Pa* and *Sa* becoming undetectable), and complete resolution of NE was generally a “by subject” phenomenon (i.e. subjects generally cleared all or none of their targeted regions), the extent of decline in these parameters could also depend on the extent of pre-existing lung damage. We tested this idea in two ways. First, we examined changes in *Pa* and *Sa* density, summed pathogen density, total bacterial load, and NE levels in the high and low damage lung regions from all subjects as separate groups, identifying no differences (Fig. 13A-F).

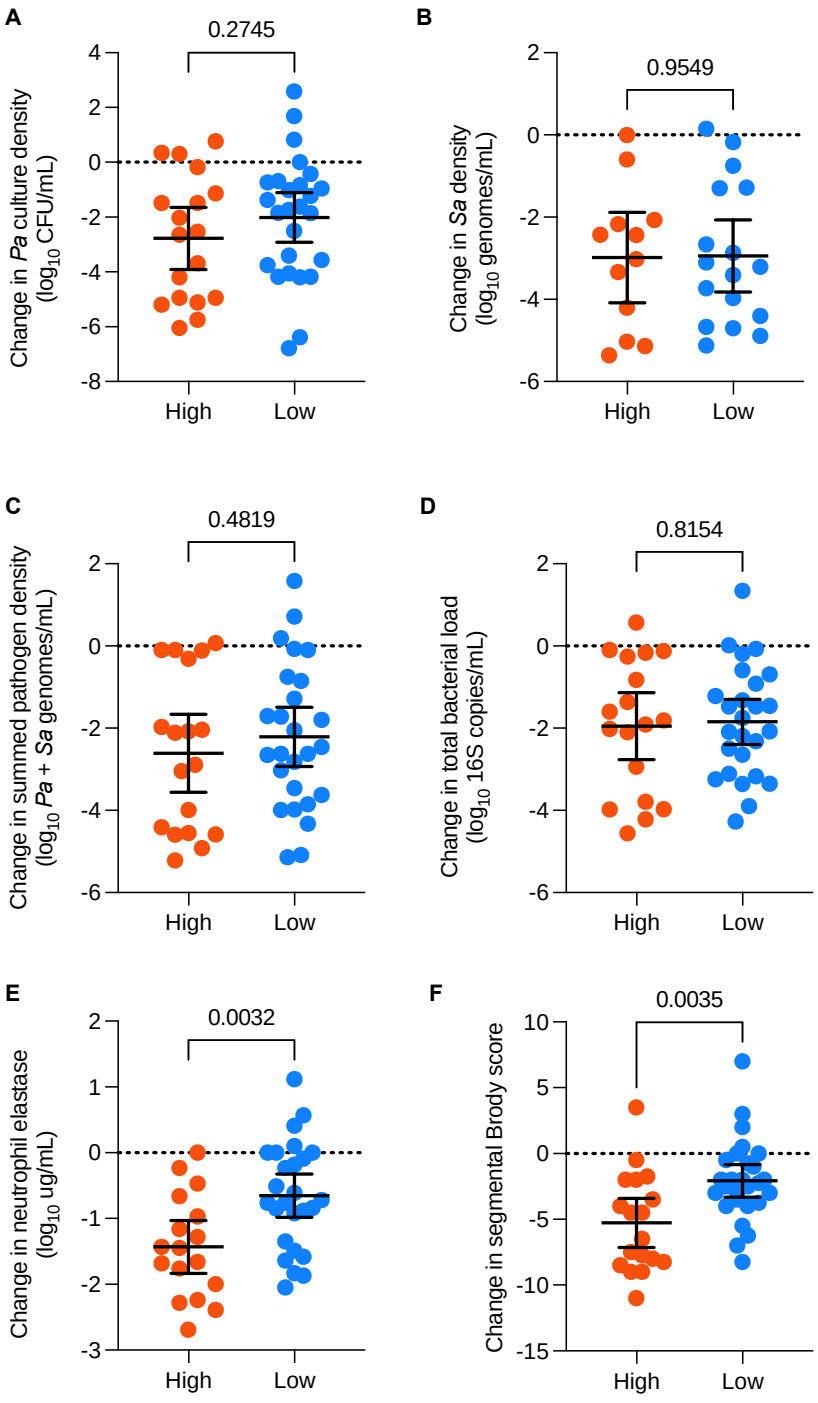

Figure 13. High and low damage regions within subjects respond similarly to ETI. High and low based on initial selection (see Fig. 2). Each circle represents a lung segment. Black lines and bars indicate mean and 95% confidence interval, respectively. P values were calculated with unpaired t-test. Concentrations expressed per mL BAL fluid. Dashed lines represent no change. Change in: (A) *Pa* culture density; (B) Sa density; (C)

Summed pathogen density; (D) Total bacterial load; (E) Neutrophil elastase; (F) Segmental Brody score. (B) Data from the 3 subjects who were *Sa*-negative pre-ETI are excluded.

Second, we investigated whether the lowest damage targeted regions experienced a larger decline in *Pa* and *Sa* density than the highest damage regions within each subject. However, neither the high or low damage regions within subjects consistently experienced greater reductions in *Pa* or *Sa* density after ETI (Fig. 14). Neither infection clearance (as defined by conversion to culture negative status) nor quantitative reductions in pathogen density appeared to be related to extent of pre-existing lung damage. Future work will investigate other factors that might affect infection outcomes after ETI (see discussion).

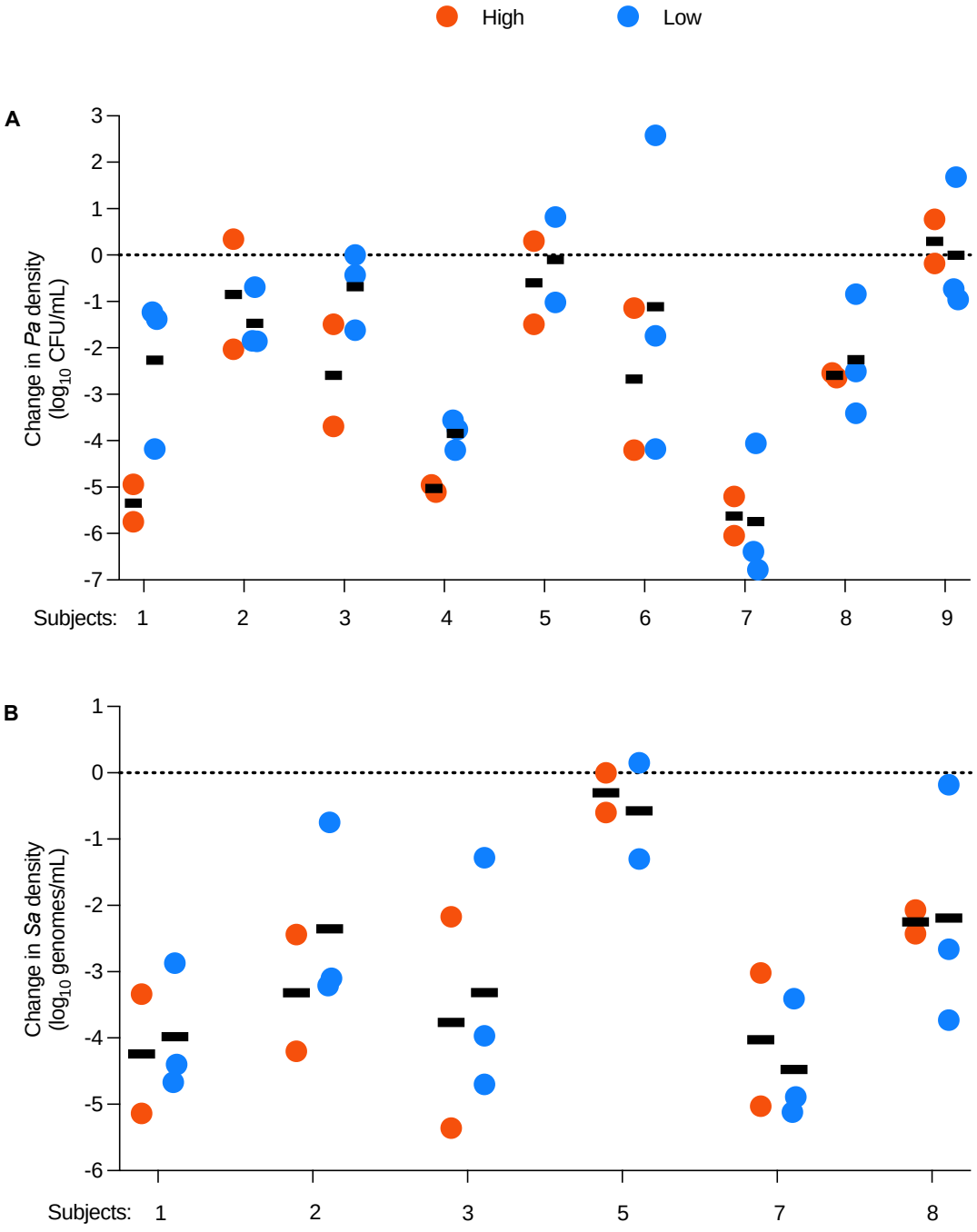

Figure 14. Change in bacterial density in high and low damage regions, displayed by subject. High and low damage based on initial selection (see Fig. 2). Each circle represents a lung segment. Black lines indicate mean. Concentrations expressed per mL BAL fluid. Dashed lines represent no change. Change in: (A) *Pa* culture density and (B) *Sa* density. (B) Data from the 3 subjects who were *Sa*-negative pre-ETI are excluded.

Discussion

Here, we performed a bronchoscopy study to sample the most and least structurally damaged lung regions within subjects before and 1.5 years after they started ETI. This work produced several findings. First, we found marked intra-lung heterogeneity in bacterial density, inflammation, and structural lung damage before ETI treatment and found strong positive associations between lung damage, bacterial density, and inflammation. Second, we found that when infection persists after ETI, it generally persists in all lung regions rather than persisting in only certain (e.g. the high damage) regions. Third, we found that persistent inflammation was strongly associated with persistent infection after ETI. Neutrophil elastase was almost never detected in *Pa*-free regions, while it was detected in most regions with persistent pathogens. Fourth, we found that the slope of the linear regression between *Pa* and neutrophil elastase was nearly identical before and after ETI. This indicates that the increase in neutrophilic inflammation per unit bacterial density was unchanged by ETI, which suggests that ETI did not alter the magnitude of the neutrophilic response to *Pa*. Finally, we found that within subjects the highest and lowest damage regions responded similarly to ETI, as measured by infection clearance, decrease in bacterial density and neutrophilic inflammation, and improvement in lung damage score.

Results presented in this thesis chapter are part of ongoing analyses. One important future direction will be to broaden our studies related to inflammation. In particular, I think it is important to investigate whether other markers of inflammation (e.g. indicators of Th1, Th2, and Th17 inflammation) show similar responses as NE both in terms of general decline after ETI, and elevation in segments that remain *Pa*-positive. A related question is whether a more comprehensive analysis of inflammatory markers will identify any type of persistent inflammation in lung segments that become *Pa*-negative after ETI.

In other ongoing analyses, we are further exploring the potential effects of pre-ETI regional heterogeneity on infection outcomes. While we found that conversion to *Pa*-culture-negative was largely a “by-subject” phenomenon, there was still a great degree of heterogeneity in the change in regional bacterial density within subjects. Our preliminary analysis found that radiologist scoring of regions as high vs low damage could not explain the heterogeneity in changes in bacterial density. However, several additional

parameters could influence the change in regional bacterial density after ETI, including pre-ETI bacterial load, inflammation (measured with NE and a panel of additional cytokines), nutritional environment, and different types of lung damage, such as small airways disease. Current work is investigating this possibility.

Our study had several limitations. First, the overall intensity of the study limited the number of subjects we could enroll. However, by sampling 5 lung regions per subject we increased our total number of observations and having multiple samples from a single subject allowed us to partially control for patient-to-patient variability in pre-ETI disease course. Second, we specifically selected patients with a known history of chronic *Pa* infection, so our findings may not apply to other organisms. However, *Pa* infections are common and are the CF infections most strongly linked to lung disease progression. We also included measurements of *Sa*, the most common CF pathogen, when possible. Third, we only sampled at two timepoints, separated by 1.5 years. This prevented us from distinguishing between short-term, likely direct effects of ETI and long-term effects that may be influenced by those short-term changes. However, long-term outcomes are important to understand as they are likely to influence patients' overall health and lifespan. Finally, we lacked a control group that was not prescribed ETI. However, other studies of CF have not observed changes in sputum bacterial density in the control group (22), suggesting it is unlikely that the changes observed here are due to study participation.

Our study also has several key strengths. First, the granularity of the study design allowed us to specifically co-locate infection, inflammation, and structural lung damage, without the concern of mixing segmental secretions, as likely occurs with sputum, which could obscure differential outcomes. Given the heterogeneity in regional lung disease we found before ETI, sputum may not fully reflect regional responses to ETI. Second, the use of bronchoscopy with a cuffed endotracheal tube also reduced contamination with upper airway secretions, again overcoming a disadvantage of sputum-based analyses. Third, we were able to capture the pre-ETI timepoint, which may be difficult in the future as ~90% of patients in the US are eligible for highly effective CFTR modulators now, including children as young as six years old. Capturing the pre-ETI timepoint also means that each lung region was able to

serve as its own control, which is significant as most bronchoscopy studies in adults are cross-sectional. Fourth, we often used multiple assays to measure our parameters of interest, increasing confidence in the results. For example, we used a combination of quantitative bacterial culture and multiple quantitative DNA-based assays, and analysis of multiplex cytokine panels are in progress to complement NE assays. Finally, our subjects were relatively homogeneous in terms of age and lung function, which limited the effects of these potential confounding factors on our measurements.

Our results demonstrate that structural lung damage, infection, and inflammation persist in most lung regions of subjects after correcting CFTR, suggesting that these pathologies do not become restricted to areas of pre-existing high damage, as has been postulated. Additionally, we found that inflammation was strongly associated with infection after ETI. This finding suggests that infection will remain a key driver of inflammation and structural lung disease progression in the post-modulator era. Future research will be needed to further address how infections are able to persist in the face of CFTR-corrected host defenses, and how to therapeutically target those functions. It will likely be of great importance to develop eradication protocols for those people who are already infected when they begin modulator therapy.

Methods

Study approval. Institutional review board approval at participating sites and written informed consent from participants were obtained prior to study participation. Study subject inclusion and exclusion criteria are listed in Table 3.

Table 3. Study subject inclusion and exclusion criteria.

Inclusion criteria

• Male or female 12-60 years of age at time of consent.
• Documentation of a CF diagnosis as evidenced by one or more clinical features consistent with CF and one or more of the following criteria:
  • Sweat chloride ≥ 60 mEq/L by quantitative pilocarpine iontophoresis test (QPIT).
  • Two well-characterized mutations in the cystic fibrosis transmembrane conductive regulator (CFTR) gene.
  • Abnormal nasal potential difference (change in NPD in response to a low chloride solution and isoproterenol of less than -6.6 mV).
• Confirmed genotype of recruitment focus (F508del/F508del or F508del/minimal function CFTR mutation).
• Subject is a candidate to begin ETI therapy as determined by their primary treating CF physician.
• FEV_1 percent predicted of >50%.
• Confirmed bronchiectasis by historical CT or chest X ray.
• Chronic Pa infection and generally sputum producing. Chronic Pa infection is defined as >50% of cultures positive for Pa for a minimum of one preceding year.
• Stable healthcare regimen for 28 days (patients may be cycling inhaled antibiotics as part of their chronic Pa management regimen).
• Written informed consent (and assent when applicable) obtained from subject or subject's legal representative and ability to comply with the requirements of the study.
• Willingness to consider travel if needed to reach the participating CF center for study participation.
• Willing to hold oral, inhaled, and IV antibiotics (except oral azithromycin) for 2 weeks prior to bronchoscopy and BAL.

Table 3 cont. Study subject inclusion and exclusion criteria.

Exclusion criteria

• Presence of a medical condition, abnormality, or laboratory value(s) in the opinion of the onsite principal investigator and/or collaborating bronchoscopist may compromise the quality of the data or place the subject at significant risk by undergoing the research related bronchoscopy, including:
  • History of life-threatening hemoptysis (ICU admission for hemoptysis, > 240 ml over 24 hours, reduction in hemoglobin >4 gm/dL, hemoptysis-related chest X-ray changes) over the prior six months
  • Any of the following abnormal lab values at screening:
  • Platelets < 50 x 10^3/µL
  • Hemoglobin < 10 gm/dL
  • Hematocrit < 30%
  • WBC > 20 x 10^3/µL
  • Neutropenia (ANC < 1.5 x 10^3/µL)
  • Lymphopenia (absolute lymphocyte count < 1.5 x 10^3/µL)
  • PT/INR > 1.5
  • Other known bleeding diathesis

• Positive pregnancy blood test (for female of childbearing potential) at the study visit.
• Breastfeeding.
• Current use of drugs with significant risks of compromising immunity (e.g. oral steroid use) for >14 days prior to bronchoscopy
• History of organ transplant.
• Use of oral anticoagulant medications (e.g.: warfarin, aspirin, other platelet inactivators) within seven days prior to bronchoscopy.
• History of lung mycobacterium infection requiring antibiotic treatment in prior year.
• Unable or unwilling to withhold use of oral anticoagulant medications within seven days after bronchoscopy.
• Unable or unwilling to withhold use of oral, inhaled and IV antibiotics (except oral azithromycin) 2 weeks prior to the sputum collections and bronchoscopies.

Computed tomography scans and scoring. Low dose CT scanning protocol was adapted from the protocol used for the multi-center SPIROMICS trial and consisted of obtaining multi-detector CT (MDCT) images of the entire lung at full inspiration (total lung capacity or TLC) and at Functional Residual Volume (RV). Scans were collected at 120 kV and current of 110 mA for inspiratory scans and 65 mA for expiratory scans. The slice thickness was 0.625 mm with an interval of 0.5 mm and a pitch of 0.984:1. Spatial resolution was matched at baseline and follow-up using a similar diameter field of view for both scanning sessions. Scans were reconstructed with filtered back projection and standard kernel. Subjects were instructed in specialized breathing techniques to acquire the scans. Briefly, the subject was instructed to inhale deeply and exhale 2 times and then hold their breath one of two different ways: with the lungs full of air (TLC) and at the end of a full expiratory effort (RV). Finally, scans were de-identified prior to transfer between the University of Washington, University of Iowa, and University of Cincinnati for subsequent analyses.

The scans were initially examined by an expert radiologist and CF clinician who selected the 2 “highest damage” and 3 “lowest damage” lung segments for sampling (excluding the lower lobes). This first selection was purely subjective, and only completed on the pre-ETI scans for the sole purpose of identifying lung segments to sample via bronchoscopy.

Scoring of the CT scans for quantitative measures of lung damage was subsequently completed in two ways by a second expert radiologist, who was blinded to the first radiologist’s assessment of degrees of damage across the regions. First, total structural lung disease was assessed via standard Brody score applied to the entire lung CT. The Brody score consists of 5 measures of CF-related lung pathologies visible on CT scans: bronchiectasis, peri-bronchial wall thickening, mucus plugging, parenchymal damage, and air trapping (229). Second, segmental lung disease was assessed via Brody score applied to segmental scans. Segmental delineation of CT’s was done with Apollo software (VIDA Diagnostics), and then the segmental scans were sent to the second expert radiologist for Brody scoring applied to each of the 5 sampled lung segments.

Bronchoscopy. Subjects underwent bronchoscopy under anesthesia with a cuffed endotracheal tube (ETT) in place utilizing established procedures standard at each study institution. BAL fluid samples were

obtained via sterile single use/disposable bronchoscopes (Ambu, Ballerup Denmark). Lavage volumes were 20mL of normal saline per region, and did not exceed 100mL/ subject to reduce risk of lung edema. The 2 “most diseased” and 3 “least diseased” lung segments were sampled. Most and least diseased were based on subjective review of pre-ETI CT scans, as described above.

BAL fluid processing for quantitation of bacterial density and inflammatory biomarkers, and culturing of *Pa*. BAL fluid was homogenized with needle and syringe. One aliquot of homogenized BAL fluid was serially diluted and plated on MacConkey agar (Difco) to quantify *Pa*. Homogenized BAL aliquots were also processed for quantification of sputum inflammatory markers and DNA extraction (see below).

Quantification of BAL fluid inflammatory biomarkers. BAL fluid was processed according to the CF Therapeutics Development Network Coordinating Center standard operating procedure. Briefly, aliquots of BAL fluid were centrifuged at 250xg for 10 min at 4°C, and supernatants were then centrifuged at 4000xg for 20 min at 4°C. Supernatants from the second spin were frozen directly at -80°C until analysis. Specimens were analyzed for free neutrophil elastase (NE) activity [Spectrophotometric assay, Sigma Diagnostics; St. Louis, MO]. The lower limit of detection for this assay was 0.5 ug/mL free neutrophil elastase.

Bacterial DNA extraction. DNA was extracted from 200uL whole BAL fluid using the Qiagen DNeasy PowerSoil Pro Qiacube Kit and eluted in 100uL Solution C6 (10 mM Tris). The purified DNA sample was stored at -20°C.

Bacterial quantification. In addition to the culture-based quantification of *Pa* described above, we also measured bacterial density using 4 additional DNA-based droplet digital PCR (ddPCR) assays: total bacterial load, *Sa* density, *Pa* density, and a “summed pathogen” density, where the *Pa* and *Sa* DNA-based densities were added together. Total bacteria, *Pa*, and *Sa* were quantified using previously validated primers and probes (Table 3) (125, 164). For most samples, ddPCR was performed using 1 uL

of undiluted DNA (BioRad QX200 ddPCR system) using the ddPCR Multiplex Supermix (BioRad). The PCR was performed following manufacturer's recommendations for cycling conditions, with an annealing temperature of 56°C and extension time of 1 minute. Results were analyzed with QX software to determine target DNA concentrations. Positive controls (DNA isolated from bacterial cultures) and negative controls (no sample added) were run with each assay.

Table 4. Primers used in this study.

Primer set	Sequence
16S PCR for sequencing	Forward: TCGTCGGCAGCGTCAGATGTGTATAAGAGACAGCCTACGGGNGGCWGCAG Reverse: GTCTCGTGGGCTCGGAGATGTGTATAAGAGACAGGACTACHVGGGTATCTAATCC
P. aeruginosa ddPCR	Forward: CCGTGGTGGTAGACCTGTTCCCAGACC Reverse: CGCAGCAGGATGCCGACGCC Probe: CCGTGGTGGTAGACCTGTTCCCAGACC
S. aureus ddPCR	Forward: GCGATTGATGGTGATACGGTT Reverse: AGCCAAGCCTTGACGAACTAAAGC Probe: GGTGTAGAGAAATATGGTCCTGAAGCAAGT
16S ddPCR	Forward: TCCTACGGGAGGCAGCAG Reverse: GGACTACCAGGGTATCTAATCCTGTT Probe: CGTATTACCGCGGCTGCTGGCA

Spirometry. Spirometric measurements were obtained in accordance with the American Thoracic Society Standards (226). The forced expiratory volume in one second percent predicted (FEV_{1pp}) values are based on the GLI 2012 values for adults (227).

Sweat chloride measurements. Pre-ETI sweat chloride values were obtained from subjects' medical records. Post-ETI sweat was collected with the Macroduct® collection system (Wescor, Logan UT), and sweat chloride levels were measured using routine standard laboratory techniques.

Statistics. All data with a lognormal distribution were log-transformed before statistical analyses were performed. Simple linear regressions were used to test for associations between quantitative parameters. Pre vs post p-values were calculated with paired t-test, and 2-tailed p-values are reported. High vs low p-values were calculated with unpaired t-test, and 2-tailed p-values are reported. All statistical analyses were performed in Prism (Graphpad).

CHAPTER 5: Conclusions & Future Directions

Overview

This is an exciting era for cystic fibrosis research and treatment. The development of CFTR modulators, the first successful drugs to correct the physiologic defect in CF, offers great hope to people with CF. Many clinical measures of health improve, including lung function, nutritional status, and frequency of disease flares ("exacerbations") (104, 108, 192, 232, 246). Unfortunately, despite marked improvements in overall health, there are hints that full health may yet be out of reach. In people taking ivacaftor, lung function continues to decline (247). Many patients remain infected with their chronic bacterial pathogens, and these patients' lungs generally remain inflamed (108, 125, 164). In the pre-modulator era, infection and inflammation were the main drivers of lung disease progression and ultimately death (32–34). The failure of modulators to resolve these pathologies suggests that lung disease may continue to progress even in those patients who are able to access CFTR modulators.

The work in this thesis has contributed to our understanding of persistent infection and inflammation after treatment with CFTR modulators, and highlights some of the challenges and opportunities that lay ahead. In chapter 2, we developed a method to enumerate and quantify the bacterial strains present in a pool of thousands of cultured isolates or directly from sputum of people with CF. In chapter 3, we tested an eradication protocol that combined intensive antibiotic treatment with initial modulator therapy. In chapter 4, we sampled many lung regions within each subject to identify characteristics of regions which remain persistently infected compared to those that clear infection. This work sets the stage for several exciting future directions.

Future directions

The most exciting future direction to me is to understand why CF infections persist after modulator treatment. Using bronchoscopy sampling, we found that when infections persisted after ETI, they persisted in nearly all sampled lung regions, including those with the mildest damage. This was surprising because high damage regions often contain permanently damaged local epithelia, airway structure, and vascular supply, so we expected that high damage regions may not respond well to ETI.

While a straightforward explanation for these results is that the *Pa* subpopulations inhabiting individual lung regions persist after treatment, a possible alternative hypothesis is that *Pa* from particular regions preferentially survive post-ETI, and subsequently re-colonize other lung regions. This is of interest because it raises the possibility that regionally localized host conditions or bacterial functions could be targeted to reduce post-ETI infection. These two possibilities could be distinguished using genetic relatedness of the pre- and post-ETI *Pa* populations.

I have begun to investigate this by collecting ~100 *Pa* isolates/ region/ timepoint, and generating whole genome sequences from these isolates. Analyzing phylogenetic trees inferred from those sequences could distinguish which pre-ETI regional populations the post-ETI populations are descended from. If we found that most regional subpopulations persisted, it would suggest that either modulators cannot generally correct host defense defects, or that many bacterial subpopulations are capable of resisting modulator-corrected host defenses. However, if only certain regional subpopulations persist and colonize other regions via migration, it would suggest that either certain regional characteristics predispose to persistence or certain *Pa* subpopulations can resist corrected host defenses. These possibilities could be further distinguished by identifying commonalities among regions and/or subpopulations that give rise to migrants.

Final remarks:

In this work we have demonstrated the recalcitrance of chronic infections to eradication, even in the face of a corrected host defect. We developed a method to improve our understanding of strain dynamics in post-CFTR modulator infections. We also tested an eradication protocol that combined intensive antibiotics with CFTR modulators. Finally, we identified the characteristics of lung regions with persistent infection and inflammation after correcting CFTR, suggesting mechanisms of their persistence. While not definitive, this study identified interesting associations to be followed up on further. Ultimately, our work suggests that modulators will not resolve all pathologies affecting people with CF and the continued development of anti-infection treatments will be required for patients to achieve full health.

REFERENCES:

1. Guo J, Garratt A, Hill A. Worldwide rates of diagnosis and effective treatment for cystic fibrosis. *J Cyst Fibros* 2022;21:456–462.
2. Andersen DH. Cystic Fibrosis Of The Pancreas And Its Relation To Celiac Disease: A Clinical And Pathologic Study. *Am J Dis Child* 1938;56:344.
3. Andersen DH, Hodges RG. Celiac Syndrome: V. Genetics of Cystic Fibrosis of the Pancreas With a Consideration of Etiology. *Am J Dis Child* 1946;72:62.
4. Kessler WR, Andersen DH. Heat prostration in fibrocystic disease of the pancreas and other conditions. *Pediatrics* 1951;8:648–656.
5. Di Sant'agnese P, Darling RC, Perara GA, Shea E. Abnormal electrolyte composition of sweat in cystic fibrosis of the pancreas. *AMA Am J Dis Child* 1953;86:618–619.
6. Gibson LE, Cooke RE. A test for concentration of electrolytes in sweat in cystic fibrosis of the pancreas utilizing pilocarpine by iontophoresis. *Pediatrics* 1959;23:545–549.
7. Quinton PM. Chloride impermeability in cystic fibrosis. *Nature* 1983;301:421–422.
8. Knowles MR, Stutts MJ, Spock A, Fischer N, Gatzy JT, Boucher RC. Abnormal Ion Permeation Through Cystic Fibrosis Respiratory Epithelium. *Science* 1983;221:1067–1070.
9. Boucher RC, Stutts MJ, Knowles MR, Cantley L, Gatzy JT. Na+ transport in cystic fibrosis respiratory epithelia- Abnormal basal rate and response to adenylate cyclase activation. *J Clin Invest* 1986;78:1245–1252.
10. Itani OA, Chen J-H, Karp PH, Ernst S, Keshavjee S, Parekh K, *et al.* Human cystic fibrosis airway epithelia have reduced Cl^- conductance but not increased Na^+ conductance. *Proc Natl Acad Sci* 2011;108:10260–10265.
11. Kerem B, Rommens JM, Buchanan JA, Markiewicz D, Cox TK, Chakravarti A, *et al.* Identification of the cystic fibrosis gene: genetic analysis. *Science* 1989;245:1073–1080.
12. Riordan JR, Rommens JM, Kerem B, Alon N, Rozmahel R, Grzelczak Z, *et al.* Identification of the cystic fibrosis gene: cloning and characterization of complementary DNA. *Science* 1989;245:1066–1073.

13. Rommens JM, Iannuzzi MC, Kerem B, Drumm ML, Melmer G, Dean M, *et al.* Identification of the cystic fibrosis gene: chromosome walking and jumping. *Science* 1989;245:1059–1065.
14. Tsui LC. The spectrum of cystic fibrosis mutations. *Trends Genet* 1992;8:392–398.
15. Clancy JP, Cotton CU, Donaldson SH, Solomon GM, VanDevanter DR, Boyle MP, *et al.* CFTR modulator theratyping: Current status, gaps and future directions. *J Cyst Fibros* 2019;18:22–34.
16. Welsh MJ, Smith AE. Molecular mechanisms of CFTR chloride channel dysfunction in cystic fibrosis. *Cell* 1993;73:1251–1254.
17. De Boeck K, Amaral MD. Progress in therapies for cystic fibrosis. *Lancet Respir Med* 2016;4:662–674.
18. Allan JD. Nutritional Supplementation in Treatment of Cystic Fibrosis of the Pancreas. *Arch Pediatr Adolesc Med* 1973;126:22.
19. Fuchs HJ, Borowitz DS, Christiansen DH, Morris EM, Nash ML, Ramsey BW, *et al.* Effect of Aerosolized Recombinant Human DNase on Exacerbations of Respiratory Symptoms and on Pulmonary Function in Patients with Cystic Fibrosis. *N Engl J Med* 1994;331:637–642.
20. Wark P, McDonald VM. Nebulised hypertonic saline for cystic fibrosis. *Cochrane Database Syst Rev* 2018;doi:10.1002/14651858.CD001506.pub4.
21. Warnock L, Gates A. Chest physiotherapy compared to no chest physiotherapy for cystic fibrosis. *Cochrane Database Syst Rev* 2015;doi:10.1002/14651858.CD001401.pub3.
22. Ramsey BW, Pepe MS, Quan JM, Otto KL, Montgomery AB, Williams-Warren J, *et al.* Intermittent Administration of Inhaled Tobramycin in Patients with Cystic Fibrosis. *N Engl J Med* 1999;340:23–30.
23. McCoy KS, Quittner AL, Oermann CM, Gibson RL, Retsch-Bogart GZ, Montgomery AB. Inhaled Aztreonam Lysine for Chronic Airway *Pseudomonas aeruginosa* in Cystic Fibrosis. *Am J Respir Crit Care Med* 2008;178:921–928.
24. Southern KW, Barker PM, Solis-Moya A, Patel L. Macrolide antibiotics for cystic fibrosis. *Cochrane Database Syst Rev* 2004;doi:10.1002/14651858.CD002203.pub2.
25. Goss CH, Sykes J, Stanojevic S, Marshall B, Petren K, Ostrenga J, *et al.* Comparison of Nutrition and Lung Function Outcomes in Patients with Cystic Fibrosis Living in Canada and the United States. *Am J Respir Crit Care Med* 2018;197:768–775.

26. Davis PB. Cystic Fibrosis Since 1938. *Am J Respir Crit Care Med* 2006;173:475–482.
27. Burgel P-R, Bellis G, Olesen HV, Viviani L, Zolin A, Blasi F, *et al.* Future trends in cystic fibrosis demography in 34 European countries. *Eur Respir J* 2015;46:133–141.
28. 2021 CFF Registry Annual Data Report. 2021;
29. Arias E, Tejada-Vera B, Kochanek K, Ahmad F. Provisional Life Expectancy Estimates for 2021. *Vital Stat Rapid Release No 23 Natl Cent Health Stat* 2022;doi:https://dx.doi.org/ 10.15620/cdc:118999.
30. Plasschaert LW, Žilionis R, Choo-Wing R, Savova V, Knehr J, Roma G, *et al.* A single-cell atlas of the airway epithelium reveals the CFTR-rich pulmonary ionocyte. *Nature* 2018;560:377–381.
31. Montoro DT, Haber AL, Biton M, Vinarsky V, Lin B, Birket SE, *et al.* A revised airway epithelial hierarchy includes CFTR-expressing ionocytes. *Nature* 2018;560:319–324.
32. Davis PB, Drumm M, Konstan MW. Cystic fibrosis: State of the Art. *Am J Respir Crit Care Med* 1996;154:1229–1256.
33. Gibson RL, Burns JL, Ramsey BW. Pathophysiology and Management of Pulmonary Infections in Cystic Fibrosis. *Am J Respir Crit Care Med* 2003;168:918–951.
34. Lyczak JB, Cannon CL, Pier GB. Lung Infections Associated with Cystic Fibrosis. *Clin Microbiol Rev* 2002;15:194–222.
35. Elborn JS. Cystic fibrosis. *The Lancet* 2016;388:2519–2531.
36. Cutting GR. Cystic fibrosis genetics: From molecular understanding to clinical application. *Nat Rev Genet* 2015;16:45–56.
37. Cohen TS, Prince A. Cystic fibrosis: a mucosal immunodeficiency syndrome. *Nat Med* 2012;18:509–519.
38. Rosenow T, Oudraad MCJ, Murray CP, Turkovic L, Kuo W, de Bruijne M, *et al.* PRAGMA-CF. A Quantitative Structural Lung Disease Computed Tomography Outcome in Young Children with Cystic Fibrosis. *Am J Respir Crit Care Med* 2015;191:1158–1165.
39. Sly PD, Gangell CL, Chen L, Ware RS, Ranganathan S, Mott LS, *et al.* Risk Factors for Bronchiectasis in Children With Cystic Fibrosis. *N Engl J Med* 2014;58:82.

40. Ramsey KA, Ranganathan S, Park J, Skoric B, Adams A-M, Simpson SJ, *et al.* Early Respiratory Infection Is Associated with Reduced Spirometry in Children with Cystic Fibrosis. *Am J Respir Crit Care Med* 2014;190:1111–1116.
41. Muhlebach MS, Zorn BT, Esther CR, Hatch JE, Murray CP, Turkovic L, *et al.* Initial acquisition and succession of the cystic fibrosis lung microbiome is associated with disease progression in infants and preschool children. *PLOS Pathog* 2018;14:e1006798.
42. Jorth P, Ehsan Z, Rezayat A, Caldwell E, Pope C, Brewington JJ, *et al.* Direct Lung Sampling Indicates That Established Pathogens Dominate Early Infections in Children with Cystic Fibrosis. *Cell Rep* 2019;27:1190–1204.
43. Esther CR, Muhlebach MS, Ehre C, Hill DB, Wolfgang MC, Kesimer M, *et al.* Mucus accumulation in the lungs precedes structural changes and infection in children with cystic fibrosis. *Sci Transl Med* 2019;11:.
44. Fischer AJ, Singh SB, LaMarche MM, Maakestad LJ, Kienenberger ZE, Peña TA, *et al.* Sustained Coinfections with *Staphylococcus aureus* and *Pseudomonas aeruginosa* in Cystic Fibrosis. *Am J Respir Crit Care Med* 2020;rccm.202004-1322OC.doi:10.1164/rccm.202004-1322OC.
45. Konstan MW, Morgan WJ, Butler SM, Pasta DJ, Craib ML, Silva SJ, *et al.* Risk Factors For Rate of Decline in Forced Expiratory Volume in One Second in Children and Adolescents with Cystic Fibrosis. *J Pediatr* 2007;151:134–139.
46. Sanders DB, Bittner RCL, Rosenfeld M, Redding GJ, Goss CH. Pulmonary exacerbations are associated with subsequent FEV_1 decline in both adults and children with cystic fibrosis: Pulmonary Exacerbations and FEV_1 Decline. *Pediatr Pulmonol* 2011;46:393–400.
47. Nixon GM, Armstrong DS, Carzino R, Carlin JB, Olinsky A, Robertson CF, *et al.* Clinical outcome after early Pseudomonas aeruginosa infection in cystic fibrosis. *J Pediatr* 2001;138:699–704.
48. Emerson J, Rosenfeld M, McNamara S, Ramsey B, Gibson RL. Pseudomonas aeruginosa and other predictors of mortality and morbidity in young children with cystic fibrosis. *Pediatr Pulmonol* 2002;34:91–100.

49. Treggiari MM, Rosenfeld M, Mayer-Hamblett N, Retsch-Bogart G, Gibson RL, Williams J, *et al.* Early anti-pseudomonal acquisition in young patients with cystic fibrosis: Rationale and design of the EPIC clinical trial and observational study. *Contemp Clin Trials* 2009;30:256–268.
50. Treggiari MM, Retsch-Bogart G, Mayer-Hamblett N, Khan U, Kulich M, Kronmal R, *et al.* Comparative Efficacy and Safety of 4 Randomized Regimens to Treat Early Pseudomonas aeruginosa Infection in Children With Cystic Fibrosis. *Arch Pediatr Adolesc Med* 2011;165:10.
51. Mayer-Hamblett N, Kronmal RA, Gibson RL, Rosenfeld M, Retsch-Bogart G, Treggiari MM, *et al.* Initial *Pseudomonas aeruginosa* treatment failure is associated with exacerbations in cystic fibrosis: *P. aeruginosa* and Exacerbations in CF. *Pediatr Pulmonol* 2012;47:125–134.
52. Struelens MJ, Schwam V, Deplano A, Baran D. Genome macrorestriction analysis of diversity and variability of Pseudomonas aeruginosa strains infecting cystic fibrosis patients. *J Clin Microbiol* 1993;31:2320–2326.
53. Rogers CS, Stoltz DA, Meyerholz DK, Ostedgaard LS, Rokhlina T, Taft PJ, *et al.* Disruption of the *CFTR* Gene Produces a Model of Cystic Fibrosis in Newborn Pigs. *Science* 2008;321:1837–1841.
54. Sun X, Sui H, Fisher JT, Yan Z, Liu X, Cho H-J, *et al.* Disease phenotype of a ferret CFTR-knockout model of cystic fibrosis. *J Clin Invest* 2010;120:3149–3160.
55. Tuggle KL, Birket SE, Cui X, Hong J, Warren J, Reid L, *et al.* Characterization of Defects in Ion Transport and Tissue Development in Cystic Fibrosis Transmembrane Conductance Regulator (CFTR)-Knockout Rats. *PLoS ONE* 2014;9:.
56. Stoltz DA, Meyerholz DK, Welsh MJ. Origins of Cystic Fibrosis Lung Disease. In: Longo DL, editor. *N Engl J Med* 2015;372:351–362.
57. Hoegger MJ, Fischer AJ, McMenimen JD, Ostedgaard LS, Tucker AJ, Awadalla MA, *et al.* Impaired mucus detachment disrupts mucociliary transport in a piglet model of cystic fibrosis. *Science* 2014;345:818–22.
58. Birket SE, Chu KK, Liu L, Houser GH, Diephuis BJ, Wilsterman EJ, *et al.* A Functional Anatomic Defect of the Cystic Fibrosis Airway. *Am J Respir Crit Care Med* 2014;190:421–432.
59. Shah VS, Meyerholz DK, Tang XX, Reznikov L, Abou Alaiwa M, Ernst SE, *et al.* Airway acidification initiates host defense abnormalities in cystic fibrosis mice. *Science* 2016;351:503–507.

60. Alaiwa MHA, Launspach JL, Grogan B, Carter S, Zabner J, Stoltz DA, *et al.* Ivacaftor-induced sweat chloride reductions correlate with increases in airway surface liquid pH in cystic fibrosis. *JCI Insight* 2018;3:e121468.
61. Abou Alaiwa MH, Reznikov LR, Gansemer ND, Sheets KA, Horswill AR, Stoltz DA, *et al.* pH modulates the activity and synergism of the airway surface liquid antimicrobials β-defensin-3 and LL-37. *Proc Natl Acad Sci* 2014;111:18703–18708.
62. Pezzulo AA, Tang XX, Hoegger MJ, Abou Alaiwa MH, Ramachandran S, Moninger TO, *et al.* Reduced airway surface pH impairs bacterial killing in the porcine cystic fibrosis lung. *Nature* 2012;487:109–113.
63. Abou Alaiwa MH, Beer AM, Pezzulo AA, Launspach JL, Horan RA, Stoltz DA, *et al.* Neonates with cystic fibrosis have a reduced nasal liquid pH; A small pilot study. *J Cyst Fibros* 2014;13:373–377.
64. Simonin J, Bille E, Crambert G, Noel S, Dreano E, Edwards A, *et al.* Airway surface liquid acidification initiates host defense abnormalities in Cystic Fibrosis. *Sci Rep* 2019;9:6516.
65. Khan TZ, Wagener JS, Bost T, Martinez J, Accurso FJ, Riches DW. Early pulmonary inflammation in infants with cystic fibrosis. *Am J Respir Crit Care Med* 1995;151:1075–1082.
66. Rosenfeld M, Gibson RL, McNamara S, Emerson J, Burns JL, Castile R, *et al.* Early pulmonary infection, inflammation, and clinical outcomes in infants with cystic fibrosis. *Pediatr Pulmonol* 2001;32:356–366.
67. Muhlebach MS, Noah TL. Endotoxin Activity and Inflammatory Markers in the Airways of Young Patients with Cystic Fibrosis. *Am J Respir Crit Care Med* 2002;165:911–915.
68. McKeon DJ, Condliffe AM, Cowburn AS, Cadwallader KC, Farahi N, Bilton D, *et al.* Prolonged survival of neutrophils from patients with Delta F508 CFTR mutations. *Thorax* 2008;63:660–661.
69. Moriceau S, Kantari C, Mocek J, Davezac N, Gabillet J, Guerrera IC, *et al.* Coronin-1 Is Associated with Neutrophil Survival and Is Cleaved during Apoptosis: Potential Implication in Neutrophils from Cystic Fibrosis Patients. *J Immunol* 2009;182:7254–7263.
70. Moriceau S, Lenoir G, Witko-Sarsat V. In Cystic Fibrosis Homozygotes and Heterozygotes, Neutrophil Apoptosis Is Delayed and Modulated by Diamide or Roscovitine: Evidence for an Innate Neutrophil Disturbance. *J Innate Immun* 2010;2:260–266.

71. Saba S, Soong G, Greenberg S, Prince A. Bacterial Stimulation of Epithelial G-CSF and GM-CSF Expression Promotes PMN Survival in CF Airways. *Am J Respir Cell Mol Biol* 2002;27:561–567.
72. Gray RD, Hardisty G, Regan KH, Smith M, Robb CT, Duffin R, *et al.* Delayed neutrophil apoptosis enhances NET formation in cystic fibrosis. *Thorax* 2018;73:134–144.
73. Berger M, Norvell TM, Tosi MF, Emancipator SN, Konstan MW, Schreiber JR. Tissue-specific Fc gamma and complement receptor expression by alveolar macrophages determines relative importance of IgG and complement in promoting phagocytosis of Pseudomonas aeruginosa. *Pediatr Res* 1994;35:68–77.
74. Vandivier RW, Fadok VA, Hoffmann PR, Bratton DL, Penvari C, Brown KK, *et al.* Elastase-mediated phosphatidylserine receptor cleavage impairs apoptotic cell clearance in cystic fibrosis and bronchiectasis. *J Clin Invest* 2002;109:661–670.
75. Sedor J, Hogue L, Akers K, Boslaugh S, Schreiber J, Ferkol T. Cathepsin-G Interferes with Clearance of Pseudomonas aeruginosa from Mouse Lungs. *Pediatr Res* 2007;61:26–31.
76. Hayes E, Murphy MP, Pohl K, Browne N, McQuillan K, Saw LE, *et al.* Altered Degranulation and pH of Neutrophil Phagosomes Impacts Antimicrobial Efficiency in Cystic Fibrosis. *Front Immunol* 2020;11:600033.
77. Bruscia EM, Bonfield TL. Cystic Fibrosis Lung Immunity: The Role of the Macrophage. *J Innate Immun* 2016;8:550–563.
78. del Fresno C, Gómez-Piña V, Lores V, Soares-Schanoski A, Fernández-Ruiz I, Rojo B, *et al.* Monocytes from Cystic Fibrosis Patients Are Locked in an LPS Tolerance State: Down-Regulation of TREM-1 as Putative Underlying Mechanism. *PLoS ONE* 2008;3:e2667.
79. Sorio C, Montresor A, Bolomini-Vittori M, Caldrer S, Rossi B, Dusi S, *et al.* Mutations of Cystic Fibrosis Transmembrane Conductance Regulator Gene Cause a Monocyte-Selective Adhesion Deficiency. *Am J Respir Crit Care Med* 2016;193:1123–1133.
80. Dasenbrook EC, Lu L, Donnola S, Weaver DE, Gulani V, Jakob PM, *et al.* Normalized T1 Magnetic Resonance Imaging for Assessment of Regional Lung Function in Adult Cystic Fibrosis Patients - A Cross-Sectional Study. *PLoS ONE* 2013;8:e73286.

81. Li Z, Sanders DB, Rock MJ, Kosorok MR, Collins J, Green CG, *et al.* Regional differences in the evolution of lung disease in children with cystic fibrosis: Regional Difference in CF Lung Disease. *Pediatr Pulmonol* 2012;47:635–640.
82. Maffessanti M, Candusso M, Brizzi F, Piovesana F. Cystic fibrosis in children: HRCT findings and distribution of disease. *J Thorac Imaging* 1996;11:27–38.
83. Mott LS, Park J, Gangell CL, de Klerk NH, Sly PD, Murray CP, *et al.* Distribution of Early Structural Lung Changes due to Cystic Fibrosis Detected with Chest Computed Tomography. *J Pediatr* 2013;163:243–248.
84. Nemec SF, Bankier AA, Eisenberg RL. Upper Lobe–Predominant Diseases of the Lung. *Am J Roentgenol* 2013;200:W222–W237.
85. Carzino R, Frayman KB, King L, Vidmar S, Ranganathan S. Regional differences in infection and structural lung disease in infants and young children with cystic fibrosis. *J Cyst Fibros* 2020;19:917–922.
86. Davis SD, Fordham LA, Brody AS, Noah TL, Retsch-Bogart GZ, Qaqish BF, *et al.* Computed Tomography Reflects Lower Airway Inflammation and Tracks Changes in Early Cystic Fibrosis. *Am J Respir Crit Care Med* 2007;175:943–950.
87. Gutierrez JP, Grimwood K, Armstrong DS, Carlin JB, Carzino R, Olinsky A, *et al.* Interlobar differences in bronchoalveolar lavage fluid from children with cystic. *Eur Respir J* 2001;17:281–286.
88. Hogan DA, Willger SD, Dolben EL, Hampton TH, Stanton BA, Morrison HG, *et al.* Analysis of Lung Microbiota in Bronchoalveolar Lavage, Protected Brush and Sputum Samples from Subjects with Mild-To-Moderate Cystic Fibrosis Lung Disease. *PLOS ONE* 2016;11:e0149998.
89. Malhotra S, Hayes D, Wozniak DJ. Mucoid Pseudomonas aeruginosa and regional inflammation in the cystic fibrosis lung. *J Cyst Fibros* 2019;18:796–803.
90. Meyer KC, Sharma A, Rosenthal NS, Peterson K, Brennan L. Regional Variability of Lung Inflammation in Cystic Fibrosis. *Am J Respir Crit Care Med* 1997;156:1536–1540.
91. Gilchrist FJ, Salamat S, Clayton S, Peach J, Alexander J, Lenney W. Bronchoalveolar lavage in children with cystic fibrosis: how many lobes should be sampled? *Arch Dis Child* 2011;96:215–217.

92. Jorth P, Staudinger BJ, Wu X, Hisert KB, Hayden H, Garudathri J, *et al.* Regional Isolation Drives Bacterial Diversification within Cystic Fibrosis Lungs. *Cell Host Microbe* 2015;18:307–319.
93. Van Goor F, Hadida S, Grootenhuis PDJ, Burton B, Cao D, Neuberger T, *et al.* Rescue of CF airway epithelial cell function in vitro by a CFTR potentiator, VX-770. *Proc Natl Acad Sci U S A* 2009;106:18825–18830.
94. McKone EF, Emerson SS, Edwards KL, Aitken ML. Effect of genotype on phenotype and mortality in cystic fibrosis: a retrospective cohort study. *The Lancet* 2003;361:1671–1676.
95. Accurso FJ, Durie PR, Donaldson SH, Uluer AZ, Mayer-Hamblett N, Ordoñez CL. Effect of VX-770 in Persons with Cystic Fibrosis and the G551D-CFTR Mutation. *N Engl J Med* 2010;13.
96. Rowe SM, Clancy JP, Wilschanski M. Nasal Potential Difference Measurements to Assess CFTR Ion Channel Activity. In: Amaral MD, Kunzelmann K, editors. *Cyst Fibros Methods Mol Biol* Humana Press; 2011. p. 69–86.
97. Ramsey BW, Davies J, McElvaney NG, Tullis E, Bell SC, Dřevínek P, *et al.* A CFTR Potentiator in Patients with Cystic Fibrosis and the *G551D* Mutation. *N Engl J Med* 2011;365:1663–1672.
98. Bardin E, Pastor A, Semeraro M, Golec A, Hayes K, Chevalier B, *et al.* Modulators of CFTR. Updates on clinical development and future directions. *Eur J Med Chem* 2021;213:113195.
99. Skilton M, Krishan A, Patel S, Sinha IP, Southern KW. Potentiators (specific therapies for class III and IV mutations) for cystic fibrosis. *Cochrane Database Syst Rev* 2019;doi:10.1002/14651858.CD009841.pub3.
100. Wainwright CE, Elborn JS, Ramsey BW, Marigowda G, Huang X, Cipolli M, *et al.* Lumacaftor–Ivacaftor in Patients with Cystic Fibrosis Homozygous for Phe508del *CFTR*. *N Engl J Med* 2015;373:220–231.
101. Taylor-Cousar JL, Munck A, McKone EF, van der Ent CK, Moeller A, Simard C, *et al.* Tezacaftor–Ivacaftor in Patients with Cystic Fibrosis Homozygous for Phe508del. *N Engl J Med* 2017;377:2013–2023.
102. Davies JC, Moskowitz SM, Brown C, Horsley A, Mall MA, McKone EF, *et al.* VX-659–Tezacaftor–Ivacaftor in Patients with Cystic Fibrosis and One or Two Phe508del Alleles. *N Engl J Med* 2018;379:.

103. Keating D, Marigowda G, Burr L, Daines C, Mall MA, McKone EF, *et al.* VX-445–Tezacaftor–Ivacaftor in Patients with Cystic Fibrosis and One or Two Phe508del Alleles. *N Engl J Med* 2018;379:1612–1620.

104. Nichols DP, Paynter AC, Heltshe SL, Donaldson SH, Frederick CA, Freedman SD, *et al.* Clinical Effectiveness of Elexacaftor/Tezacaftor/Ivacaftor in People with Cystic Fibrosis: A Clinical Trial. *Am J Respir Crit Care Med* 2022;205:529–539.

105. Bell SC, Mall MA, Gutierrez H, Macek M, Madge S, Davies JC, *et al.* The future of cystic fibrosis care: a global perspective. *Lancet Respir Med* 2020;8:65–124.

106. Davies JC, Wainwright CE, Canny GJ, Chilvers MA, Howenstine MS, Munck A, *et al.* Efficacy and Safety of Ivacaftor in Patients Aged 6 to 11 Years with Cystic Fibrosis with a G551D Mutation. *Am J Respir Crit Care Med* 2013;187:1219–1225.

107. De Boeck K, Munck A, Walker S, Faro A, Hiatt P, Gilmartin G, *et al.* Efficacy and safety of ivacaftor in patients with cystic fibrosis and a non-G551D gating mutation. *J Cyst Fibros* 2014;13:674–680.

108. Rowe SM, Heltshe SL, Gonska T, Donaldson SH, Borowitz D, Gelfond D, *et al.* Clinical mechanism of the cystic fibrosis transmembrane conductance regulator potentiator ivacaftor in G551D-mediated cystic fibrosis. *Am J Respir Crit Care Med* 2014;190:175–184.

109. Morrison CB, Shaffer KM, Araba KC, Markovetz MR, Wykoff JA, Quinney NL, *et al.* Treatment of cystic fibrosis airway cells with CFTR modulators reverses aberrant mucus properties *via* hydration. *Eur Respir J* 2022;59:2100185.

110. Pohl K, Hayes E, Keenan J, Henry M, Meleady P, Molloy K, *et al.* A neutrophil intrinsic impairment affecting Rab27a and degranulation in cystic fibrosis is corrected by CFTR potentiator therapy. *Blood* 2014;124:999–1009.

111. Hardisty GR, Law SM, Carter S, Grogan B, Singh PK, McKone EF, *et al.* Ivacaftor modifies cystic fibrosis neutrophil phenotype in subjects with R117H residual function CFTR mutations. *Eur Respir J* 2021;57:2002161.

112. Hisert KB, Birkland TP, Schoenfelt KQ, Long ME, Grogan B, Carter S, *et al.* Ivacaftor decreases monocyte sensitivity to interferon-γ in people with cystic fibrosis. *ERJ Open Res* 2020;6:00318–02019.

113. Hisert KB, Birkland TP, Schoenfelt KQ, Long ME, Grogan B, Carter S, *et al.* CFTR Modulator Therapy Enhances Peripheral Blood Monocyte Contributions to Immune Responses in People With Cystic Fibrosis. *Front Pharmacol* 2020;11:1219.

114. Hisert KB, Schoenfelt KQ, Cooke G, Grogan B, Launspach JL, Gallagher CG, *et al.* Ivacaftor-Induced Proteomic Changes Suggest Monocyte Defects May Contribute to the Pathogenesis of Cystic Fibrosis. *Am J Respir Cell Mol Biol* 2016;54:594–597.

115. Hisert KB, Heltshe SL, Pope C, Jorth P, Wu X, Edwards RM, *et al.* Restoring Cystic Fibrosis Transmembrane Conductance Regulator Function Reduces Airway Bacteria and Inflammation in People with Cystic Fibrosis and Chronic Lung Infections. *Am J Respir Crit Care Med* 2017;195:1617–1628.

116. Durfey SL, McGeer K, Ratjen AM, Carter SC, Grogan B, Gallagher CG, *et al.* Six-Year Follow-Up of Ivacaftor-Treated Subjects With CFTR-G551D: An Update on the Dublin Cohort. *Pediatr Pulmonol* 2019. p. S334–S334.

117. Heltshe SL, Mayer-Hamblett N, Burns JL, Khan U, Baines A, Ramsey BW, *et al.* Pseudomonas aeruginosa in cystic fibrosis patients with G551D-CFTR treated with ivacaftor. *Clin Infect Dis* 2015;60:703–712.

118. Volkova N, Moy K, Evans J, Campbell D, Tian S, Simard C, *et al.* Disease progression in patients with cystic fibrosis treated with ivacaftor: Data from national US and UK registries. *J Cyst Fibros* 2020;19:68–79.

119. Singh SB, McLearn-Montz AJ, Milavetz F, Gates LK, Fox C, Murry LT, *et al.* Pathogen acquisition in patients with cystic fibrosis receiving ivacaftor or lumacaftor/ivacaftor. *Pediatr Pulmonol* 2019;doi:10.1002/ppul.24341.

120. Kawala CR, Ma X, Sykes J, Stanojevic S, Coriati A, Stephenson AL. Real-world use of ivacaftor in Canada: A retrospective analysis using the Canadian Cystic Fibrosis Registry. *J Cyst Fibros* 2021;doi:10.1016/j.jcf.2021.03.008.

121. Harris JK, Wagner BD, Zemanick ET, Robertson CE, Stevens MJ, Heltshe SL, *et al.* Changes in Airway Microbiome and Inflammation with Ivacaftor Treatment in Patients with Cystic Fibrosis and the G551D Mutation. *Ann Am Thorac Soc* 2020;17:212–220.

122. Einarsson GG, Ronan NJ, Mooney D, McGettigan C, Mullane D, NiChroinin M, *et al.* Extended-culture and culture-independent molecular analysis of the airway microbiota in cystic fibrosis following CFTR modulation with ivacaftor. *J Cyst Fibros* 2021;doi:10.1016/j.jcf.2020.12.023.

123. Sheikh S, Britt RD, Ryan-Wenger NA, Khan AQ, Lewis BW, Gushue C, *et al.* Impact of elexacaftor–tezacaftor–ivacaftor on bacterial colonization and inflammatory responses in cystic fibrosis. *Pediatr Pulmonol* 2022;doi:10.1002/ppul.26261.

124. Zhang S, Shrestha CL, Robledo-Avila F, Jaganathan D, Wisniewski BL, Brown N, *et al.* Cystic fibrosis macrophage function and clinical outcomes after elexacaftor/tezacaftor/ivacaftor. *Eur Respir J* 2022;doi:10.1183/13993003.02861-2021.

125. Nichols DP, Morgan SJ, Skalland M, Vo AT, Van Dalfsen JM, Singh SBP, *et al.* Pharmacologic improvement of CFTR function rapidly decreases sputum pathogen density but lung infections generally persist. *J Clin Invest* 2023;doi:10.1172/JCI167957.

126. Gjodsbol K, Christensen JJ, Karlsmark T, Jorgensen B, Klein BM, Krogfelt KA. Multiple bacterial species reside in chronic wounds: a longitudinal study. *Int Wound J* 2006;3:225–31.

127. McGeachie J. Recurrent Infection of Urinary Tract - Reinfection or Recrudescence. *Br Med J* 1966;1:952–954.

128. Frederick J, Braude A. Anaerobic Infection of Paranasal Sinuses. *N Engl J Med* 1974;290:135–137.

129. Branger C, Gardye C, LambertZechovsky N. Persistence of Staphylococcus aureus strains among cystic fibrosis patients over extended periods of time. *J Med Microbiol* 1996;45:294–301.

130. Kahl BC, Duebbers A, Lubritz G, Haeberle J, Koch HG, Ritzerfeld B, *et al.* Population Dynamics of Persistent *Staphylococcus aureus* Isolated from the Airways of Cystic Fibrosis Patients during a 6-Year Prospective Study. *J Clin Microbiol* 2003;41:4424–4427.

131. Hirschhausen N, Block D, Bianconi I, Bragonzi A, Birtel J, Lee JC, *et al.* Extended Staphylococcus aureus persistence in cystic fibrosis is associated with bacterial adaptation. *Int J Med Microbiol* 2013;303:685–692.

132. Burns JL, Gibson RL, McNamara S, Yim D, Emerson J, Rosenfeld M, *et al.* Longitudinal Assessment of Pseudomonas aeruginosa in Young Children with Cystic Fibrosis. *J Infect Dis* 2001;183:444–452.

133. Smith EE, Buckley DG, Wu Z, Saenphimmachak C, Hoffman LR, D'Argenio DA, *et al.* Genetic adaptation by Pseudomonas aeruginosa to the airways of cystic fibrosis patients. *Proc Natl Acad Sci* 2006;103:8487–8492.

134. Goerke C, Gressinger M, Endler K, Breitkopf C, Wardecki K, Stern M, *et al.* High phenotypic diversity in infecting but not in colonizing Staphylococcus aureus populations. *Environ Microbiol* 2007;9:3134–3142.

135. Long DR, Wolter DJ, Lee M, Precit M, McLean K, Holmes E, *et al.* Polyclonality, Shared Strains, and Convergent Evolution in Chronic Cystic Fibrosis *Staphylococcus aureus* Airway Infection. *Am J Respir Crit Care Med* 2021;203:1127–1137.

136. Jelsbak L, Johansen HK, Frost A-L, Thøgersen R, Thomsen LE, Ciofu O, *et al.* Molecular Epidemiology and Dynamics of *Pseudomonas aeruginosa* Populations in Lungs of Cystic Fibrosis Patients. *Infect Immun* 2007;75:2214–2224.

137. Jain M, Ramirez D, Seshadri R, Cullina J, Powers C, Schulert G, *et al.* Type III secretion phenotypes of Pseudomonas aeruginosa strains change during infection of individuals with cystic fibrosis. *J Clin Microbiol* 2004;42:5229–5237.

138. Anthony M, Rose B, Pegler M, Elkins M, Service H, Thamotharampillai K, *et al.* Genetic analysis of Pseudomonas aeruginosa isolates from the sputa of Australian adult cystic fibrosis patients. *J Clin Microbiol* 2002;40:2772–2778.

139. Syrmis M, O'Carroll M, Sloots T, Coulter C, Wainwright C, Bell S, *et al.* Rapid genotyping of Pseudomonas aeruginosa isolates harboured by adult and paediatric patients with cystic fibrosis using repetitive-element-based PCR assays. *J Med Microbiol* 2004;53:1089–1096.

140. Mahenthiralingam E, Campbell M, Foster J, Lam J, Speert D. Random amplified polymorphic DNA typing of Pseudomonas aeruginosa isolates recovered from patients with cystic fibrosis. *J Clin Microbiol* 1996;34:1129–1135.

141. Hogardt M, Hoboth C, Schmoldt S, Henke C, Bader L, Heesemann J. Stage-specific adaptation of hypermutable Pseudomonas aeruginosa isolates during chronic pulmonary infection in patients with cystic fibrosis. *J Infect Dis* 2007;195:70–80.

142. Langhanki L, Berger P, Treffon J, Catania F, Kahl B, Mellmann A. In vivo competition and horizontal gene transfer among distinct Staphylococcus aureus lineages as major drivers for adaptational changes during long-term persistence in humans. *BMC Microbiol* 2018;18:.

143. Oliver A, Canton R, Campo P, Baquero F, Blazquez J. High frequency of hypermutable Pseudomonas aeruginosa in cystic fibrosis lung infection. *SCIENCE* 2000;288:1251–1253.

144. McCallum S, Corkill J, Gallagher M, Ledson M, Hart C, Walshaw M. Superinfection with a transmissible strain of Pseudomonas aeruginosa in adults with cystic fibrosis chronically colonised by P aeruginosa. *LANCET* 2001;358:558–560.

145. Salunkhe P, Smart C, Morgan J, Panagea S, Walshaw M, Hart C, *et al.* A cystic fibrosis epidemic strain of Pseudomonas aeruginosa displays enhanced virulence and antimicrobial resistance. *J Bacteriol* 2005;187:4908–4920.

146. Parkins MD, Glezerson BA, Sibley CD, Sibley KA, Duong J, Purighalla S, *et al.* Twenty-five-year outbreak of Pseudomonas aeruginosa infecting individuals with cystic fibrosis: Identification of the prairie epidemic strain. *J Clin Microbiol* 2014;52:1127–1135.

147. Duong J, Booth S, McCartney N, Rabin H, Parkins M, Storey D. Phenotypic and Genotypic Comparison of Epidemic and Non-Epidemic Strains of Pseudomonas aeruginosa from Individuals with Cystic Fibrosis. *PLOS ONE* 2015;10:.

148. Yagci S, Hascelik G, Dogru D, Ozcelik U, Sener B. Prevalence and genetic diversity of Staphylococcus aureus small-colony variants in cystic fibrosis patients. *Clin Microbiol Infect* 2013;19:77–84.

149. Lieberman TD, Flett KB, Yelin I, Martin TR, McAdam AJ, Priebe GP, *et al.* Genetic variation of a bacterial pathogen within individuals with cystic fibrosis provides a record of selective pressures. *Nat Genet* 2014;46:82–87.

150. Williams D, Evans B, Haldenby S, Walshaw MJ, Brockhurst MA, Winstanley C, *et al.* Divergent, Coexisting Pseudomonas aeruginosa Lineages in Chronic Cystic Fibrosis Lung Infections. *Am J Respir Crit Care Med* 2015;191:775–785.

151. Allendorf F, Lundquist L. Introduction: Population biology, evolution, and control of invasive species. *Conserv Biol* 2003;17:24–30.

152. Frederiksen B, Koch C, Hoiby N. Antibiotic treatment of initial colonization with Pseudomonas aeruginosa postpones chronic infection and prevents deterioration of pulmonary function in cystic fibrosis. *Pediatr Pulmonol* 1997;23:330–335.

153. Hansen C, Pressler T, Hoiby N. Early aggressive eradication therapy for intermittent Pseudomonas aeruginosa airway colonization in cystic fibrosis patients: 15 years experience. *J Cyst Fibros* 2008;7:523–530.

154. Ratjen F, Doring G, Nikolaizik W. Effect of inhaled tobramycin on early Pseudomonas aeruginosa colonisation in patients with cystic fibrosis. *LANCET* 2001;358:983–984.

155. Treggiari M, Rosenfeld M, Retsch-Bogart G, Gibson R, Ramsey B. Approach to eradication of initial Pseudomonas aeruginosa infection in children with cystic fibrosis. *Pediatr Pulmonol* 2007;42:751–756.

156. Tenover F, Arbeit R, Goering R, Mickelsen P, Murray B, Persing D, *et al.* Interpreting Chromosomal DNA Restriction Patterns Produced By Pulsed-Field Gel-Electrophoresis - Criteria For Bacterial Strain Typing. *J Clin Microbiol* 1995;33:2233–2239.

157. van Belkum A, Melles D, Nouwen J, van Leeuwen W, van Wamel W, Vos M, *et al.* Co-evolutionary aspects of human colonisation and infection by Staphylococcus aureus. *Infect Genet Evol* 2009;9:32–47.

158. Kidd TJ, Grimwood K, Ramsay KA, Rainey PB, Bell SC. Comparison of three molecular techniques for typing Pseudomonas aeruginosa isolates in sputum samples from patients with cystic fibrosis. *J Clin Microbiol* 2011;49:263–268.

159. Waters V, Zlosnik J, Yau Y, Speert D, Aaron S, Guttman D. Comparison of three typing methods for Pseudomonas aeruginosa isolates from patients with cystic fibrosis. *Eur J Clin Microbiol Infect Dis* 2012;31:3341–3350.

160. Gentili V, Gianesini S, Balboni P, Menegatti E, Rotola A, Zuolo M, *et al.* Panbacterial real-time PCR to evaluate bacterial burden in chronic wounds treated with Cutimed (TM) Sorbact (TM). *Eur J Clin Microbiol Infect Dis* 2012;31:1523–1529.

161. Yusuf E, Jordan X, Clauss M, Borens O, Mader M, Trampuz A. High bacterial load in negative pressure wound therapy (NPWT) foams used in the treatment of chronic wounds. *Wound Repair Regen* 2013;21:677–681.

162. Rudkjobing V, Aanaes K, Wolff T, von Buchwald C, Johansen H, Thomsen T. An exploratory study of microbial diversity in sinus infections of cystic fibrosis patients by molecular methods. *J Cyst Fibros* 2014;13:645–652.

163. Fischer A, Singh S, LaMarche M, Maakestad L, Kienenberger Z, Pena T, *et al.* Sustained Coinfections with Staphylococcus aureus and Pseudomonas aeruginosa in Cystic Fibrosis. *Am J Respir Crit Care Med* 2021;203:328–338.

164. Hisert KB, Heltshe SL, Pope C, Jorth P, Wu X, Edwards RM, *et al.* Restoring Cystic Fibrosis Transmembrane Conductance Regulator Function Reduces Airway Bacteria and Inflammation in People with Cystic Fibrosis and Chronic Lung Infections. *Am J Respir Crit Care Med* 2017;195:1617–1628.

165. Shevchenko SG, Radey M, Tchesnokova V, Kisiela D, Sokurenko EV. Escherichia coli Clonobiome: Assessing the Strain Diversity in Feces and Urine by Deep Amplicon Sequencing. *Appl Environ Microbiol* 2019;85:.

166. Rosen M, Davison M, Bhaya D, Fisher D. Fine-scale diversity and extensive recombination in a quasisexual bacterial population occupying a broad niche. *SCIENCE* 2015;348:1019–1023.

167. Gan GL, Willie E, Chauve C, Chindelevitch L. Deconvoluting the diversity of within-host pathogen strains in a multi-locus sequence typing framework. *BMC Bioinformatics* 2019;20:637.

168. Curran B, Jonas D, Grundmann H, Pitt T, Dowson C. Development of a multilocus sequence typing scheme for the opportunistic pathogen Pseudomonas aeruginosa. *J Clin Microbiol* 2004;42:5644–5649.

169. Enright MC, Day NPJ, Davies CE, Peacock SJ, Spratt BG. Multilocus sequence typing for characterization of methicillin-resistant and methicillin-susceptible clones of Staphylococcus aureus. *J Clin Microbiol* 2000;38:1008–1015.

170. Jolley KA, Bray JE, Maiden MCJ. Open-access bacterial population genomics: BIGSdb software, the PubMLST.org website and their applications. *Wellcome Open Res* 2018;3:124.

171. Callahan BJ, McMurdie PJ, Rosen MJ, Han AW, Johnson AJA, Holmes SP. DADA2: High-resolution sample inference from Illumina amplicon data. *Nat Methods* 2016;13:581–583.

172. Polz M, Cavanaugh C. Bias in template-to-product ratios in multitemplate PCR. *Appl Environ Microbiol* 1998;64:3724–3730.

173. Nakamura K, Oshima T, Morimoto T, Ikeda S, Yoshikawa H, Shiwa Y, *et al.* Sequence-specific error profile of Illumina sequencers. *Nucleic Acids Res* 2011;39:.

174. Schirmer M, D'Amore R, Ijaz U, Hall N, Quince C. Illumina error profiles: resolving fine-scale variation in metagenomic sequencing data. *BMC Bioinformatics* 2016;17:.

175. McAdam P, Holmes A, Templeton K, Fitzgerald J. Adaptive Evolution of Staphylococcus aureus during Chronic Endobronchial Infection of a Cystic Fibrosis Patient. *PLOS ONE* 2011;6:.

176. Morgan S, Lippman S, Bautista G, Harrison J, Harding C, Gallagher L, *et al.* Bacterial fitness in chronic wounds appears to be mediated by the capacity for high-density growth,not virulence or biofilm functions. *PLOS Pathog* 2019;15:.

177. Wen C, Wu L, Qin Y, Van Nostrand J, Ning D, Sun B, *et al.* Evaluation of the reproducibility of amplicon sequencing with Illumina MiSeq platform. *PLoS ONE* 2017;12:.

178. Feigelman R, Kahlert C, Baty F, Rassouli F, Kleiner R, Kohler P, *et al.* Sputum DNA sequencing in cystic fibrosis: non-invasive access to the lung microbiome and to pathogen details. *Microbiome* 2017;5:.

179. Wolcott R, Hanson J, Rees E, Koenig L, Phillips C, Wolcott R, *et al.* Analysis of the chronic wound microbiota of 2,963 patients by 16S rDNA pyrosequencing. *Wound Repair Regen* 2016;24:163–174.

180. Loesche M, Gardner S, Kalan L, Horwinski J, Zheng Q, Hodkinson B, *et al.* Temporal Stability in Chronic Wound Microbiota Is Associated With Poor Healing. *J Invest Dermatol* 2017;137:237–244.

181. Price L, Liu C, Melendez J, Frankel Y, Engelthaler D, Aziz M, *et al.* Community Analysis of Chronic Wound Bacteria Using 16S rRNA Gene-Based Pyrosequencing: Impact of Diabetes and Antibiotics on Chronic Wound Microbiota. *PLOS ONE* 2009;4:.

182. Stokell J, Gharaibeh R, Hamp T, Zapata M, Fodor A, Steck T. Analysis of Changes in Diversity and Abundance of the Microbial Community in a Cystic Fibrosis Patient over a Multiyear Period. *J Clin Microbiol* 2015;53:237–247.

183. Zhao J, Schloss PD, Kalikin LM, Carmody LA, Foster BK, Petrosino JF, *et al.* Decade-long bacterial community dynamics in cystic fibrosis airways. *Proc Natl Acad Sci* 2012;109:5809–5814.

184. Klepac-Ceraj V, Lemon K, Martin T, Allgaier M, Kembel S, Knapp A, *et al.* Relationship between cystic fibrosis respiratory tract bacterial communities and age, genotype, antibiotics and Pseudomonas aeruginosa. *Environ Microbiol* 2010;12:1293–1303.

185. Cox MJ, Allgaier M, Taylor B, Baek MS, Huang YJ, Daly RA, *et al.* Airway Microbiota and Pathogen Abundance in Age-Stratified Cystic Fibrosis Patients. *PLoS ONE* 2010;5:e11044.

186. Coburn B, Wang PW, Diaz Caballero J, Clark ST, Brahma V, Donaldson S, *et al.* Lung microbiota across age and disease stage in cystic fibrosis. *Sci Rep* 2015;5:1–12.

187. Whiteside S, Razvi H, Dave S, Reid G, Burton J. The microbiome of the urinary tract-a role beyond infection. *Nat Rev Urol* 2015;12:81–90.

188. Al-Aloul M, Crawley J, Winstanley C, Hart C, Ledson M, Walshaw M. Increased morbidity associated with chronic infection by an epidemic Pseudomonas aeruginosa strain in CF patients. *THORAX* 2004;59:334–336.

189. McCallum S, Gallagher M, Corkill J, Hart C, Ledson M, Walshaw M. Spread of an epidemic Pseudomonas aeruginosa strain from a patient with cystic fibrosis (CF) to non-CF relatives. *THORAX* 2002;57:559–560.

190. Camacho C, Coulouris G, Avagyan V, Ma N, Papadopoulos J, Bealer K, *et al.* BLAST plus : architecture and applications. *BMC Bioinformatics* 2009;10:.

191. Dave K, Dobra R, Scott S, Saunders C, Matthews J, Simmonds NJ, *et al.* Entering the era of highly effective modulator therapies. *Pediatr Pulmonol* 2021;56:.

192. Ramsey BW, Bell SC, Wainwright CE, Sermet-Gaudelus I, Yen K. A CFTR Potentiator in Patients with Cystic Fibrosis and the G551D Mutation. *N Engl J Med* 2011;10.

193. Heltshe SL, Mayer-Hamblett N, Burns JL, Khan U, Baines A, Ramsey BW, *et al.* Pseudomonas aeruginosa in cystic fibrosis patients with G551D-CFTR treated with ivacaftor. *Clin Infect Dis* 2015;60:703–712.

194. Hoppe JE, Wagner BD, Accurso FJ, Zemanick ET, Sagel SD. Characteristics and outcomes of oral antibiotic treated pulmonary exacerbations in children with cystic fibrosis. *J Cyst Fibros* 2018;17:760–768.

195. Nelson MT, Wolter DJ, Eng A, Weiss EJ, Vo AT, Brittnacher MJ, *et al.* Maintenance tobramycin primarily affects untargeted bacteria in the CF sputum microbiome. *Thorax* 2020;75:780–790.

196. Lam JC, Somayaji R, Surette MG, Rabin HR, Parkins MD. Reduction in Pseudomonas aeruginosa sputum density during a cystic fibrosis pulmonary exacerbation does not predict clinical response. *BMC Infect Dis* 2015;15:145.

197. Stuart Elborn J, Geller DE, Conrad D, Aaron SD, Smyth AR, Fischer R, *et al.* A phase 3, open-label, randomized trial to evaluate the safety and efficacy of levofloxacin inhalation solution (APT-1026) versus tobramycin inhalation solution in stable cystic fibrosis patients. *J Cyst Fibros* 2015;14:507–514.

198. Alaiwa MHA, Launspach JL, Grogan B, Carter S, Zabner J, Stoltz DA, *et al.* Ivacaftor-induced sweat chloride reductions correlate with increases in airway surface liquid pH in cystic fibrosis. *JCI Insight* 2018;3:.

199. Zharkova MS, Orlov DS, Golubeva OYu, Chakchir OB, Eliseev IE, Grinchuk TM, *et al.* Application of Antimicrobial Peptides of the Innate Immune System in Combination With Conventional Antibiotics—A Novel Way to Combat Antibiotic Resistance? *Front Cell Infect Microbiol* 2019;9:128.

200. Brook I. Inoculum effect. *Rev Infect Dis* 1989;11:361–368.

201. Udekwu KI, Parrish N, Ankomah P, Baquero F, Levin BR. Functional relationship between bacterial cell density and the efficacy of antibiotics. *J Antimicrob Chemother* 2009;63:745–757.

202. Alvarez-Ortega C, Harwood CS. Responses of *Pseudomonas aeruginosa* to low oxygen indicate that growth in the cystic fibrosis lung is by aerobic respiration. *Mol Microbiol* 2007;65:153–165.

203. Kragh KN, Alhede M, Jensen PØ, Moser C, Scheike T, Jacobsen CS, *et al.* Polymorphonuclear Leukocytes Restrict Growth of Pseudomonas aeruginosa in the Lungs of Cystic Fibrosis Patients. *Infect Immun* 2014;82:4477–4486.

204. Brown MRW, Anwar H, Lambert PA. Evidence that mucoid *Pseudomonas aeruginosa* in the cystic fibrosis lung grows under iron-restricted conditions. *FEMS Microbiol Lett* 1984;21:113–117.

205. Baltimore RS, Christie CDC, Smith GJW. Immunohistopathologic Localization of Pseudomonas aeruginosa in Lungs from Patients with Cystic Fibrosis: Implications for the Pathogenesis of Progressive Lung Deterioration. *Am Rev Respir Dis* 1989;140:1650–1661.

206. Worlitzsch D, Tarran R, Ulrich M, Schwab U, Cekici A, Meyer KC, *et al.* Effects of reduced mucus oxygen concentration in airway Pseudomonas infections of cystic fibrosis patients. *J Clin Invest* 2002;109:317–325.

207. Ashish A, Paterson S, Mowat E, Fothergill JL, Walshaw MJ, Winstanley C. Extensive diversification is a common feature of Pseudomonas aeruginosa populations during respiratory infections in cystic fibrosis. *J Cyst Fibros* 2013;12:790–793.

208. Darch SE, McNally A, Harrison F, Corander J, Barr HL, Paszkiewicz K, *et al.* Recombination is a key driver of genomic and phenotypic diversity in a Pseudomonas aeruginosa population during cystic fibrosis infection. *Sci Rep* 2015;5:1–12.

209. Shade A, Peter H, Allison SD, Baho DL, Berga M, Bürgmann H, *et al.* Fundamentals of microbial community resistance and resilience. *Front Microbiol* 2012;3:1–19.

210. Moss RB, Flume PA, Elborn JS, Cooke J, Rowe SM, McColley SA, *et al.* Efficacy and safety of ivacaftor in patients with cystic fibrosis who have an Arg117His-CFTR mutation: A double-blind, randomised controlled trial. *Lancet Respir Med* 2015;3:524–533.

211. Lucotte G, Hazout S. Geographic and Ethnic Distributions of the More Frequent Cystic Fibrosis Mutations in Europe Show That a Founder Effect Is Apparent for Several Mutant Alleles. *Hum Biol* 1995;67:16.

212. Zolin A, Orenti A, Naehrlich L, Jung A, van Rens J. ECFSPR Annual Report 2018. 2020;175.

213. Morgan SJ, Durfey SL, Ravishankar S, Jorth P, Ni W, Skerrett DT, *et al.* A population-level strain genotyping method to study pathogen strain dynamics in human infections. *JCI Insight* 2021;6:e152472.

214. Vu-Thien H, Hormigos K, Corbineau G, Fauroux B, Corvol H, Moissenet D, *et al.* Longitudinal survey of Staphylococcus aureus in cystic fibrosis patients using a multiple-locus variable-number of tandem-repeats analysis method. *BMC Microbiol* 2010;10:24.

215. Saiman L. Improving outcomes of infections in cystic fibrosis in the era of CFTR modulator therapy. *Pediatr Pulmonol* 2019;54:.

216. Seeley JJ, Ghosh S. Molecular mechanisms of innate memory and tolerance to LPS. *J Leukoc Biol* 2017;101:107–119.

217. Yang L, Jelsbak L, Marvig RL, Damkiaer S, Workman CT, Rau MH, *et al.* Evolutionary dynamics of bacteria in a human host environment. *Proc Natl Acad Sci U S A* 2011;108:7481–6.

218. Kopf SH, Sessions AL, Cowley ES, Reyes C, Van Sambeek L, Hu Y, *et al.* Trace incorporation of heavy water reveals slow and heterogeneous pathogen growth rates in cystic fibrosis sputum. *Proc Natl Acad Sci* 2016;113:E110–E116.

219. Rossi E, Falcone M, Molin S, Johansen HK. High-resolution in situ transcriptomics of Pseudomonas aeruginosa unveils genotype independent patho-phenotypes in cystic fibrosis lungs. *Nat Commun* 2018;9:3459.

220. Ibberson CB, Whiteley M. The Staphylococcus aureus Transcriptome during Cystic Fibrosis Lung Infection. *mBio* 2019;10:.

221. Poole K. Pseudomonas Aeruginosa: Resistance to the Max. *Front Microbiol* 2011;2:.

222. Faure E, Kwong K, Nguyen D. Pseudomonas aeruginosa in Chronic Lung Infections: How to Adapt Within the Host? *Front Immunol* 2018;9:2416.

223. Amiel E, Lovewell RR, O'Toole GA, Hogan DA, Berwin B. *Pseudomonas aeruginosa* Evasion of Phagocytosis Is Mediated by Loss of Swimming Motility and Is Independent of Flagellum Expression. *Infect Immun* 2010;78:2937–2945.

224. Lieleg O, Caldara M, Baumgärtel R, Ribbeck K. Mechanical robustness of Pseudomonas aeruginosa biofilms. *Soft Matter* 2011;7:3307.

225. Döring G, Conway SP, Heijerman HGM, Hodson ME, Høiby N, Smyth A, *et al.* Antibiotic therapy against Pseudomonas aeruginosa in cystic fibrosis: a European consensus. *Eur Respir J* 2000;16:749.

226. Standardization of Spirometry, 1994 Update. American Thoracic Society. *Am J Respir Crit Care Med* 1995;152:1107–1136.

227. Quanjer PH, Stanojevic S, Cole TJ, Baur X, Hall GL, Culver BH, *et al.* Multi-ethnic reference values for spirometry for the 3–95-yr age range: the global lung function 2012 equations. *Eur Respir J* 2012;40:1324–1343.

228. Brody AS, Klein JS, Molina PL, Quan J, Bean JA, Wilmott RW. High-resolution computed tomography in young patients with cystic fibrosis: Distribution of abnormalities and correlation with pulmonary function tests. *J Pediatr* 2004;145:32–38.

229. Brody AS, Kosorok MR, Laxova A, Bandla H. Reproducibility of a Scoring System for Computed Tomography Scanning in Cystic Fibrosis. *J Thorac Imaging* 2006;21:8.

230. Foster Z, Grünwald N. Analysis of Microbiome Community Data in R. 2018;doi:XXX.

231. O'Brien KL, Bronsdon MA, Dagan R, Yagupsky P, Janco J, Elliott J, *et al.* Evaluation of a Medium (STGG) for Transport and Optimal Recovery of *Streptococcus pneumoniae* from Nasopharyngeal Secretions Collected during Field Studies. *J Clin Microbiol* 2001;39:1021–1024.

232. Keating D, Marigowda G, Burr L, Daines C, Mall MA, McKone EF, *et al.* VX-445–Tezacaftor–Ivacaftor in Patients with Cystic Fibrosis and One or Two Phe508del Alleles. *N Engl J Med* 2018;379:1612–1620.

233. Jorth P, Durfey S, Rezayat A, Garudathri J, Ratjen A, Staudinger BJ, *et al.* Cystic Fibrosis Lung Function Decline after Within-Host Evolution Increases Virulence of Infecting *Pseudomonas aeruginosa*. *Am J Respir Crit Care Med* 2021;203:637–640.

234. Jensen PØ, Moser C, Kharazmi A, Presler T, Koch C, Høiby N. Increased serum concentration of G-CSF in cystic fibrosis patients with chronic Pseudomonas aeruginosa pneumonia. *J Cyst Fibros* 2006;5:145–151.

235. Norman D, Elborn JS, Cordon SM, Rayner RJ, Wiseman MS, Hiller EJ, *et al.* Plasma tumour necrosis factor alpha in cystic fibrosis. *Thorax* 1991;46:91–95.

236. Dean TP, Dai Y, Shute JK, Church MK, Warner JO. Interleukin-8 Concentrations Are Elevated in Bronchoalveolar Lavage, Sputum, and Sera of Children with Cystic Fibrosis. *Pediatr Res* 1993;34:159–161.

237. Wilmott RW, Frenzke M, Kociela V, Peng L. Plasma interleukin-1α and β, tumor necrosis factor-α, and lipopolysaccharide concentrations during pulmonary exacerbations of cystic fibrosis. *Pediatr Pulmonol* 1994;18:21–27.

238. Schmittgrohe S. Interleukin-8 in whole blood and clinical status in cystic fibrosis. *Cytokine* 2004;doi:10.1016/j.cyto.2004.09.004.

239. McColley SA, Stellmach V, Boas SR, Jain M, Crawford SE. Serum vascular endothelial growth factor is elevated in cystic fibrosis and decreases with treatment of acute pulmonary exacerbation. *Am J Respir Crit Care Med* 2000;161:1877–1880.

240. Aris RM, Stephens AR, Ontjes DA, Denene Blackwood A, Lark RK, Hensler MB, *et al.* Adverse Alterations in Bone Metabolism Are Associated with Lung Infection in Adults with Cystic Fibrosis. *Am J Respir Crit Care Med* 2000;162:1674–1678.

241. Bell, Bowerman, Nixon, Macdonald, Elborn, Shale. Metabolic and inflammatory responses to pulmonary exacerbation in adults with cystic fibrosis: REE during pulmonary exacerbation in CF adults. *Eur J Clin Invest* 2000;30:553–559.

242. Limoli DH, Yang J, Khansaheb MK, Helfman B, Peng L, Stecenko AA, *et al.* Staphylococcus aureus and Pseudomonas aeruginosa co-infection is associated with cystic fibrosis-related diabetes and poor clinical outcomes. *Eur J Clin Microbiol Infect Dis* 2016;35:947–953.

243. Elborn JS, Cordon SM, Parker D, Delamere FM, Shale DJ. The host inflammatory response prior to death in patients with cystic fibrosis and chronic Pseudomonas aeruginosa infection. *Respir Med* 1993;87:603–607.

244. Chalmers JD, Moffitt KL, Suarez-Cuartin G, Sibila O, Finch S, Furrie E, *et al.* Neutrophil Elastase Activity Is Associated with Exacerbations and Lung Function Decline in Bronchiectasis. *Am J Respir Crit Care Med* 2017;195:1384–1393.

245. Saiman L, Marshall BC, Mayer-Hamblett N, Burns JL, Quittner AL, Cibene DA, *et al.* Azithromycin in Patients With Cystic Fibrosis Chronically Infected With Pseudomonas aeruginosa: A Randomized Controlled Trial. *JAMA* 2003;290:1749.

246. McKone E, Rodriguez S, Yen K, Davies J. Long-term safety and efficacy of ivacaftor in subjects with CF who have the G551D-CFTR mutation. *Eur Respir J* 2012;40:1842.

247. Guimbellot JS, Baines A, Paynter A, Heltshe SL, VanDalfsen J, Jain M, *et al.* Long term clinical effectiveness of ivacaftor in people with the G551D CFTR mutation. *J Cyst Fibros* 2021;20:213–219.